

University of Dundee

MASTER OF SCIENCE

## Evaluation of the Potential Expansion Mechanisms of Bottom Ash in Unbound Sub-base Materials

Mac Giolla Bhride, Padraic

*Award date:*  
2015

[Link to publication](#)

### General rights

Copyright and moral rights for the publications made accessible in the public portal are retained by the authors and/or other copyright owners and it is a condition of accessing publications that users recognise and abide by the legal requirements associated with these rights.

- Users may download and print one copy of any publication from the public portal for the purpose of private study or research.
- You may not further distribute the material or use it for any profit-making activity or commercial gain
- You may freely distribute the URL identifying the publication in the public portal

### Take down policy

If you believe that this document breaches copyright please contact us providing details, and we will remove access to the work immediately and investigate your claim.



UNIVERSITY OF DUNDEE

# EVALUATION OF THE POTENTIAL EXPANSION MECHANISMS OF BOTTOM ASH IN UNBOUND SUB- BASE MATERIALS

---

**Pádraic Mac Giolla Bhríde**

**Project Supervisor: Dr. Tom D Dyer**

**Student ID: 070009965**

## Abstract

The aim of this dissertation is to evaluate the potential for bottom ash from the incineration of municipal solid waste to undergo chemical reactions which could lead to expansion when used as an unbound granular fill

This paper sets out the experimental results obtained from testing of the Incinerator Bottom Ash under several procedures. A literature review was carried out to determine the common characteristics of bottom ash, from the literature review a series of tests were chosen to characterise certain properties of the material.

Several mix proportions of IBA and chemical additions of sodium sulphate ( $\text{Na}_2\text{SO}_4$ ), sodium hydroxide ( $\text{NaOH}$ ) and Calcium Chloride ( $\text{CaCl}_2$ ) were made to hasten chemical reactions. Several standard tests and new hybrid tests were performed to determine the properties of the mix proportions. Tests such as rapid evaluation of expansion, X-Ray diffraction, X-Ray fluorescence, pH testing, microscopic examination, magnetic separation analysis, Thermogravimetry, Scanning Electron Microscopy and accelerated chemical reactions.

Results showed that expansion appears to be through two mechanisms, unpredictable relaxation of compacted material and more notably the formation of expansive gels promoted by alkaline conditions.

## Table of Contents

Abstract.....	i
Table of Contents.....	ii
Table of Figures.....	v
Table of Tables.....	ix
Acknowledgements.....	x
1 Introduction.....	1
1.1 Background.....	1
1.2 Municipal Solid Waste and Incinerator Bottom Ash.....	1
1.3 Scope of Study, Aims and objectives.....	2
1.4 Outline of the Study.....	2
2 Literature Review.....	4
2.1 Introduction.....	4
2.2 Municipal Solid Waste.....	4
2.2.1 Municipal Waste Incineration.....	5
2.3 Incinerator Bottom Ash.....	6
2.3.1 Treatment of IBA.....	6
2.3.2 Unbound Road Materials – Mechanical Properties and Current Test Methods.....	7
2.3.3 Applications in Roads.....	7
2.3.4 Other Applications in Industry.....	8
2.4 IBA Composition.....	8
2.4.1 Physical Properties of Incinerator Bottom Ash.....	8
2.4.2 Chemical Composition.....	9
2.4.3 Optimum Moisture Content/Maximum dry density.....	9
2.5 Mechanisms of Expansion.....	10
2.5.1 Slag Expansion.....	10
2.5.2 Oxidation of Aluminium.....	12
2.5.3 Hydrogen Evolution.....	14
2.5.4 Expansion Due to Sulphates.....	15

2.5.5	Alkali Silica Reaction .....	17
2.5.6	Freeze-Thaw .....	20
2.5.7	Frost Heave .....	21
2.6	Literature Review Conclusion .....	21
3	Methodology .....	22
3.1	Introduction.....	22
3.2	Materials .....	22
3.2.1	Incinerator Bottom Ash.....	22
3.2.2	Chemicals.....	22
3.3	Experimental Procedures .....	23
3.3.1	Initial Testing of Ash .....	23
3.4	Rapid Evaluation of Expansion.....	24
3.4.1	Preparation of Specimens.....	24
3.5	X-Ray Diffraction .....	28
3.6	X-Ray Fluorescence.....	28
3.7	pH Testing.....	28
3.8	Microscopic Examination .....	29
3.8.1	Preparation of Samples .....	29
3.8.2	Magnetic Separation Analysis .....	31
3.9	Thermogravimetry .....	31
3.10	Scanning Electron Microscopy .....	32
3.11	Thermal Analysis .....	34
4	Results and Discussion .....	35
4.1	Initial Testing Results .....	35
4.1.1	Normal Proctor Test.....	35
4.1.2	Particle Size Distribution .....	38
4.1.3	Chemical Composition.....	38
4.1.4	Mineralogical Composition.....	39
4.1.5	Magnetic Separation Analysis .....	40

4.2	Swelling Results.....	40
4.2.1	Specimens Containing Na <sub>2</sub> SO <sub>4</sub> .....	41
4.2.2	Specimens Containing NaOH .....	43
4.2.3	Specimens Containing CaCl <sub>2</sub> .....	45
4.2.4	Specimens Containing no Chemical Addition (Control) .....	47
4.2.5	Discussion of Rapid Evaluation of Expansion Test Results .....	48
4.2.6	Summary of Expansion.....	50
4.3	X-ray Diffraction .....	52
4.3.1	Specimens Containing Na <sub>2</sub> SO <sub>4</sub> .....	52
4.3.2	Specimens Containing NaOH .....	54
4.3.3	Specimens Containing CaCl <sub>2</sub> .....	57
4.3.4	Specimens Containing No Chemical Addition (Controls) .....	58
4.3.5	Summary of X-Ray Diffraction .....	61
4.4	pH Testing.....	61
4.5	Microscopic Analysis.....	61
4.5.1	Specimens Containing Na <sub>2</sub> SO <sub>4</sub> .....	62
4.5.2	Specimens Containing NaOH .....	64
4.6	Scanning Electron Microscope and EDAX analysis.....	65
4.6.1	Specimens Containing Na <sub>2</sub> SO <sub>4</sub> .....	65
4.6.2	Specimens Containing NaOH .....	69
4.6.3	Specimens Containing CaCl <sub>2</sub> .....	78
4.6.4	Specimens without chemical addition.....	82
4.7	Thermal Analysis .....	89
5	Discussion of Results.....	98
6	Conclusions.....	101
6.1	Proposed further study .....	103
7	Bibliography .....	104
	Journals and Books .....	104
	Standards.....	105

Websites.....	106
---------------	-----

## Table of Figures

Figure 1-1 Timetable for proposed project .....	3
Figure 2-1 IBA Cleveland site .....	8
Figure 2-2 . Development of expansion pressure from steel slag particles (Wang, 2010). ....	11
Figure 2-3 IBA swelling under various conditions .....	13
Figure 2-4 Axial swell deformation versus time .....	14
Figure 2-5. Change in specimen dimensions and compressive strength versus time for a PC mortar exposed to a 25,000 ppm sulphate (or 37,000ppm Na <sub>2</sub> SO <sub>4</sub> ) solution at 23°C. ....	16
Figure 2-6 Expansion curves for concrete containing combination of coarse and fine aggregate known to display reactivity [Dyer and Dhir, 2010]. ....	19
Figure 3-1 Test cylinder.....	26
Figure 3-2 Test cylinder, rubber seal and end cap .....	27
Figure 3-3 pH test of moisture from a Castle Bromwich Specimen .....	29
Figure 3-4 Leica DC 300F microscope.....	30
Figure 3-5 Ash with epoxy resin coating .....	30
Figure 3-6 Ash sample prepared for microscopic analysis. ....	31
Figure 3-7 Netzsch simultaneous thermal analysis PC .....	32
Figure 3-8 Samples for SEM .....	33
Figure 3-9 Cressington Sputter coater .....	33
Figure 3-10 Environmental scanning electron microscope.....	34
Figure 4-1. Standard Proctor test curve for gravelly soil .....	36
Figure 4-2. Relative Bulk Density from the Cleveland ash. ....	36
Figure 4-3. Relative Bulk Density from the Birmingham ash. ....	37
Figure 4-4 PSD comparing both IBAs .....	38
Figure 4-5 Expansion measurements taken from Cleveland IBA specimens containing Na <sub>2</sub> SO <sub>4</sub> .....	41
Figure 4-6 Expansion measurements taken from Cleveland IBA specimens containing Na <sub>2</sub> SO <sub>4</sub> with additions of water.....	41
Figure 4-7 Expansion measurements taken from Castle Bromwich IBA specimens containing Na <sub>2</sub> SO <sub>4</sub> .....	42
Figure 4-8 Expansion measurements taken from control Castle Bromwich and Cleveland IBA specimens.....	42
Figure 4-9 Expansion measurements taken from Cleveland IBA specimens containing NaOH.....	43

Figure 4-10 Expansion measurements taken from Cleveland IBA specimens containing NaOH with additions of water.....	43
Figure 4-11 Expansion measurements taken from Castle Bromwich IBA specimens containing NaOH .....	44
Figure 4-12 Expansion measurements taken from Castle Bromwich IBA specimens containing NaOH with additions of water.....	44
Figure 4-13 Expansion measurements taken from Cleveland IBA specimens containing $\text{CaCl}_2$ .....	45
Figure 4-14 Expansion measurements taken from Cleveland IBA specimens containing $\text{CaCl}_2$ with additions of water.....	45
Figure 4-15 Expansion measurements taken from Castle Bromwich IBA specimens containing $\text{CaCl}_2$ .....	46
Figure 4-16 Expansion measurements taken from Castle Bromwich IBA specimens with added water containing $\text{CaCl}_2$ .....	46
Figure 4-17 Expansion measurements taken from control Castle Bromwich and Cleveland IBA specimens.....	47
Figure 4-18 Expansion measurements taken from control Castle Bromwich and Cleveland IBA specimens with the additional water. ....	47
Figure 4-19 Ranges and average expansion values for different types of chemical exposure.....	51
Figure 4-20 Ranges and average expansion values for different test temperatures. ....	51
Figure 4-21 Ranges and average expansion values for different moisture conditions.....	52
Figure 4-22 X-ray diffraction traces from the Cleveland ash before and after exposure to $\text{Na}_2\text{SO}_4$ 20 with added water. Th = Thernardite ( $\text{Na}_2\text{S}_{04}$ )Castle Bromwich.....	53
Figure 4-23 X-ray diffraction traces from the Castle Bromwich ash before and after exposure to $\text{Na}_2\text{SO}_4$ 40°C .....	54
Figure 4-24 X-ray diffraction traces from the Cleveland ash before and after exposure to NaOH at 40oC. N = cancrinite; B = bayerite. ....	55
Figure 4-25 X-ray diffraction traces from the Cleveland ash before and after exposure to NaOH with added water. N = cancrinite; B = bayerite; CA = calcium aluminates.....	55
Figure 4-26 X-ray diffraction traces from the Castle Bromwich ash before and after exposure to NaOH at 20oC. Et = ettringite; B = bayerite.....	56
Figure 4-27 X-ray diffraction traces from the Castle Bromwich ash before and after exposure to NaOH at 40oC. CA = calcium aluminate; N = cancrinite; M = mullite; G = gibbsite; B = bayerite; T = tridymite; C = cristobalite. ....	57
Figure 4-28 X-ray diffraction traces from the Castle Bromwich ash before and after exposure to NaOH at 20oC with added water. Ca = calcium aluminates; N = cancrinite; G = gibbsite.....	57



Figure 4-29 X-ray diffraction traces from the Castle Bromwich ash before and after exposure to $\text{CaCl}_2$ at 40°C .....	58
Figure 4-30 X-ray diffraction traces from the Cleveland ash with no chemical addition before and after storage at 20°C. B = bayerite .....	59
Figure 4-31 X-ray diffraction traces from the Castle Bromwich ash with no chemical addition before and after storage at 20°C with additional water. CA = calcium aluminate .....	59
Figure 4-32 Background of the Cleveland IBA XRD trace and the background of the same material after exposure to NaOH at 40°C with additional water .....	60
Figure 4-33 Background of the Castle Bromwich IBA XRD trace and the background of the same material after exposure to NaOH at 40°C .....	60
Figure 4-34 Microscopic image from a particle taken from CL $\text{Na}_2\text{SO}_4$ 40 specimen .....	62
Figure 4-35 CL Microscopic image from a particle taken from $\text{Na}_2\text{SO}_4$ 40 specimen .....	62
Figure 4-36 Microscopic image from a particle taken from CB $\text{Na}_2\text{SO}_4$ 40 specimen .....	63
Figure 4-37 Microscopic image from a particle taken from CB $\text{Na}_2\text{SO}_4$ 40 S specimen .....	63
Figure 4-38 Microscopic image from a particle taken from CL NaOH 40 specimen .....	64
Figure 4-39 SEM image from a particle taken from the CL $\text{Na}_2\text{SO}_4$ 40 Specimen .....	66
Figure 4-40 SEM image from a particle taken from the CL $\text{Na}_2\text{SO}_4$ 40 specimen .....	66
Figure 4-41 EDAX spectrum from the crystals present on the CL $\text{Na}_2\text{SO}_4$ 40 specimen .....	67
Figure 4-42 SEM image from a particle taken from the CL $\text{Na}_2\text{SO}_4$ 40 S specimen .....	67
Figure 4-43 SEM image from a particle taken from the CB $\text{Na}_2\text{SO}_4$ 40 specimen .....	68
Figure 4-44 SEM image from a particle taken from the CB $\text{Na}_2\text{SO}_4$ 40 specimen .....	69
Figure 4-45 EDAX spectrum of particle taken from the CB $\text{Na}_2\text{SO}_4$ 40 specimen .....	69
Figure 4-46 SEM image from a particle taken from CL NaOH 40 .....	70
Figure 4-47 EDAX spectrum of particle taken from the CL $\text{Na}_2\text{SO}_4$ 40 specimen .....	70
Figure 4-48 SEM image from a particle taken from the CL NaOH 40 S specimen .....	71
Figure 4-49 EDAX spectrum from the reaction product present on the particle taken from the .....	72
Figure 4-50 SEM image of a thin layer of material developing on a glass particle taken from the CL NaOH 40 S specimen .....	72
Figure 4-51 SEM image of reaction products on the surface of a glass particle taken from the CL NaOH 40 S .....	73
Figure 4-52 EDAX spectrum of suspected CSH gel on the CL NaOH 40 S specimen .....	73
Figure 4-53 SEM image from the surface of a particle taken from the CB NaOH 20 specimen .....	74
Figure 4-54 EDAX spectrum of particle taken from the CB NaOH 20 specimen .....	74
Figure 4-55 SEM image from a particle taken from the CB NaOH 40 specimen .....	75
Figure 4-56 SEM image of Clusters of needle like crystals in the CB NaOH 40 specimen (1 of 2) ....	75

Figure 4-57 SEM image of Needle shaped and hexagonal crystals in the CB NaOH 40 specimen. (2 of 2 @ 10x magnification) .....	76
Figure 4-58 SEM image from a particle taken from the CB NaOH 20 S specimen .....	77
Figure 4-59 EDAX spectrum of particle taken from the CB NaOH 20 S specimen.....	77
Figure 4-60 SEM image of reaction products from a particle taken from the CB NaOH 20 S specimen .....	78
Figure 4-61 SEM images of the surface of a particle from the CL CaCl <sub>2</sub> 40 specimen .....	79
Figure 4-62 SEM image of Crystals of CaCl <sub>2</sub> powder on surface of a particle taken from CB CaCl <sub>2</sub> 40 S, .....	80
Figure 4-63 SEM images of a Gel layer on the surface of a particle taken from CB CaCl <sub>2</sub> 40 S.....	80
Figure 4-64 SEM images of a particle taken from CB CaCl <sub>2</sub> 40 S specimen. (2) @ 5x magnification, gel like surface leading to aggregate not yet reacted .....	81
Figure 4-65 SEM images of a particle taken from CB CaCl <sub>2</sub> 40 S specimen.....	81
Figure 4-66 EDAX spectrum of particle taken from the CB CaCl <sub>2</sub> 40 specimen.....	82
Figure 4-67 SEM images of Corrosion products on the surface of a particle taken from CL control 20 specimen .....	83
Figure 4-68 EDAX spectrum from the CL control 20 specimen .....	83
Figure 4-69 SEM images of Corrosion products on the surface of a particle taken from the CL Control 20 specimen .....	84
Figure 4-70 EDAX Spectrum from CL control 20 specimen .....	84
Figure 4-71 SEM images of a layer of reaction product on the surface of a particle from CB Control 20 S .....	85
Figure 4-72 EDAX spectrum from CB Control 20 S.....	85
Figure 4-73 SEM image of Unburnt organic material on a particle taken from CB Control 20 S specimen .....	86
Figure 4-74. EDAX spectrum of unburnt organic material in CB Control 20 S.....	86
Figure 4-75 SEM images of a particle taken from CB Control 40 S specimen .....	87
Figure 4-76 EDAX spectrum of particle taken from the CB Control 40 S specimen.....	87
Figure 4-77 Thermal analysis results from the unreacted Castle Bromwich IBA .....	90
Figure 4-78 Thermal analysis results from the powdered Castle Bromwich IBA after storage in the presence of water at 40oC for 6 weeks. ....	91
Figure 4-79 Thermal analysis results from the powdered Castle Bromwich IBA after storage in the presence of a solution of NaOH at 40oC for 4 weeks.....	91
Figure 4-80 Thermal analysis results from the powdered Castle Bromwich IBA after storage in the presence of a solution of CaCl <sub>2</sub> at 40oC for 4 weeks.....	92
Figure 4-81 Thermal analysis results from the powdered Castle Bromwich IBA after storage in the presence of a solution of Na <sub>2</sub> SO <sub>4</sub> at 40oC for 4 weeks .....	92

Figure 4-82 X-ray diffraction traces from the powdered Castle Bromwich specimens exposed to different chemical environments.....	93
Figure 4-83 X-ray diffraction traces from the original powdered Castle Bromwich specimen, plus the material after exposure to NaOH. ....	93
Figure 4-84 Thermal analysis results from the unreacted Cleveland IBA.....	94
Figure 4-85 Thermal analysis results from the powdered Cleveland IBA after storage in the presence of water at 40oC for 6 weeks. ....	94
Figure 4-86 Thermal analysis results from the powdered Cleveland IBA after storage in the presence of a solution of NaOH at 40oC for 4 weeks.....	95
Figure 4-87 Thermal analysis results from the powdered Cleveland IBA after storage in the presence of a solution of CaCl <sub>2</sub> at 40oC for 4 weeks.....	95
Figure 4-88 Thermal analysis results from the powdered Castle Bromwich IBA after storage in the presence of a solution of Na <sub>2</sub> SO <sub>4</sub> at 40oC for 4 weeks.....	96
Figure 4-89 X-ray diffraction traces from the powdered Cleveland specimens exposed to different chemical environments .....	96
Figure 4-90 X-ray diffraction traces from the original powdered Cleveland specimen, plus the material after exposure to NaOH .....	97

## Table of Tables

Table 2-1 Composition of IBA from selected literature .....	9
Table 2-2 Common sulphur bearing minerals and their solubilities .....	16
Table 3-1 Specimens investigated during the rapid evaluation of expansion testing programme and the labelling system used to identify the specimens. ....	25
Table 3-2 Water content of samples .....	26
Table 4-1 Major oxide analysis of ash.....	39
Table 4-2 mineralogical analysis of ash.....	39
Table 4-3 Summary of Expansion .....	48
Table 4-4 pH values obtained from IBA specimens with excess liquid. ....	61
Table 4-5 Summary of reaction products found in EDAX and Thermal analysis .....	88

## Acknowledgements

I would like to sincerely thank Dr. Tom D. Dyer, Dr. Dyer's continuous assistance and guidance and understanding was vital to the successful completion of the dissertation. I would like to thank the technicians and fellow research students in Dundee's Concrete Technology Unit for all of their help and support.

I would also like to thank my friends whose support throughout the duration of the dissertation was vital. I would also like to remember friends and family which were have lost throughout this period, you will never be forgotten.

Ba mhaith liom buíochas a ghlacadh le mo chuid tuismitheorí agus Ailbhe, Jack agus Cian a thug cúnamh dhom agus a chuir suas liom i rith treimhse na h-oibre. Go raibh míle maith agaibh.

## **1 Introduction**

### **1.1 Background**

Ballast Phoenix Limited is the leading UK producer of Incinerator Bottom Ash Aggregate (IBAA) with a view to address issues relating to the risk of expansion mechanisms in IBAA. IBAA is a product of municipal waste incineration (MSWI) and is the product of bottom clinker material being cooled in a quench bath of water, stockpiled for a period of 4 weeks (on average) and then processed using various physical and magnetic separation techniques to produce a graded aggregate.

Ballast Phoenix Limited engaged the University of Dundee to carry out research on their product to firstly establish its physical and chemical characteristics and to then use previous research to guide further experimentation. The application scenario of most interest for this research project is that for unbound sub-base materials where IBAA is used as foundations to road and building projects. Use of IBAA as an aggregate in concrete is also of importance.

There have been some unfounded comparisons of IBAA to other secondary materials in the market place such as steel slags and blast furnace slag, which need to be addressed in a comprehensive and scientifically rigorous manner.

Some issues with IBAA such as expansion in road bases, embankment fill and aggregates for concrete building blocks are a concern for industry; this expansion is believed to be mainly attributed to the level of heavy metals within the aggregate. (HSE, 2010)

### **1.2 Municipal Solid Waste and Incinerator Bottom Ash**

The incineration of municipal solid waste (MSW) is becoming increasingly important for waste management. This is due to the increasing cost of landfill since the introduction of the new Landfill Tax 2008 and the revised EU Waste Framework Directive for England and Wales which advocates that 50% of all household waste and 70% of all construction waste must be recycled by 2020 (EEA, 2013)

This increased use of incineration produces a by-product, Incinerator Bottom Ash (IBA). IBA consists of non-combustible materials and is made up of a mix of materials such as sand, stone, glass, porcelain, metals and ash from un-burnt materials. IBA produced from a typical municipal incinerator represents about 20-30% of the input waste and Approximately 1 million tonnes of IBA are produced in England and Wales each year. The use of IBA is a positive advance in sustainable development, by saving natural resources and decreasing waste volume stored in landfills.

IBAA is the product of IBA being cooled in a quench bath of water and stockpiled for a period of 4 weeks (on average) and then processed using various physical and magnetic separation techniques to produce a graded aggregate. IBAA can be used in a number of engineering applications, the main application being a fill material in road construction as an unbound sub base material.

### 1.3 Scope of Study, Aims and objectives

The scope of this study is to study samples of unprocessed IBA from two MSW plants in the U.K., Cleveland, a county located in the North-East of England and Castle Bromwich, a suburb situated within the northern part of the Metropolitan Borough of Solihull in the English county of the West Midlands. The unprocessed IBA will be used to rapidly identify any issues which have been encountered in the use of IBA. These issues will be identified by adjusting the composition of compacted ash specimens, or the test temperature, and measuring dimensional changes. The ash used in this study is unprocessed ash which was initially quenched and then bagged and sent directly from the MSW Incineration facility to the laboratory labelled IBA.

The aim of this dissertation is to evaluate, on behalf of ballast phoenix limited, the potential for bottom ash from the incineration of municipal solid waste to undergo chemical reactions which could lead to expansion when used as an unbound granular fill. Where expansion issues are identified, more detailed examination will be conducted in a manner which will allow a judgement of whether the level of physical and gaseous expansion is likely to be acceptable within limits set by standards. The increased usage of IBAA has led to the need to evaluate the typical characteristics of the material. The aims of the dissertation are listed below:

- Complete a Literature review outlining the following
  - Origin and Background of IBA.
  - Composition of IBA
  - Possible mechanisms of expansion
  - Possible experimental procedures to be used in the study.
- Laboratory Testing
  - Characterisation of IBA in terms of selected physical and chemical properties.
  - Carry out an experimental programme to classify the expansion of IBA under a range of different conditions.
  - Continuously monitor expansive behaviour
  - Further Analysis of expansive material to investigate reactive materials.
- Evaluation of Experimental procedures
- Using the findings of this dissertation, highlight future work which can be carried out

### 1.4 Outline of the Study

The 12 month programme of works is shown in Figure 1-1 below, the experimental procedures and research was carried out within this timeframe. Following is an outline of the study;

Chapter 2 is a literature review: This chapter gives an outline of the reasons behind the use of IBA in industry, the formation of IBA and the application of the material. Once familiar with IBA, the physical characteristics of the material were then evaluated. This was done through researching past studies on IBA which classify the typical characteristics of the material. These studies also outlined the methods of classification which were then used in the experimental programme.

From the findings of the Literature review a laboratory based experimental programme was conducted which examined the tendency for compacted IBA to undergo expansion under a range of different conditions. These conditions were elevated temperatures, increased moisture contents and the addition of high concentrations of chemical substances which had the potential to cause reactions which lead to expansion.

The Methodology, Chapter 3, outlines the approach taken to investigate possible expansion mechanisms of IBA. The materials used, the experimental procedures and the preparation of samples are explained here. The labelling system is also explained, this labelling system will be used extensively throughout the document.

Chapter 4, results and discussion gives the initial testing results which are the characteristics of the IBA being used in this study. The experimental programme results are presented and discussed in detail, beginning with the expansion of the specimens. The influence of the ambient conditions in which the specimens were stored will have an effect on the overall expansion. Each specimen which showed some expansive properties are discussed here. The results are presented individually through the summation of the effect that each chemical addition has on the IBA. For example, rapid expansion results will be categorised by the chemical addition and the effects of the additions will be discussed.

The results of the expansion led to more intensive testing of the IBA. The testing criteria for the purposes of this study were chosen through investigation in the literature review. Testing included, X-ray Diffraction, X-ray fluorescence, magnetic separation analysis, thermogravimetry, Scanning electron microscopy and accelerated chemical reactions were all undertaken to give a better picture of the reactions occurring in the ash when rapid evaluation of expansion had ceased.

Chapter 5 is the discussion of the results. The summation of the processes which were individually discussed in chapter 4 are summarised here.

The conclusions of this study are summarised in chapter 6 along with suggestions for future work.

ACTIVITY	MONTH											
	1	2	3	4	5	6	7	8	9	10	11	12
<b>Work step 1. Literature Review</b>												
<i>Literature search</i>												
<i>Review document</i>												
<b>Work step 2. Laboratory Study</b>												
<i>Experimental programme plan</i>												
<i>Laboratory activities</i>												
<i>Final report</i>												

Figure 1-1 Timetable for proposed project

## 2 Literature Review

### 2.1 Introduction

This chapter gives an outline of the reasons behind the use of IBA in industry, the formation of IBA and the application of the material. Once familiar with IBA, the physical characteristics of the material were then evaluated. This was done through researching past studies on IBA which classify the typical characteristics of the material. These studies also outlined the methods of classification which were then used in the experimental programme.

Incineration is an important component of the integral management of municipal solid wastes (MSWs) in many countries. Incineration of these wastes produces Incinerator Bottom ash's (IBA) and if processed, incinerator bottom ash aggregate (IBAA) can be produced. These aggregates are recycled materials which are used in road construction and many other engineering applications such as foamed concrete, aggregate for asphalt and aggregate for concrete building blocks to name a few. For these materials to be used in the correct manner it is necessary to know their properties and how these properties effect their intended purposes. Existing literature on IBA and IBAA will be investigated in this literature review.

The literature review will address the following issues relating to IBA

- History of IBA
- The production of IBA
- The constituent materials and the material properties of IBA
- The applications of IBA in construction
- The issues dealing with the use of IBA
- Mechanisms of expansion of IBA

### 2.2 Municipal Solid Waste

In recent years the European Union (EU) has placed restrictions on landfilling waste materials, household landfilled materials are commonly known as Municipal solid waste (MSW). MSW is defined as *"all types of solid waste generated by households or commercial establishments"*. MSW has traditionally been deposited in landfills.

However, due to new EU laws which prohibit storing of untreated waste in landfills, and increasing cost of landfill disposal and the shortage of appropriate sites for locating landfill facilities incineration is becoming an increasingly popular option (Müller and Rübner 2006). In England and Wales, approximately 28 million tonnes of MSW are currently produced each year, of which about 90% is sent to landfill. (Qiao, Tyrer et al. 2008) Qiao also states that this figure is increasing by 3% per annum.

MSW contains everyday items which are used and then discarded within the household. Many of the constituents of MSW are recyclable. The waste is made up of both organic and inorganic materials



from residential, commercial, institutional and industrial sources. MSW contains Biodegradable waste, recyclable material, and inert waste and domestic hazardous waste.

### 2.2.1 Municipal Waste Incineration

Municipal solid waste is treated in incineration plants to reduce the volume, the toxicity and the reactivity of the waste (Klein, Baumann et al. 2001). 10% of MSW is sent to one of 14 operational energy from waste (EfW) plants in England and Wales for incineration, the majority goes to landfill. Incineration produces over 800 kilotons of IBA, most of which is land filled. (Klein, Baumann et al. 2001)

The incineration of MSW is set to increase in the UK and many other EU Countries that have limited availability of land for landfill. Incineration is highly effective, The most obvious effect of the incineration is the volume and mass reduction of the waste, the volume of the waste is reduced by 70 – 90% (Juric, Hanzic et al. 2006) and the mass by 60% (Arm 2003).

The moving grate furnace system is the most commonly used combustion system for high throughput MSW processing in the UK. First, the waste is sorted and oversized material is shredded. The sorted waste is then stored in the waste bunker before it is incinerated. During incineration, the waste is slowly driven through the furnace by a mechanically actuated grate. Waste continuously enters one end of the furnace and ash is discharged through the other. In the furnace the waste is heated up to 800–1,000°C. This is done gradually, which first makes the waste dry and at approximately 500°C it starts to burn. The combustion process results in bottom ash and flue gas. Plants are designed to ensure full combustion of the material as it moves through the furnace. The end of the grate normally passes the hot ash to a quench to rapidly cool the remaining non-combustibles.

To allow efficient combustion a sufficient amount of oxygen is required to fully oxidise the fuel. The incinerator process transforms organic materials into Carbon dioxide (CO<sub>2</sub>) and water (H<sub>2</sub>O) and also produces inorganic residues. These residues range from ferrous and non-ferrous metals to silicates. In other words, Incinerator plant combustion temperatures are in excess of 850°C and the waste is mostly converted into carbon dioxide and water and any non-combustible materials remain as a solid, known as incinerator bottom ash, these remaining materials are metals, glass and stone. IBA always contains small amounts of residual carbon.

Two types of ashes are produced as a result of the incineration process; bottom ash and fly ash. Bottom ash residues are large and heavy particles which are removed from the bed of the incinerator whereas fly ash residues are very fine particles entrained in exhaust gases. In Europe, most facilities isolate and manage the bottom ash and fly ash streams separately.

To identify what happens during incineration Loss of ignition (LOI) testing is carried out. Loss of ignition is a test used in inorganic analytical chemistry, mainly to analyse minerals. It consists of strongly heating a sample of material at a specified temperature, allowing volatile substances to escape until its mass ceases to change. This may be done in air, or in some other reactive or inert atmosphere. The simple test typically consists of placing a few grams of the material in a tared, pre-ignited crucible and determining its mass, placing it in a temperature-controlled furnace for a set

time, cooling it in a controlled (e.g. water-free, CO<sub>2</sub>-free) atmosphere, and predetermining the mass. The process may be repeated to show that mass-change is complete.

M. Arm (2003) studied IBA from sources in Sweden and found LOI in inorganic material at 550°C. Juric et al. found that incineration occurred at between 600°C and 800°C with 70% of required air added. The conditions used ensured warming, drying and semi-pyrolitic gasification of waste where most of the metals cannot evaporate and remain in the bottom ash. (Juric, Hanzic et al. 2006)

## 2.3 Incinerator Bottom Ash

The end of the grate normally passes the hot bottom ash to a water filled quench bath to rapidly cool the remaining combustibles. The resulting material can then be disposed of to landfill facilities. However, more recently, the use of bottom ash as a construction material has become an established practice. IBA is an inert material comprising of a mix of ceramics, slags, glassy materials and some metals. When used in this way, the ash is normally stockpiled for a period of time prior to being screened to remove oversize particles and also, in some cases, processed to remove ferrous metals. Many studies have been undertaken to find possibilities of incorporating IBA into building materials or structures.

### 2.3.1 Treatment of IBA

After the incineration and quenching of the MSW various technological options are available to treat the IBA prior to its reuse or disposal, such options are size separation, magnetic separation, washing, ageing/weathering, carbonation, chemical extraction and sintering.

Chimenos *et al* state that the most common method used in natural ageing of the IBA where IBA is stockpiled on the ground, this includes reactions such as oxidation, carbonation, neutralization of pH, dissolution, precipitation and sorption. All done through storage in stockpiles open to the atmosphere for a period of 1 – 3 months. (Chimenos *et al*. 1999) Bayuseno et al. state that the treatment of IBA after processing has a major impact on IBA characteristics. However these characteristics are poorly understood and there is a lack of quantification and testing in this area, i.e. they have not been studied in depth.

After incineration the material is quenched, early alteration products formed by the quenching of the products are ettringite and hydrocalumite, which are found in bottom ash particles. (Bayuseno and Schmahl 2010) The mineral assemblage of IBA is thermodynamically unstable and subject to ageing and weathering processes, leading to the formation of secondary minerals (e.g. ettringite, hydrocaluminate and C-S-H phase) the options available for reuse are discussed below and it is in the options stated below that the formation of secondary minerals transpires.

Under more heat IBA can have pozzolanic properties similar to that of cement (Qiao, Tyrer et al. 2008) Qiao found that milled IBA showed a low reactivity due to high organic content and large amount of inert minerals present after the incineration process. The IBA was then subject to thermal treatment at 800°C, this showed increases in reactivity by decreasing the LOI (BSEN196-2 2005) and decomposing CaCO<sub>3</sub> to give CaO. This helps to produce new active phases such as mayenite and gehelite.

### 2.3.2 Unbound Road Materials – Mechanical Properties and Current Test Methods

A major use for IBA in engineering is as an unbound aggregate in road construction and similar applications. Unbound road materials are significant in road bases and pavements because they act as a stable platform on which the upper layers of the pavement can be compacted and constructed. The unbound layers should be permeable and non-frost susceptible, to act as an insulating layer for the subgrade. All layers in a road base should be able to spread the traffic load to reduce stress on the underlying pavement layer and the subgrade, preventing overstress and rutting in the subgrade (Alkemade, Eymael et al. 1994).

Particle size and shape plays a major role in the final deformation properties of a road base. For the deformation properties of a road to remain the same over the course of its life, the particle size and shape must not change. The road base is always compacted but the variety of the material in IBA can generate issues. These issues can be created through environmental changes or loading on the material. Therefore, the material must be resistant to mechanical and climatic action.

M. Arm (2003) states that the resistance to mechanical action depends on the particle strength, which depends on the geometrical shape, the mineral composition and cohesion and the structure and texture of the particle. In an unbound layer of materials the contact between the particles and the size distribution of the material exerts an influence on this. Forteza (2004) studied IBAA physical characteristics and found that IBAA is an excellent material for granular layers (bases and sub-bases). However, the author mentions that particle size distribution should be refined to achieve a better level of compaction, e.g. by refining some of the larger particles, material left in a 10mm sieve and the finer particles below 1mm, this greater compaction will improve the longevity of the sub-base material in roads. (Forteza, 2004)

There are many standard test methods to measure the suitability of materials being considered through the deformation properties of material under load. The methods used are California bearing ratio, the static plate bearing test. Tests on organic matter content are loss of ignition (LOI) method and colorimetric measurement and determination of total organic carbon (TOC)

### 2.3.3 Applications in Roads

The department of transport's design manual for roads and bridges identifies that IBA can replace primary and secondary aggregates in most applications. (The Highways Agency, 2004) IBA may be used in many road applications for example, IBA is used in bitumen bound materials and concrete where the relevant material and grading requirements are met (D. François , A. Jullien, 2009). IBA can also be used as an unbound mixture for sub base, in the construction of embankments or as fill. Forteza, Far *et. al.* found that IBA can be used in road bases as the metal content and its leachates fulfilled the environmental regulations required. They found that the engineering properties of the bottom ash are similar to those of natural aggregates like gravels and crushed rock and that its use is feasible in road construction, as a sub base material and banking material.

### 2.3.4 Other Applications in Industry

IBA can be used to produce lightweight masonry units, as an additive in foamed concrete. The ceramic industry can use IBA in the production of tiles and also used in landfill engineering projects and in brownfield remediation projects.

Powdered IBA has been used experimentally as a partial replacement for cement in concrete. IBA contains some quantities of typical cement minerals, although in a lesser quantity than cement clinker. IBA is similar to class C pozzolans. Pera, Coutaz et al. (1997) found that when Raw IBA was introduced in concrete instead of gravel, problems of swelling and cracking occur due to the reaction between metallic aluminium and cement causing the corrosion of aluminium metal. Al-Rawas *et al.* (2005) found that at 20% replacement for cement IBA produced a higher compressive strength than the use of cement alone.

## 2.4 IBA Composition

The raw materials which are found in IBA are everyday items. The main constituents are glass, slag, ceramics, metals and other materials which are not as abundant (Bayuseno and Schmahl 2010). These base materials are the make-up of IBA. The material properties before and after incineration are discussed in more detail below.

### 2.4.1 Physical Properties of Incinerator Bottom Ash

IBA is a grey to black amorphous material that contains high levels of glasses and metals. Figure 2-1 shows IBA which was acquired from the Cleveland site. The nature of the aggregate depends greatly on the nature of the waste, type of combustion unit and nature of the air-pollution-control device.



Figure 2-1 IBA Cleveland site

IBA is a relatively lightweight material compared to sands and aggregate. It has a bulk specific gravity of 1.9- 2.4 for coarse particle and a bulk specific gravity of 1.5 – 2.2 for fine particles. Compare this to

2.6 – 2.8 for conventional aggregates (Siddique 2008). As well as being lightweight IBA is highly absorptive with absorption values of 4 -10% for coarse particles and 5 – 17% for finer particles. Conventional aggregates exhibit absorptive values of less than 2% (Siddique 2008)

#### 2.4.2 Chemical Composition

Siddique states that the composition of the material varies from facility to facility and regionally between plants. However, studies have shown that the difference is not substantial and many of the characteristics found in the UK are also found abroad. The main constituents of the IBA should remain similar. Bayuseno states that fresh IBA consists of amorphous and major crystalline phases such as silicates, oxides and carbonates. The mineral assemblage of fresh bottom ash is unstable and an aging process occurs by reaction towards an equilibrium mineral phase composition in the environmental conditions. (Bayuseno and Schmahl 2010)

Chemical compositions of IBA analysis in literature are shown in Table 2-1. The materials are, Germany sourced IBA (Müller and Rübner 2006), A Swedish ash whose composition was determined by Arm (2003) and a weathered Spanish bottom ash (Ginés, Chimenos et al. 2009)

The chemical composition of IBA is similar to the UK. In Sweden the chemical composition of IBA was found by Arm. Ginés et al. found that the composition of Spanish IBA

The results show that the composition of the German and ballast phoenix samples is similar in nature and will be due to similar incineration techniques or a similar trend in waste disposal in the region. The Swedish results show a lower level of SiO<sub>2</sub>. This may be due to practices within the country, e.g. a high rate of glass recycling etc, results can be seen in Table 2-1 below. All show a high level of siliceous material (SiO<sub>2</sub>), all close to or over 50% in composition. The remainder are composed of ceramic materials and unburned material. Calcium oxide (CaO) makes up between 10 and 15% of all the materials.

**Table 2-1 Composition of IBA from selected literature**

Component	SiO <sub>2</sub>	CaO	MgO	Al <sub>2</sub> O <sub>3</sub>	Fe <sub>2</sub> O <sub>3</sub>	Na <sub>2</sub> O	K <sub>2</sub> O	SO <sub>3</sub>	Na <sub>2</sub> O+K <sub>2</sub> O+TiO <sub>2</sub>
Amount	%	%	%	%	%	%	%	%	%
Northern Germany	55.7	11.9	2.7	14.1	8.8	1.4	1.2	0.7	
Sweden 2000	46	15	2	10	9	-	-	-	8
Spain 2009	49.38	14.68	2.32	6.58	8.38	7.78	1.41	0.57	

#### 2.4.3 Optimum Moisture Content/Maximum dry density

IBA has varying optimum moisture contents; EU standards are originally developed for natural aggregates which are uniform, such as gravel or crushed rock, which may not be appropriate to accurately assess IBA. (CEN, 2005) Finding compaction parameters are essential to ensure good design. Natural aggregates are uniform and give consistent and accurate results, in comparison to

IBA which can have an abundance of varying materials (Forteza, 2004). Glass from domestic sources can be found at between 50 – 60%, glass occurs in angular and flaky or a circular morphology which accounts for the high flakiness index of IBA samples, these particles have a lower strength when load is applied and are more susceptible to break down during compaction. Slag like particles have a highly porous and vesicular structure, this means that they have a higher capacity for absorbing water comparatively to natural aggregates. (Chimenos, Segarra et al. 1999) The above mentioned materials have great bearing on the proctor compaction method results, by means of their inconsistent variability as part of IBA.

Proctor compaction is the process by which solid particles are packed more closely together, thereby increasing the dry density of the soil. The dry density which can be achieved depends on the degree of compaction applied and the amount of water present in the soil. For a given degree of compaction of a given cohesive soil, there is an optimum moisture content at which the dry density obtained reaches a maximum value. In order to determine the water content that allows compaction to maximum density, a series of Proctor tests must be carried out. Due to the variable nature of the material being used, IBA the results of the normal Proctor test are inconsistent with those of a more homogeneous material e.g. sand or clay. (Izquierdo, Querol et al. 2011)

Izquierdo found that it is common practice in industry to re-compact a single sample of material to determine proctor curves. However, this overvalues the optimum moisture contents and maximum dry densities leading to inaccurate results. However, since IBA is a material with the capacity of absorbing large amounts of water, optimum moisture contents are markedly high i.e. 14 – 15%.

## 2.5 Mechanisms of Expansion

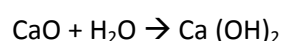
In certain conditions, expansion of aggregate and other materials used in construction applications is encountered. This is potentially problematic since the deflections and stresses resulting from expansion can damage structures containing them and render structures unserviceable.

There are many mechanisms of expansion observed. Many of the main types of expansion can be best seen in concrete applications. In most cases expansion is a result of chemical reactions occurring within the concrete. There are numerous types of chemical attack which cause expansion - sulphate attack, thaumasite sulphate attack, alkali-silica reaction and corrosion of steel reinforcement. The mechanisms of expansion are dependent on specific aggressive substances being present in the constituent materials, but all have one requirement which remains constant - moisture.

### 2.5.1 Slag Expansion

Steel slags are a by-product of steel production. Fluxes such as lime are added in steel making process to remove unwanted components from the steel. It is these fluxes and non-metallic components that combine to form steel slag. When cooled the slag can then be processed into aggregate, most if not all of this aggregate is used as a foundation layer in road construction.

Steel slags may contain un-hydrated (free) lime which will expand in the presence moisture via the reaction:



The formation of calcium hydroxide ( $\text{Ca(OH)}_2$ ) is believed to contribute to expansion as a result of crystallisation pressures between crystals formed in the spaces between slag particles and the sides of these particles. Different theories have been proposed regarding how crystallisation pressures arise. One theory states that they are produced when repulsive forces (electrostatic and solvation forces) exist between crystal faces and pore walls (Wang, 2010). Their existence permits a thin layer of water to occupy the space between the two surfaces which acts as a means for new material to be supplied to the crystal face. This supply of material allows the crystal to grow to the extent that sufficient pressures develop to fracture the confining material (Scherer, 2004). An alternative theory is that the pressures are created as a result of an increase in the concentration of dissolved species in pore solutions, which in turn are produced by the increase in solubility of calcium hydroxide crystals resulting from pressures caused by their growth in a confined space (Ping and Beaudoin, 1992).

Figure 2-2 shows how expansion force develops in concrete containing steel slag aggregate in tension in a cement mortar matrix.

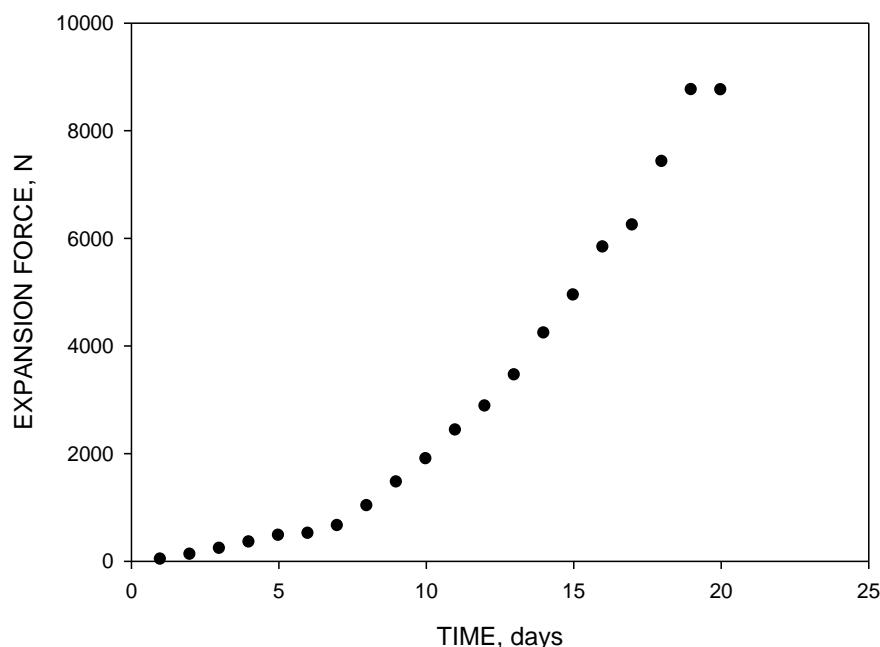
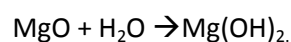


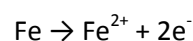
Figure 2-2 . Development of expansion pressure from steel slag particles (Wang, 2010).

Steel slag expansion may also be caused by magnesia hydration and oxidation of elemental iron.

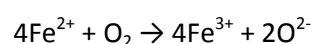
Magnesia hydration occurs by a similar mechanism to lime hydration, and follows the reaction:



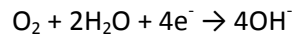
The oxidation of iron involves a series of reactions which start with ionisation at its surface:



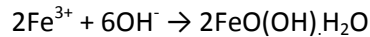
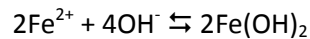
Where the metal ion dissolves. The iron can undergo further oxidation in the presence of water:



At the other metal surface, under neutral pH conditions, a reduction reaction occurs:



Iron hydroxides are then formed:



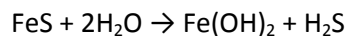
The hydroxides may subsequently undergo reactions to give a mixture of hydroxides and FeO, FeO(OH) and Fe<sub>2</sub>O<sub>3</sub>, which collectively make up the substance referred to as rust.

Rust is considerably less dense than iron metal, meaning that rust formation leads to an expansion in volume of up to four times.

Air cooled blast furnace slag is a by-product of iron production and are also potentially prone to expansion, although through two different mechanisms – dicalcium silicate transformation and a reaction involving iron sulphide.

Dicalcium silicate transformation occurs when β-dicalcium silicate is present in the slag. β-dicalcium silicate is a metastable form of dicalcium silicate (2CaO.SiO<sub>2</sub>) which will over time, undergo a phase transformation to the more stable γ-dicalcium silicate. This transformation involves an increase in volume which leads to disintegration of slag particles. A method for testing the β form is described in BS EN 1744-1, which involves the inspection of split slag particles under ultra-violet light.

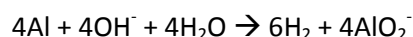
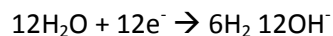
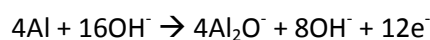
Iron sulphide ( and magnesium sulphide ) also cause disintegration, this time via the hydrolysis of the sulphide, an example of the hydrolysis reaction is.



A method for determining the potential for sulphide disintegration is also described in BS EN 1744-1, which involves submerging particles of slag in water for a number of days and observing the extent to which disintegration occurs.

### 2.5.2 Oxidation of Aluminium

The formation of gel from oxidation of metallic aluminium occurs at high pH (>10), i.e. the metal is dissolved with the emission of hydrogen.



The reaction occurs when the metal is in contact with water or OH<sup>-</sup> ions.

Alkemade et al. theorise that aluminium will be oxidised in cement bound IBA resulting in the formation of soluble aluminate ions. The aluminate will diffuse only a little if the moisture content is



low. And, therefore, the concentration of aluminate could be high near aluminium particles. After time, the pH of the cement based ash will decrease, if carbonation is taking place. Aluminium will be converted into aluminium hydroxide,  $\text{Al}(\text{OH})_3$  and due to these changing conditions there will be a subsequent increase in volume. Alkemade et. al also found that IBA stored outside depots are subject to higher levels of expansion because carbonation has already begun during storage. (Alkemade, Eymael et al. 1994)

The results of expansion found by Alkemade et al. show that the largest amount of expansion was observed under wet air conditions (samples kept in a wet place where oxygen and humidity foster expansion from aluminium oxidation). Figure 2-3 shows expansion as a result of aluminium hydroxide formation (and probably rust formation) under different storage conditions. The test specimen stored in air displayed the most expansion, indicating that access to oxygen is an important factor.

The IBA was also treated using lime + slag and 3% artificial Portland cement with a low  $\text{C}_3\text{A}$  content (CPA), Figure 2-4 below shows the effect of treatment on the IBA. The 3% CPA lowers the expansion due to the effect of the cement on the pH of the aggregate. As mentioned above, a high pH will increase the expansion rate of IBA. The swell deformation is due to oxidation of metals such as aluminium and/or iron.

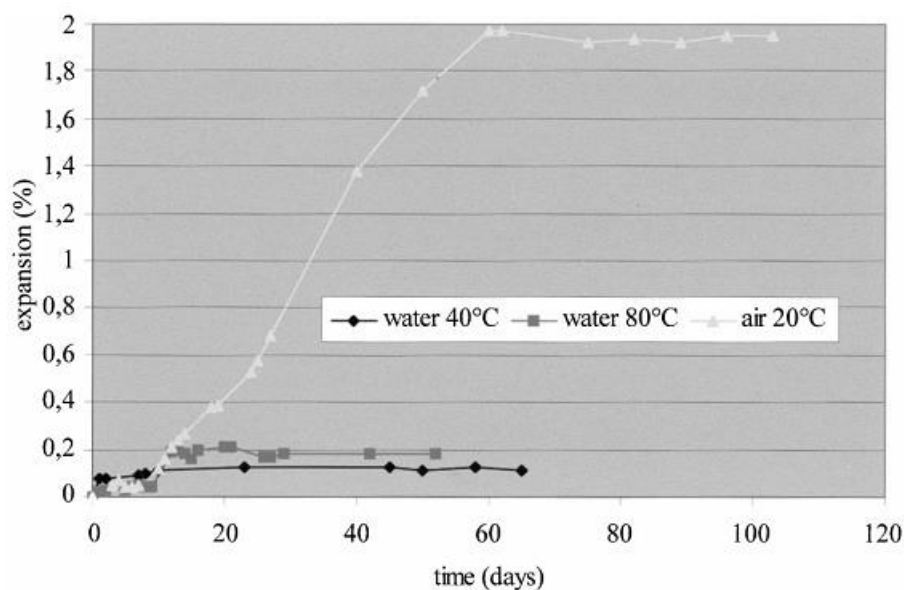


Figure 2-3 IBA swelling under various conditions

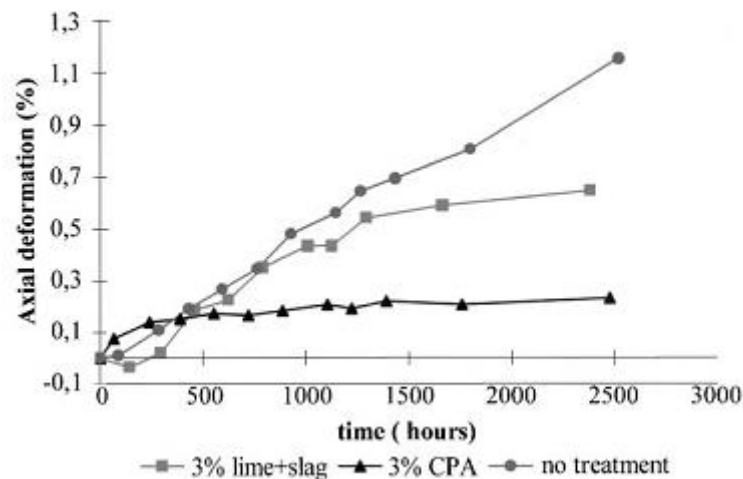


Figure 2-4 Axial swell deformation versus time

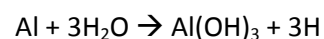
### 2.5.3 Hydrogen Evolution

Hydrogen evolution in IBA is attributed to chemical reactions involved in the transformation of IBA inorganic matter. This includes the oxidation of scrap iron, the hydroxylation of metals, the carbonation of alkaline and alkaline earth metals, and the dissolution of lime and calcium sulphate. (Bayuseno and Schmahl 2010) Bottom ash is unstable, this is due to the make-up of the material. Fresh bottom ash consists of amorphous and major crystalline phases such as silicates, oxides and carbonates.

The phase assemblage that is present after the processing of IBA i.e. rapid combustion, cooling and quenching is not in equilibrium. The ash is characteristically metastable under environmental conditions. Therefore, the ash is highly susceptible to chemical and mineralogical alteration over time.

#### 2.5.3.1 *Reaction between IBA and an Alkaline Environment,*

(Müller and Rübner 2006) studied the interaction of IBA, when utilized as an aggregate in concrete, with the cement matrix. In the alkaline environment produced by the hydrogen of Portland cement, corrosion of some metals produces a great amount of gaseous hydrogen. They found that the most prominent reactions observed were the formation of aluminium hydroxide and the release of hydrogen gas from the aluminium grains reacting in the alkaline environment:



The formation of pockets of hydrogen gas has been found to lead to a reduction in strength in fresh concrete. In consolidated materials, it is feasible that pressures could develop which are sufficient to disrupt the compacted material.

#### 2.5.4 Expansion Due to Sulphates

Expansion can occur as the result of reactions of materials containing aluminium and calcium with sulphate ions. This is sometimes observed in concrete, where it is referred to as sulphate attack. Sulphate attack occurs as a result of the ingress of dissolved ions into concrete which subsequently undergo reactions with the hardened cement. Laboratory tests show that the first effect of the reactions is to increase the strength and density of the concrete as the reaction products fill the pore space. When it is filled, further ettringite formation induces internal stresses in the concrete which may disrupt causing expansion of the affected region (BRE, 2001). To aid the understanding of sulphate attack it is useful to examine where sulphates arise in the environment.

##### 2.5.4.1 *Sulphates in the Environment*

The extent to which sulphate in soil is available for ingress into concrete depends on the solubility of the minerals present, as well as the extent to which groundwater is present and its mobility. Soil can potentially contain a number of sulphate minerals, although some of these are of low solubility. Common sulphate minerals are shown in Table 2-2 (Dyer, 2014), which shows that the most soluble are sodium and magnesium sulphates.

Sulfide minerals such as pyrite, marcasite and pyrrhotite may also be present. Most of these sulphide minerals are of very low solubility. In undisturbed soils rich in sulphide minerals, sulphate will only be present in significant quantities in the first 2-10 metres of soil which has undergone long-term weathering processes which have led to the gradual oxidation of sulphides. Moreover, the first metre of soil will typically contain relatively low levels of sulphate resulting from leaching to lower levels by infiltrating rainwater (Dyer 2014).

Disruption of soil during construction can potentially bring sulphide minerals in contact with air, which allows the minerals to be oxidised to sulphate minerals at a relatively high rate. In high pH conditions this process can be accelerated (Casanova et al, 1996; Casanova et al, 1997). Sulphur-oxidising bacteria, which may be present in soil are also capable of converting sulphide minerals into sulphates (Trudinger, 1971). In both cases, sulphide is oxidised to sulphuric acid, which proceeds to react with other cations in the soil to form sulphate compounds.

Peaty soils are also rich in sulphur, although much of this is present as organic compounds, rather than inorganic minerals (Spratt et al, 1987). However, this too can be oxidised to sulphate as a result of soil disruption.

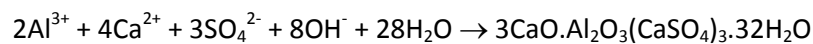
Human activities may also introduce sulphur onto sites. Previous industrial operations – particularly those involving the handling and processing of fossil fuels may contaminate soil with sulfates and sulfides. Activities of this type include coal mining, gas and coke processing plants and iron and steel manufacture. Additionally activities such as fertilizer manufacture and metal finishing may also introduce sulfates onto a site. In some cases, sulphate-bearing by-products from industrial activities may be introduced onto sites as granular fill. These include blast furnace slag, colliery spoil, furnace bottom ash from coal-fired power generation and IBA (BRE, 2005). Demolition rubble can also potentially contain reasonably large quantities of soluble sulphate (Musson et al, 2008).

Table 2-2 Common sulphur bearing minerals and their solubilities

c	CHEMICAL FORMULA	SOLUBILITY at 25°C, mg/l
Barite	BaSO <sub>4</sub>	2
Anhydrite	CaSO <sub>4</sub>	3,178
Gypsum	CaSO <sub>4</sub> ·2H <sub>2</sub> O	2,692
Epsomite	MgSO <sub>4</sub> ·7H <sub>2</sub> O	1,481,658
Jarosite	KFe <sub>3</sub> (OH) <sub>6</sub> (SO <sub>4</sub> ) <sub>2</sub>	5
Mirabilite	Na <sub>2</sub> SO <sub>4</sub> ·10H <sub>2</sub> O	340,561
Glauberite	Na <sub>2</sub> Ca(SO <sub>4</sub> ) <sub>2</sub>	78,146
Pyrite	FeS <sub>2</sub>	0
Marcasite	FeS <sub>2</sub>	0
Pyrrhotite	FeS	0

#### 2.5.4.2 Sulphate Expansion Mechanism

The most commonly encountered form of sulphate expansion occurs as the result of ettringite (3CaO·Al<sub>2</sub>O<sub>3</sub>(CaSO<sub>4</sub>)<sub>3</sub>·32H<sub>2</sub>O) formation. The reaction is as follows:



As for lime hydration, it is believed that the expansion results from crystallisation pressures. The expansion of mortar undergoing sulphate expansion is shown in Figure 2-5 (Al-Dulaijan, 2007). Also shown in this plot is the loss of strength of the material, illustrating the disruptive action of the expansion process.

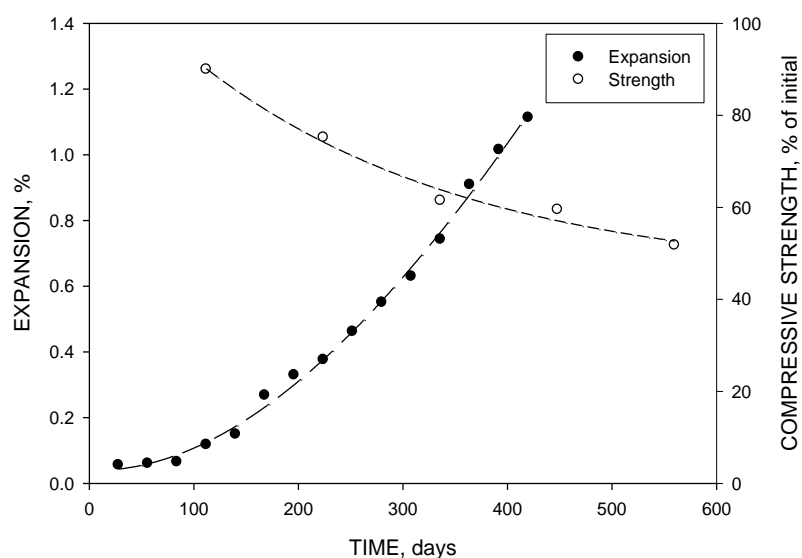


Figure 2-5. Change in specimen dimensions and compressive strength versus time for a PC mortar exposed to a 25,000 ppm sulphate (or 37,000ppm Na<sub>2</sub>SO<sub>4</sub>) solution at 23°C.

#### 2.5.4.3 *How Sulphates affect IBA*

Sulfates commonly occur in the solid part of the ground, soil, rock or fill, and in groundwater. IBA is affected by sulphate attack through the ingress of dissolved ions into IBA. Ingress could come from the application in which the IBA is used, for example, IBA used as a cement replacement can undergo reactions with hardened cement. IBA used as a fill material for road bases can also come into contact with groundwater or Soils rich in sulphates.

Unfortunately the author could not find direct research on the effects of sulphates on IBA, however, the reaction products should be relatively similar to those in concrete. Sulphate attack in concrete occurs as a result of the ingress of dissolved ions into concrete which subsequently undergo reactions with the hardened cement. The expansion of ettringite can give rise to spalling or cracking in concrete. Sulphate attack in IBA can occur in a similar manner, the ingress of dissolved ions into the IBA can react with the constituents of the IBA to form ettringite. Ettringite typically fills the pore space of concrete before inducing further internal stresses causing expansion/cracking of the affected region. As IBA is generally used as a sub base fill material, it is compacted on placing and voids will still occur. If excessive ettringite formation occurs within IBA it could potentially have the same adverse effects (BRE 2012). Water can give rise to a faster diffusion of the ions in the material thus speeding the effects of sulphate.

#### 2.5.5 **Alkali Silica Reaction**

Alkali-aggregate reaction occurs when certain constituents in aggregates react with alkali hydroxides in concrete. There are three forms of alkali-aggregate reaction of which one is alkali-silica reaction and the others alkali-carbonate reaction and Alkali-silicate reaction. To properly explain Alkali-silica reaction we must know the basics behind alkali-aggregate reaction and also the processes of Alkali-Carbonate Reaction, Alkali-silica reaction and Alkali-silicate reaction. Each form is briefly discussed below:

- **Alkali-Carbonate Reaction:** Reactions observed with certain dolomitic rocks are associated with alkali-carbonate reaction (ACR). Reactive rocks contain dolomite surrounded by a matrix of calcium and clay. ACR is rare because rocks which are prone to ACR are usually unsuitable as aggregate because of other reasons, i.e. a lack of strength (Farny and Kosmatka, 1997).
- **Alkali Silicate Reaction:** Alkali-silicate reaction is the same as ASR except that in this case the reactive constituent is not free silica but silica that is present in the combined form of silicates (e.g. chlorite, vermiculate, micas) it is probable that the phyllosilicates are reactive only if fine grained. Phyllosilicates are sheet silicates, formed by parallel sheets of silicate tetrahedra with  $\text{Si}_2\text{O}_5$  (Farny and Kosmatka, 1997).
- **Alkali-silica Reaction:** ASR is a reaction between the hydroxyl ions in the pore water of concrete and certain forms of silica. This reaction produces a gel which expands and can lead to cracking of concrete (Farny and Kosmatka, 1997).

Alkali-Silica reaction is a reaction between the hydroxyl ions in the pore water of concrete and certain forms of silica which occur in aggregates. The hydration of Portland cement results in the formation of an alkaline pore solution. This solution contains sodium ions  $\text{Na}^+$ , potassium ions  $\text{K}^+$ , calcium ions  $\text{Ca}^{2+}$  and hydroxyl ions  $\text{OH}^-$ . The quantities of these substances depend on the quantity

of sodium and potassium in the anhydrous Portland cement. The quantity of sodium and potassium is responsible for the alkalinity being higher than that of a saturated solution of calcium hydroxide. (Federico and Chidiac 2009)

The silica comes from aggregates such as crushed rock, sands, glass and gravel. In the case of IBA the silica is predominantly glass. The silica reacts with the hydroxide ions associated with these alkalis in the pore water. This reaction forms the alkali-silica gel which is hygroscopic, and the gels imbibition of the pore water causes it to swell. As the gel swells the concrete subsequently cracks and this eventually leads to failure (BRE 2004.)

For alkali-silica reaction to occur, three conditions must be present:

1. Reactive forms of silica;
2. High alkalinity (pH);
3. Sufficient moisture (Farny 1997)

Reactive forms of silica come from the aggregate, For example recycled aggregates such as glass are made of silica and are very reactive with respect to ASR. The pore solution in mortar and concrete contains almost entirely sodium, potassium and hydroxyl ions and has a pH within the range of 13 to 14.

The alkali-silica reaction is basically an attack by sodium or potassium hydroxyl solution on silica, producing an alkali-silicate gel (Concrete.Society 1999) Moisture is in the concrete mix and can be absorbed by the concrete through rain, capillary action and many other ways. The moisture that is found in the concrete allows the gel to form but in order for the gel to expand excess water must be present. The reaction can be visualised as a two-step process

1. alkalis + silica + moisture = alkali-silica gel
2. alkalis + silica + additional moisture = expansion of alkali-silica gel

Gel presence does not always coincide with distress and therefore the presence of gel does not always indicate destructive ASR. However the expansion of the gel does.

#### **2.5.5.1 Damaging Effects of ASR**

ASR is a slow process and can be found upon visual inspection and, therefore, risk of complete failure is low. ASR mainly causes serviceability problems and can worsen other deteriorative mechanisms such as freeze-thaw and sulphate exposure. Harmful ASR expansion does not occur without reactants, i.e. the silica, alkalis and moisture. ASR is characterised by a network of cracks. Typical indicators of ASR are map cracking (this is a random pattern appearing in the concrete) and in its advanced stages closed joints, spalled concrete surfaces and/or relevant displacements of different portions of a structure. Shrinkage cracking also occurs in concrete, but this type of cracking is usually found in the first year of the concretes life, the earliest time that cracking has led to concern in concrete in the UK is about 5 years (BRE 2004)

ASR cracking can allow more reactants such as alkalis, to enter the concrete increasing the damaging effects of ASR. As ASR gel absorbs water it applies a fairly uniform pressure of up to 10 MPa or more in all directions. This pressure exceeds the tensile strength capacity of most concretes. The tensile strength of concrete is roughly 10% of its compressive strength. The crack only expands enough to relieve the pressure caused and accommodate the resulting volume increase (Farny 1997). The cracks usually occur longitudinally as there is less restraint to lateral expansion. The reaction will cease when either of the reactants is consumed or when the hydroxyl ion concentration is so low that the reactive silica is no longer attacked (Hobbs 1988)

The nature of expansion observed during ASR in concrete is shown in Figure 2-6.

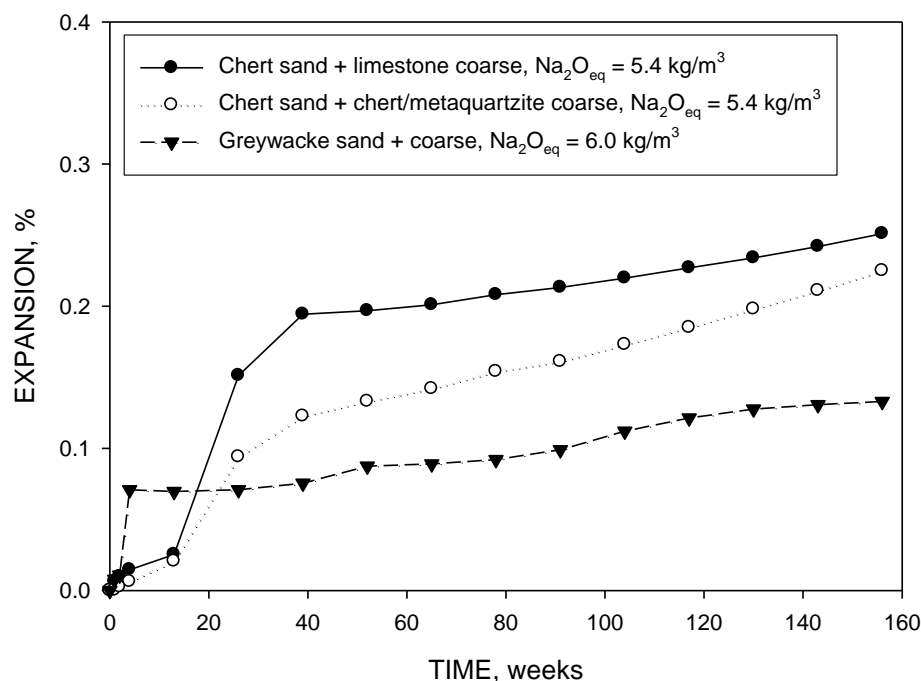


Figure 2-6 Expansion curves for concrete containing combination of coarse and fine aggregate known to display reactivity [Dyer and Dhir, 2010].

#### 2.5.5.2 ASR Found in IBA

Muller and Rubner (2006) used three different groups of concrete, two sets prepared in labs, one set of concrete was stored in water for several weeks, and one group was exposed in a humidity chamber at 40°C for 9 months. The final group consisted of drilled cores of concrete beams which were exposed outdoors for 8 years.

As well as identifying problems with hydrogen gas formation, susceptibility of glass components of the bottom ash to ASR was found to be an issue, as the glass is highly reactive. It was also seen that actual damage due to ASR is sporadic even when abundant silicate gel formation was well observed in all sample specimens (Müller and Rübner 2006).

Ichikawa and Miura (2007) carried out studies to understand why soft and fluid hydrated alkali silicate generated by ASR of aggregates by alkaline pore solution accumulates the expansive

pressure for cracking the aggregate and the surrounding concrete. The authors found that alkali silicate has no ability to generate expansive pressures unless the aggregate is tightly packed with a reaction rim, the reaction rim is slowly generated from the alkali silicate that covers the ASR affected aggregate. Therefore, their model claims that ASR does not cause the deterioration of concrete, if the ASR is completed before the formation of the reaction rim

#### **2.5.5.3 How ASR affects IBA**

ASR is classically a reaction between the hydroxyl ions in the pore water of concrete and certain forms of silica. This reaction produces a gel which expands and can lead to cracking of concrete. In IBA this is not the case, the main structure is different. However, the same reactions occur, the alkali environment created in the IBA reacts with the silica present to form ASR.

Muller and Rubner (2006) studied the microstructure of concrete made with IBA as an aggregate component. The studies found that the glass components of the bottom ash are susceptible to ASR. This is once again within a concrete matrix, IBA in sub base materials would contain constituents like silica, sodium, oxygen and calcium which could potentially lead to formation of ASR. ASR gel could be formed and fill voids left in the material and subsequently cause expansion.

#### **2.5.6 Freeze-Thaw**

Freeze-thaw is a form of physical weathering; it is caused by an expansion of moisture as it freezes. Water in a crack or void can freeze and expand in volume by 9% as it turns to ice. The expansion formed by the ice exerts great pressure in the void causing expansion. Attention should be paid to frost susceptibility and frost heaving values of alternative materials such as incinerator bottom ash aggregate intended for use in cold regions.

Water absorption levels are a useful link to the occurrence of phenomena such as freeze-thaw deterioration. Water absorption is measured in accordance to BS 812-2 (BS812-2 1995). CIRIA report C 559 states that high water absorption is only an indicator of possible aggregate susceptibility. One of the main physical differences between IBA and natural aggregate is its higher absorption rate. (Tam, Gao et al. 2008) investigated the water absorption of Recycled aggregate (RA) in comparison to natural aggregate. It was found that the higher the water absorption of the coarse aggregate, the reduced resistance to freezing and thawing than with natural aggregate. RA absorbs between 3% - 10% of water compared to less than 1% - 5% for natural aggregate.

Tan and Gao also state that the current standard BS 812-2 for testing water absorption in aggregate is unsuitable as parts of the RA can be dislodged during the soaking and drying process and can have an adverse effect on the final readings. This is likely to be true for IBA which is not a homogeneous aggregate. The new approach to testing water absorption is named real time water assessment of water absorption (RAWA) which provides an easier way to obtain the water absorption at different time intervals and without the needing of soaking and drying of the aggregate. The level and time of water absorption can be related to the supposed expansion of IBA. This can further the understanding of the mechanisms of expansion.



### 2.5.7 Frost Heave

The term frost heave is referring to the phenomena where a road will actually "heave", i.e. rise up above its normal level due to the action of frost.

As freezing temperatures penetrate the ground and the aggregate structure under pavements and slabs, moisture is frozen. Saturated pore structures are more susceptible to damage as water freezes and expand. Frost heaving occurs when additional water can be drawn into the pores between soil and aggregate particles by capillary action. The most susceptible are silt-sized materials forming a continuous path in soil or aggregate layers. They contain pores that are fine enough to hold water under tension and to draw sufficient additional water into the mass

In addition to the upward displacement caused by heaving during long frozen periods, the principal damage to highways occur during spring when thawing starts from the top down. Thawing first weakens the layer just under the pavement as ice lenses melt and the structure above collapses. As thawing continues (with the layer of frozen material below), excess water has nowhere to go and further reduces support for the pavement. This is when heavy truck traffic can do the most damage to a pavement.

## 2.6 Literature Review Conclusion

The literature review serves as a starting point for experimental procedures. The literature review set out the main characteristics of MSW, IBA and IBAA. It also highlighted previous studies carried out on IBA. From this research, the testing methods were analysed and the testing methods subsequently chosen.

### 3 Methodology

#### 3.1 Introduction

The approach taken to investigate the possible expansion mechanisms of IBA is outlined and discussed in this chapter. Testing was undertaken to investigate possible forms of expansion that were found during researching the literature review. Several likely mechanisms for expansion were discussed. The aim of the testing procedure was to screen materials for the most likely mechanism, or mechanisms of expansion.

In order to attempt to accelerate reactions, two approaches were taken. Firstly, chemical reagents were added to IBA specimens to induce some of the chemical reactions involved in the expansion mechanisms discussed in the previous section. Additionally, elevated temperatures were used as a means of accelerating such reactions. It should be stressed that elevated temperatures can potentially influence the nature of the reaction products in a manner which is not representative of normal ambient temperatures. For this reason, specimens were studied in parallel at 20°C.

The materials used for this research project were unprocessed Incinerator Bottom Ash which was delivered directly to the laboratory in the University of Dundee and used once received to avoid any ageing of the material.

#### 3.2 Materials

The materials and chemicals used in this study were chosen to represent the effect of different chemical environments on IBA. The choice of the materials was based on previous research in the subject and known chemical reactions which can occur in IBA.

##### 3.2.1 Incinerator Bottom Ash

IBA was obtained from two UK sites; the material came from facilities located in Cleveland and Castle Bromwich. The IBA had been quenched, but had not been aged, as it was felt that investigation before chemical reactions of ageing was more likely to identify any expansion issues.

##### 3.2.2 Chemicals

###### 3.2.2.1 *Sodium Sulphate ( $\text{Na}_2\text{SO}_4$ )*

Sodium Sulphate was used a reagent in the study to examine the potential for IBA to undergo expansion as a result of sulphate exposure to mimic the aggregates exposure to sulphate in soils. The influence of sulphate was explored through an addition of 5% sodium sulphate ( $\text{Na}_2\text{SO}_4$ ) by mass of dry ash to sets of specimens prior to compaction.

### 3.2.2.2 ***Sodium Hydroxide (NaOH):***

As discussed in the literature review, high pH conditions are required for the oxidation of aluminium, hydrogen gas evolution and alkali-silica reaction. Higher pH conditions were achieved through the addition of 5% of sodium hydroxide (NaOH) by mass of dry ash.

### 3.2.2.3 ***Calcium Chloride (CaCl<sub>2</sub>):***

5% CaCl<sub>2</sub> by mass was added to selected specimens to establish whether the formation of corrosion products on particles of ferrous metal in the IBA could be a source of expansion. Ferrous metal is very much sensitive to the presence of chloride ions, which shorten the period of time for corrosion to initiate. The corrosion products of steel and iron have a much larger volume relative to the metal and will therefore produce expansion.

## 3.3 **Experimental Procedures**

### 3.3.1 **Initial Testing of Ash**

Ash was used as soon as it was delivered and preliminary tests were carried out. The Ash was not dried nor had additional water unless stated otherwise. This was to ensure the ash remained in the same conditions as it would have if being delivered to a site.

#### 3.3.1.1 ***Moisture Content***

The oven-drying method was used as stated in BS 812-109 (BSI,1990) this method provides a measure of the total water present in a sample of ash. The method comprises placing a test portion in a container and drying it at a temperature of  $105 \pm 5$  °C until it reaches constant mass. Moisture content is determined by difference in mass and expressed as a percentage of the dry mass.

#### 3.3.1.2 ***Particle size Distribution***

The particle size distribution is found following BS EN 933-1(BSI, 2012). The test consists of dividing up and separating, by means of a series of sieves, a material into several particle size classifications of decreasing sizes. The aperture sizes and the number of sieves are selected in accordance with the nature of the sample and the accuracy required. The method adopted was dry sieving.

Sample reduction yielded a test portion of mass 10kg. Material was placed into the largest sieve size on the top of the sieving column; the column was then mechanically shaken. The material retained on each sieve was weighed. The results of sieving were then calculated using EN 933-1: (BSI, 1997)

#### 3.3.1.3 ***Normal Proctor Test***

Compaction is the process by which solid particles are packed more closely together, thereby increasing the dry density of the soil. The dry density which can be achieved depends on the degree of compaction applied and the amount of water present in the soil. For a given degree of compaction of a given cohesive soil, there is an optimum moisture content at which the dry density obtained reaches a maximum value.

In order to determine the water content that allows compaction to maximum density, a series of Proctor tests were been carried out. Due to the variable nature of the material being used, the results of the normal Proctor test were inconsistent with those of a more homogeneous material e.g. sand or clay.

The ash was deemed to fit under the classification of '*soils susceptible to crushing*', since the ash being used could be crushed when subject to a sufficient load. The grading obtained previously was used to establish the appropriate specimen preparation technique, using the procedure in Section 3.2.6 of BS EN 1377-4. (BS1, 1990)

The compaction of ash in the Proctor test is achieved using a 2.5kg rammer of 50mm  $\pm$  0.5mm dropped 27 times from a height 300mm. Approximately 2.5 kg of ash is used for each moisture content assessment. Each Proctor test requires 5 different moisture contents. Therefore, approximately 15kg of material was needed for each Proctor test. The quantity of ash required for this type of testing is very high; BS EN 1377-4 states that the aggregate used in the normal proctor test using soils susceptible to crushing shall be discarded after use, as crushing has altered the original properties of the sample.

### 3.4 Rapid Evaluation of Expansion

The aim of this part of the programme was to examine the materials which display the most likely mechanism, or mechanisms, of expansion. As stated in the literature review, IBA can replace primary and secondary aggregates in most applications. (The Highways Agency, 2004) IBA may be used in many road applications. IBA can also be used as an unbound mixture for sub base, in the construction of embankments or as fill. This requires compaction. Figure 2-3 shows expansion under different storage conditions. The test specimen stored in air displayed the most expansion, indicating that access to oxygen is an important factor.

A new test method was created to help establish the expansion properties of the IBA under these conditions. The testing method chosen ensured that the IBA was compacted in contact with various chemical additions and had access to oxygen under different temperatures to create a suitable environment to promote expansion. Sample preparation is outlined further on in this section.

Chemical additions were made to the IBA to promote expansive reactions of various types. The chemicals used were  $\text{Na}_2\text{SO}_4$ ,  $\text{NaOH}$  and  $\text{CaCl}_2$ , these chemicals were added at 5% by mass of the sample. Each sample of ash and chemical addition made up were tested under normal conditions to establish their expansion properties. In addition to this testing, a replica of each specimen was made up, this time with water additions (100% of the as-received moisture content). These specimens were labelled "specimens with added water".

#### 3.4.1 Preparation of Specimens

Compacted cylindrical specimens were prepared with ash provided by Ballast phoenix with and without chemical and water additions. The cylindrical samples were then stored in the environment chambers at 20°C and 40°C. 16 samples of each ash available were prepared. Specimens were labelled in terms of their source (Cleveland = CL, Castle Bromwich = CB), chemical addition (e.g. Sodium Sulphate =  $\text{Na}_2\text{SO}_4$ , Sodium hydroxide =  $\text{NaOH}$  and Calcium Chloride =  $\text{CaCl}_2$ ) temperature

(20°C or 40°C) and whether the sample has any additional water (e.g. S for specimens with added water). Therefore, a sample of Cleveland ash with sodium sulphate addition stored at 20°C with no additional water will be labelled CL Na<sub>2</sub>SO<sub>4</sub> 20, the same sample with water addition water will be labelled CL Na<sub>2</sub>SO<sub>4</sub>20 S.

**Table 3-1 Specimens investigated during the rapid evaluation of expansion testing programme and the labelling system used to identify the specimens.**

Temp. °C	Na <sub>2</sub> SO <sub>4</sub> , g	NaOH, g	CaCl <sub>2</sub> , g	Water		
20	X			No addition	CL Na <sub>2</sub> SO <sub>4</sub> 20	CB Na <sub>2</sub> SO <sub>4</sub> 20
40	X			No addition	CL Na <sub>2</sub> SO <sub>4</sub> 40	CB Na <sub>2</sub> SO <sub>4</sub> 20
20	X			Addition	CL Na <sub>2</sub> SO <sub>4</sub> 20 S	CB Na <sub>2</sub> SO <sub>4</sub> 20 S
40	X			Addition	CL Na <sub>2</sub> SO <sub>4</sub> 40 S	CB Na <sub>2</sub> SO <sub>4</sub> 20 S
20		X		No addition	CL NaOH 20	CB NaOH 20
40		X		No addition	CL NaOH 40	CB NaOH 40
20		X		Addition	CL NaOH 20 S	CB NaOH 20S
40		X		Addition	CL NaOH 40 S	CB NaOH 40 S
20			X	No addition	CL CaCl <sub>2</sub> 20	CB CaCl <sub>2</sub> 20
40			X	No addition	CL CaCl <sub>2</sub> 40	CB CaCl <sub>2</sub> H 40
20			X	Addition	CL CaCl <sub>2</sub> 20S	CB CaCl <sub>2</sub> 20S
40			X	Addition	CL CaCl <sub>2</sub> 40S	CB CaCl <sub>2</sub> 40S
20				No addition	CL Control 20	CB Control 20
40				No addition	CL Control 40	CB Control 40
20				Addition	CL Control 20S	CB Control 20S
40				Addition	CL Control 40S	CB Control 40S

It should be noted that different moisture contents were obtained in several samples due to the nature of the raw materials, for example, material was delivered in 20kg bags, each bag had a different water content and therefore a different addition was required for each to match the as received water content. This was done to ensure that all samples had uniform additions. One option which was investigated was to produce each sample the same water content, however, due to the various nature of the material within the unprocessed IBA this was not achievable. Adding 100% water addition to the as received aggregate was the most uniform method at the time.

To allow the investigation to consider the as-received condition of the ash, the ash was not subject to any drying or treatment before testing began and all aggregate samples were prepared once the raw material was received to ensure no aging could occur. The moisture contents of the batches of ash used for each specimen are shown in Table 3-2. Water additions (100% of the as-received

moisture content) were added to one specimen for each exposure type. These specimens were labelled “specimens with added water”.

**Table 3-2 Water content of samples**

Specimen	Moisture Content, % by mass	
	Clev	CB
Na <sub>2</sub> SO <sub>4</sub> 20	6.22	12.75
Na <sub>2</sub> SO <sub>4</sub> 40	6.22	12.75
Na <sub>2</sub> SO <sub>4</sub> 20 S	12.44	25.50
Na <sub>2</sub> SO <sub>4</sub> 40 S	12.44	25.50
NaOH 20	13.25	8.53
NaOH 40	13.25	8.53
NaOH 20S	26.5	17.06
NaOH 40S	26.5	17.06
CaCl <sub>2</sub> 20	6.41	10.39
CaCl <sub>2</sub> 40	6.41	10.39
CaCl <sub>2</sub> 20S	12.82	20.78
CaCl <sub>2</sub> 40S	12.82	20.78
Control 20	11.95	13.43
Control 40	11.96	13.43
Control 20S	23.92	26.86
Control 40S	23.92	26.86

The cylinder used for the test was a 400mm long PVC pipe with an internal diameter of 150mm. The bottom of the pipe should be closed in such a way that it was water-tight and able to survive the compaction process. This is done with a square plate of PVC welded to the pipe.



**Figure 3-1 Test cylinder**

The top of the pipe was capped with a water-tight end-cap (Figure 3-2).



Figure 3-2 Test cylinder, rubber seal and end cap

The specimen preparation procedure is as follows:

1. Weigh the empty cylinder.
2. Find moisture content of each sample of ash
3. Fill the cylinder with 2.5kg of IBA, or mixture of IBA and any chemical addition required for the test ( $\text{NaSO}_4$ ,  $\text{NaOH}$  or  $\text{CaCl}_2$ ).
4. Compact the material using a Hilti TE76 breaker with a compaction plate attachment of 130mm diameter. The hammer was operated for a period of time such that approximately 23000 J of energy was delivered to the material. The compaction time required is 1 minute per layer.
5. Repeat stages 3-4 two more times such that the cylinder contains 3 layers of compacted material.
6. Secure the end-cap on the cylinder.

The test procedure was as follows:

1. Weigh the cylinder.
2. Remove the end-cap.
3. Using a sounding rod, take four readings on the extremity of the specimen, plus a further four readings distributed over the specimen surface. Fixed points were marked and labelled on the cylinder to ensure the same point was being measured each time.
4. Add the required amount of water to the specimen, replace the cap and leave for precisely 10 minutes.
5. Weigh the cylinder. If the mass of the specimen has dropped, this indicates loss of water from the cylinder by evaporation. In theory this should be very low. However, if this loss exceeds 1g, additional water should be added to make up the difference.
6. Remove the cap and take another measurement, as described in 3.
7. Replace the cap.

8. Repeat 5 to 7 at test ages of 1 hour, 3 hours, 6 hours, 24 hours, and then on a daily basis for the first two weeks and then on a weekly basis for the remainder of the testing period.
9. Expression of expansion was made at the surface of the specimens at 9 fixed points and the result expressed as an average percentage of expansion obtained from the 9 fixed points relative to the original cylinder height.
10. Samples were broken when needed for further testing.

### 3.5 X-Ray Diffraction

X-ray powder diffraction (XRD) is a rapid analytical technique primarily used for phase identification of a crystalline material and can provide information relating to the crystal structure of compounds

Specimen's analysed using X-ray diffraction were dried in a desiccator at 20°C and then ground to a fine powder before being packed into specimen holders and analysed using a Phillips diffractometer with Cu-K $\alpha$  radiation source and a single crystal graphite monochromator. An angular range of 3 - 60°2 $\theta$  in 0.10°2 $\theta$  increments was used throughout.

In the case of the as-received ashes, quantitative analysis was conducted using Reitveld refinement. The non-crystalline materials in the IBA could not be quantified using this technique. However, a 5% (by mass) corundum internal standard was mixed into these specimens to allow quantification of the total amorphous content of each sample.

### 3.6 X-Ray Fluorescence

X-ray fluorescence (XRF) uses the emission of characteristic "secondary" (or fluorescent) X-rays from a material that has been excited by bombarding with high-energy X-rays to determine its chemical composition. The phenomenon is widely used for elemental analysis and chemical analysis, particularly in the investigation of metals, glass, ceramics and building materials.

Powdered specimens were compressed into pellets before being analysed using XRF

### 3.7 pH Testing

pH testing was carried out using a HANNA Pocket pHep5 pH tester. Measurements of the pH were conducted after 1 g of powdered IBA sample was combined with 50g of distilled water. In certain cases, after expansion specimens were broken, liquid was found to have settled within the cylinders. This liquid was collected and also tested for pH.





Figure 3-3 pH test of moisture from a Castle Bromwich Specimen

### 3.8 Microscopic Examination

Microscopic analysis was undertaken using a geological microscope manufactured by Leica. The microscope allowed observation using reflective light. This is where the light shines onto the specimen and reflected back into the lens. The Leica DC 300F (Figure 3-3), was used to see if any expansive products developed in the ash.

#### 3.8.1 Preparation of Samples

When specimens from expansion were broken up, the ash which appeared to be undergoing reactions, e.g. displaying rust formation or other deposits on surfaces, were prepared for the microscope. The ash was impregnated with an epoxy resin. The resin was coloured with Eosine to highlight porosity under the microscope. The ash was placed in a plastic housing and the epoxy resin coating poured onto the sample. The sample was then placed in a vacuum oven where the air was extracted from the specimens and the epoxy resin hardened at 45°C to produce an air free and solid specimen. The solid specimen can be seen in Figure 3-5 and Figure 3-6

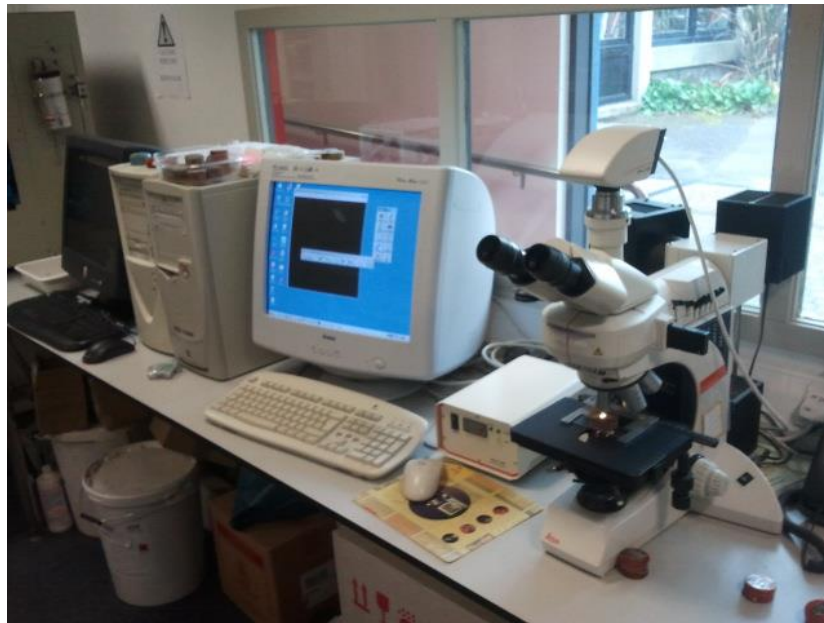


Figure 3-4 Leica DC 300F microscope



Figure 3-5 Ash with epoxy resin coating

After 24 hours when the specimen hardened the plastic housing was removed. The face of the ash and resin specimen was ground and polished for analysis under the microscope, Figure 3-6.



Figure 3-6 Ash sample prepared for microscopic analysis.

### 3.8.2 Magnetic Separation Analysis

The magnetic content of the IBAs was measured because steel and iron particles did not reduce in size during grinding for XRD and XRF analysis, and were not included in these analyses. A bulk sample of ash was subdivided by the quartering method.

1. Empty sample on a hard, clean and smooth surface that is free from cracks. Mix thoroughly and pile in a cone. Materials which tend to segregate should be dampened.
2. Flatten cone with a shovel, spreading the material to a circular layer of uniform thickness. Divide into quarters by two (2) lines intersecting at right angles at the centre of the pile.
3. Discard the two (2) diagonally opposite quarters. Sweep clean the space occupied by the discarded quarters.
4. The remaining quarters should be thoroughly mixed and further reduced by quartering if desired. "Quartering" may be performed any number of times to obtain the required sample size
5. The ash is then weighed and laid out on a flat surface
6. The steel particles were then separated from the ash magnetically.
7. After separation the ash and the steel are separately weighed.

### 3.9 Thermogravimetry

Thermogravimetry involves a continuous recording of mass changes of a sample of material, as a function of temperature. Thermogravimetry was carried out using a Netzsch simultaneous thermal analyser (Figure 3-7).

IBA from cylindrical specimens was crushed and ground in the ball mill to produce a powder. Once ground, a sample of material, approximately 150mg was placed on an arm of the recording microbalance. The microbalance was then moved into a furnace. The furnace temperature is controlled in a pre-programmed temperature/time profile. The atmosphere inside the furnace was a continuously flowing supply of nitrogen. This allows the temperature to be raised without ignition of

the sample. Analysis of materials in this way allowed examination of the thermal decomposition of the samples over a temperature of ambient to 1000°C.



Figure 3-7 Netzsch simultaneous thermal analysis PC

### 3.10 Scanning Electron Microscopy

Scanning electron microscopy uses a focused beam of high energy electrons to generate a variety of signals at the surface of solid specimens. The signals which are obtained from the interaction of the beam and solid surface can be used to generate information relating to the external morphology, chemical composition and crystalline structure of the sample.

The ESEM was used in this study to examine the specimens obtained from testing. The ESEM allows examination of the specimen's microstructure and give information on how the various chemical additions reacted differently. Preparation of samples

To prepare for the test a sample of each of the specimens was placed on a cylindrical aluminium stub of 10 mm diameter. The specimens were attached to the stubs using double coated conductive carbon tape. The tape holds the sample firmly to the surface, Figure 3-8.



**Figure 3-8 Samples for SEM**

Samples were then coated in a thin layer of conducting material, a mixture of gold and palladium. This was necessary due to the nonconductive nature of the specimens. The coating was applied at a thickness of 20 nanometres so as not to interfere with dimensions of the surface features. The coating apparatus is shown in Figure 3-9. After coating in a thin layer of gold and palladium the samples are transferred to the SEM for examination.



**Figure 3-9 Cressington Sputter coater**





Figure 3-10 Environmental scanning electron microscope

### 3.11 Thermal Analysis

One concern relating to the experimental programme was that insufficient reaction products would be present in the specimens deriving from the rapid evaluation of expansion tests to allow them to be identified by chemical analysis.

For this reason, 10g samples of finely ground samples of each IBA were placed in sealed Teflon reaction vessels with an equal mass of water with additions of NaOH and Na<sub>2</sub>SO<sub>4</sub> and stored at 40°C. Because of the higher surface area of these samples, the chemical reactions were anticipated to proceed at a much faster rate leading to higher concentrations of reaction products.

The samples were removed from the conditions of elevated temperature and dried in a desiccator containing silica gel at 20°C. Once dried, the specimens were analysed using thermal analysis (thermogravimetry) and X-ray diffraction

## 4 Results and Discussion

### 4.1 Initial Testing Results

Chapter 4, results and discussion gives the initial testing results which are the characteristics of the IBA being used in this study. The experimental programme results are presented and discussed in detail, beginning with the expansion of the specimens. The influence of the ambient conditions in which the specimens were stored will have an effect on the overall expansion. Each specimen which showed some expansive properties are discussed here. The results are presented individually through the summation of the effect that each chemical addition has on the IBA. For example, rapid expansion results will be categorised by the chemical addition and the effects of the additions will be discussed.

The results of the expansion led to more intensive testing of the IBA. The testing criteria for the purposes of this study were chosen through investigation in the literature review. Testing included, X-ray Diffraction, X-ray fluorescence, magnetic separation analysis, thermogravimetry, Scanning electron microscopy and accelerated chemical reactions were all undertaken to give a better picture of the reactions occurring in the ash when rapid evaluation of expansion had ceased.

#### 4.1.1 Normal Proctor Test

In order to determine the water content that allows compaction to maximum density, a series of Proctor tests were carried out. The IBA was deemed to fit under the classification of '*soils susceptible to crushing*', since the ash being used could be crushed when subject to a sufficient load. The grading obtained previously was used to establish the appropriate specimen preparation technique, using the procedure in Section 3.2.6 of BS EN 1377-4.

The results from the normal Proctor test were inconsistent - A Proctor test should display a curve which initially rises and then falls with water content. The highest point on the curve is the optimum moisture content for the material. In the case of IBA samples, the resulting plot shows a great deal of fluctuation. Due to the difficulties faced in the compaction of the material in question it was difficult to correctly determine the optimum moisture content of the ash for further testing. Figure 4-1 shows a standard Proctor curve for a gravelly soil sample (Virtual Soil lab, 2012). Figure 4-2 and Figure 4-3 show the results for the Cleveland and Birmingham samples respectively.

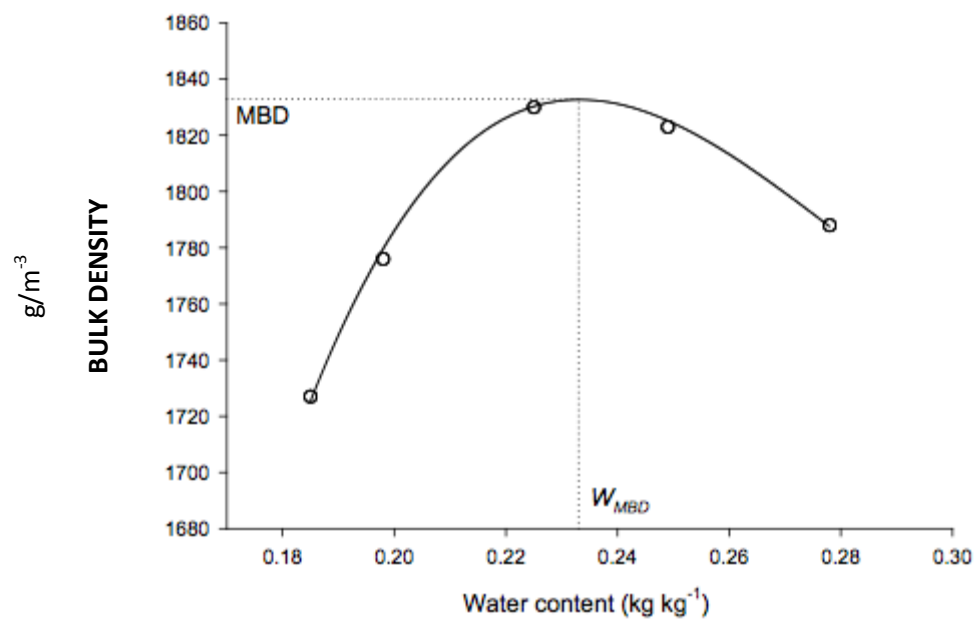


Figure 4-1. Standard Proctor test curve for gravelly soil .

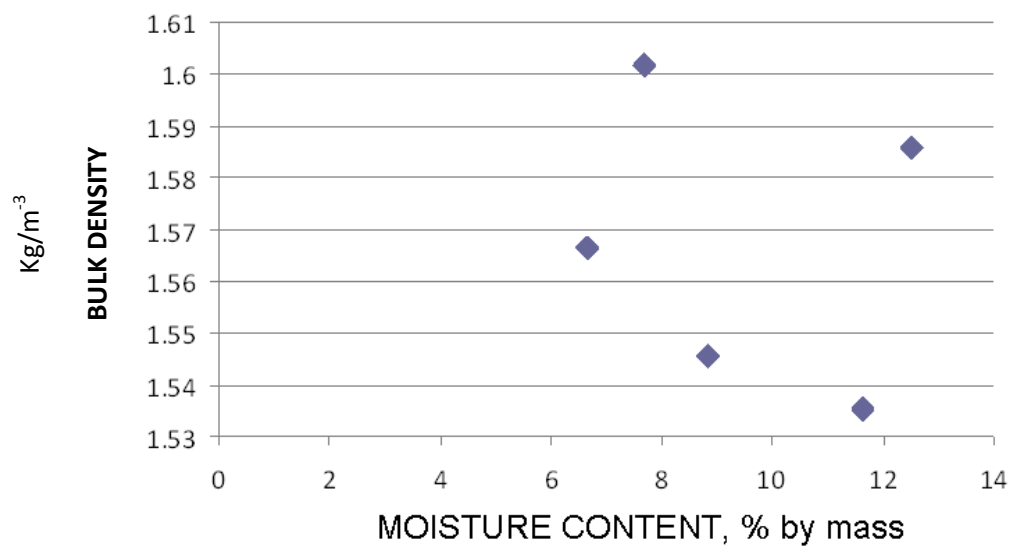


Figure 4-2. Relative Bulk Density from the Cleveland ash.



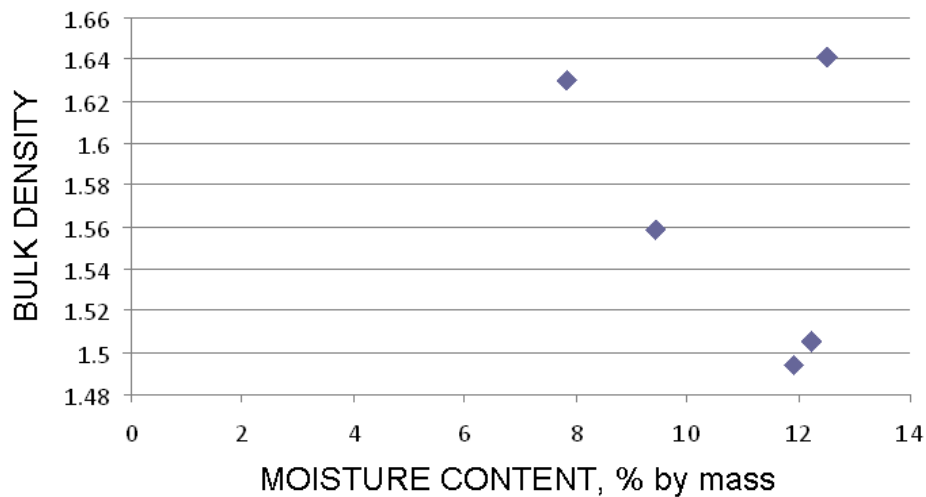


Figure 4-3. Relative Bulk Density from the Birmingham ash.

The most likely reason for the inconsistent results is the lack of control over the composition within each test specimen, meaning that the density of this volume of material varied considerably. A quartering technique was used to obtain a representative sample of the ash. However, it may be that this was not enough to ensure a statistically representative sample. Another possibility is simply that the variation in mechanical properties of the various constituent materials was affecting compaction.

Two options are proposed as a solution to this. Firstly, to address the possibility of inconsistent mechanical properties, a number of trial tests will be attempted with a rammer of higher mass, to establish whether these inconsistencies are reduced when a higher energy impact is involved.

Secondly, it was realised that it might be necessary to assume optimum moisture content based on previous work in the field. A variety of values are presented by different researchers, and therefore the most appropriate course of action was to use the values set out in previous literature. As noted in the Literature review, the optimum moisture content is 14-15%.

#### 4.1.2 Particle Size Distribution

Particle size characterisation was conducted on the IBAs. Particle size distribution was determined by sieving the sample series with aperture sizes ranging from 50mm to 73 $\mu$ m as required by BS EN 933-2.

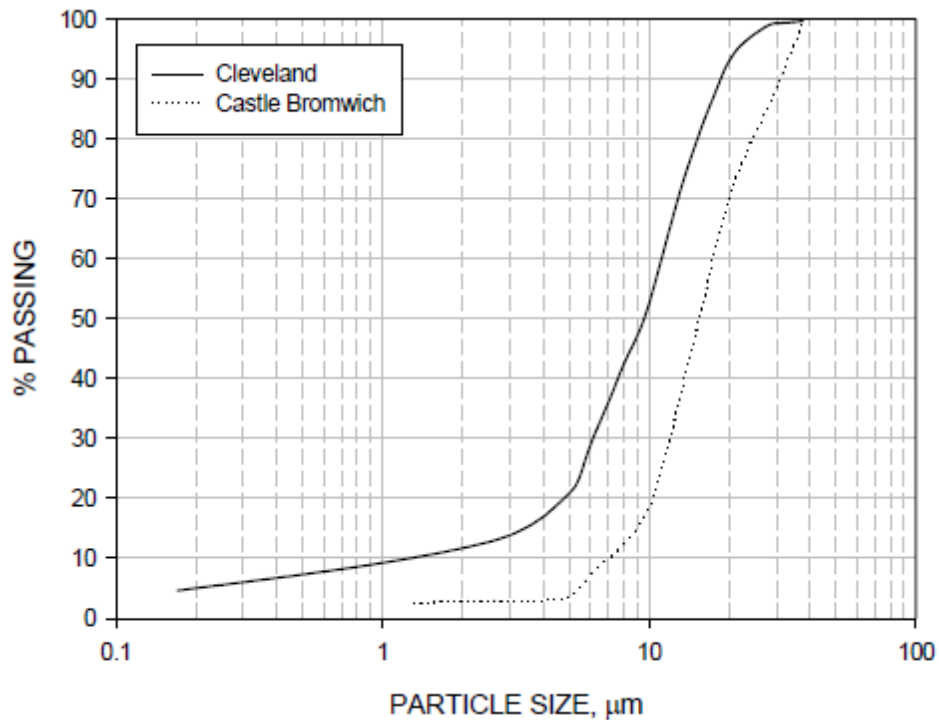


Figure 4-4 PSD comparing both IBAs

Figure 4-4 shows all PSD for both ashes. The Cleveland ash is very similar. However, there is a change in the overall grading of the Castle Bromwich ash though the curve stays on a similar line. This shows that the Cleveland ash contains a larger proportion of finer particles than the Castle Bromwich.

#### 4.1.3 Chemical Composition

Table 4-1 is mean results of samples showing the chemical composition of the as received IBAs. The materials are largely composed of  $\text{SiO}_2$ ,  $\text{CaO}$ ,  $\text{Al}_2\text{O}_3$  and  $\text{Fe}_2\text{O}_3$ . The pH values for the two IBAs were 9.3 and 9.7 for the Cleveland and Castle Bromwich IBAs respectively.

Table 4-1 Major oxide analysis of ash

Constituent	%, by mass	
	Cleveland	Castle Bromwich
CaO	15.20	16.56
SiO <sub>2</sub>	49.22	50.15
Al <sub>2</sub> O <sub>3</sub>	8.96	8.27
Fe <sub>2</sub> O <sub>3</sub>	10.17	5.94
MgO	2.53	2.10
MnO	0.12	0.13
TiO <sub>2</sub>	1.06	0.67
K <sub>2</sub> O	0.92	0.91
Na <sub>2</sub> O	5.20	6.39
P <sub>2</sub> O <sub>5</sub>	0.85	0.85
Cl	0.495	1.083
SO <sub>3</sub>	0.538	0.854
Total	95.263	93.907

#### 4.1.4 Mineralogical Composition

Table 4-2 shows the results of Rietveld refinement of the X-ray diffraction data obtained from the two sources of IBA, plus the proportion of magnetic material from magnetic separation. It can be seen that substantial parts of both materials are either amorphous material (much of which will be largely glass) or metal.

Table 4-2 mineralogical analysis of ash

Mineral	% by mass	
	Cleveland	Castle Bromwich
Quartz	6.5	5.15
Aluminium	0.1	0.1
Hematite	0.2	0.5
Magnetite	0.2	0.4
Dolomite	0.2	0.1
Lead	0.1	0.1
Halite	0.1	0.3
Calcite	2.0	2.4
Microcline	0.2	1.9
Albite	0.8	0.0
Nickel	0.1	0.1
Amorphous	57.0	68.3
Magnetic	35.8	21.1

#### 4.1.5 Magnetic Separation Analysis

Large ferrous articles do not grind up in the ball mill used to prepare specimens for chemical analysis and are set aside. Therefore, magnetic separation was carried out on representative samples of both IBAs. Microscopic analysis highlights the presence of ferrous metals in the ash, see Figure 4-38.

The presence of metals in the IBA is quite high in both ashes, however, Castle Bromwich shows nearly 15% more metallic content than the Cleveland specimen. This may have a bearing on the expansion process through reactions with ferrous and nonferrous metals.

#### 4.2 Swelling Results

Rapid evaluation of expansion measurements are summarised in this section, the aim of this part of the programme was to screen the materials for the most likely mechanism, or mechanisms of expansion. Chemical additions were made to the IBA to promote expansive reactions of various types. The chemicals used  $\text{Na}_2\text{SO}_4$ ,  $\text{NaOH}$  and  $\text{CaCl}_2$  are added at 5% by mass of the sample to encourage reactive properties within the matrix.

Figure 4-5 to Figure 4-16 show the expansion results obtained for specimens containing an addition of 5% by mass of chemicals, for the Cleveland and Castle Bromwich IBAs respectively. These are plotted alongside the results from the control specimens containing no chemical addition. The reactions occurring are not only dependant on the chemical additions but also the amount of moisture present.

Expansion results are shown with percentage of expansion of the material plotted against time. The various chemical additions are examined, with the specimens of 20 and 40°C plotted against each other as well as the control specimens of 20 and 40°C. Specimens with additional water are also examined once again using control specimens to compare expansion.

The percentage of expansion of the material within the expansion cylinder can be seen to vary between 0 – 2%. In a wholly confined environment, as would be the case in a real civil engineering application, expansion as a result of relaxation would not be observed, since the material would be wholly confined. On site, material is compacted in several layers at optimum moisture content. Additionally, relaxation would most likely occur on site relatively rapidly and before any subsequent construction activity takes place. Samples which did show expansion in excess of 1% linear strain through gel formation had been subjected to high pH conditions intended to promote a reaction. Most IBAA applications would not expose IBAA to the high pH conditions necessary for this reaction, for this reason expansion cannot be deemed to be significant and would not affect material which would be used in real applications.

As a result of this, in very large volumes of ash, overall expansion is likely to be very low, since localised expansion will be dissipated throughout the rest of the volume. Thus, in most instances, it is likely that the risk of expansion of IBA is remote.

#### 4.2.1 Specimens Containing $\text{Na}_2\text{SO}_4$

##### 4.2.1.1 *Cleveland*

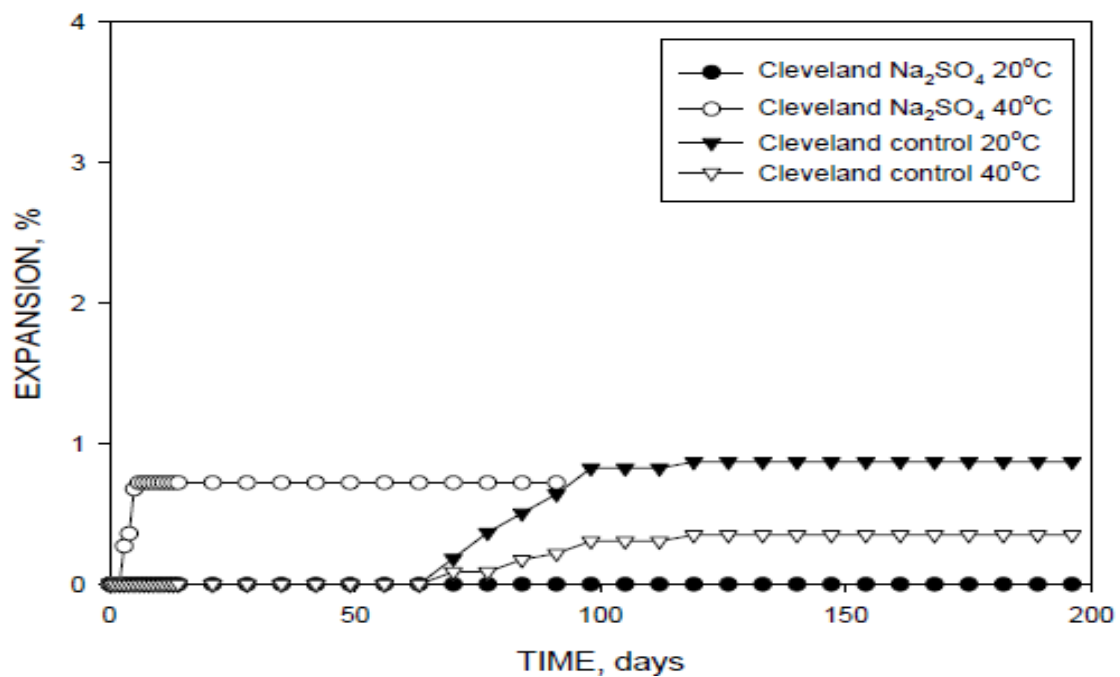


Figure 4-5 Expansion measurements taken from Cleveland IBA specimens containing  $\text{Na}_2\text{SO}_4$

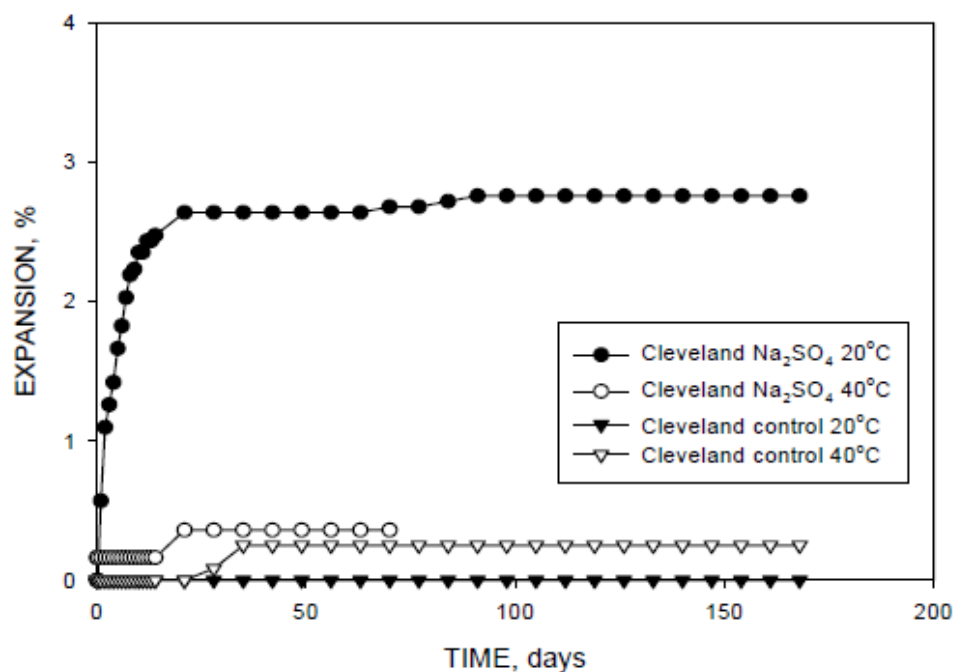


Figure 4-6 Expansion measurements taken from Cleveland IBA specimens containing  $\text{Na}_2\text{SO}_4$  with additions of water

#### 4.2.1.2 *Castle Bromwich*

In Cleveland specimens seen in Figure 4-7, expansion is observed in all specimens. Figure 4-8 shows the effect of Saturation on the specimens.

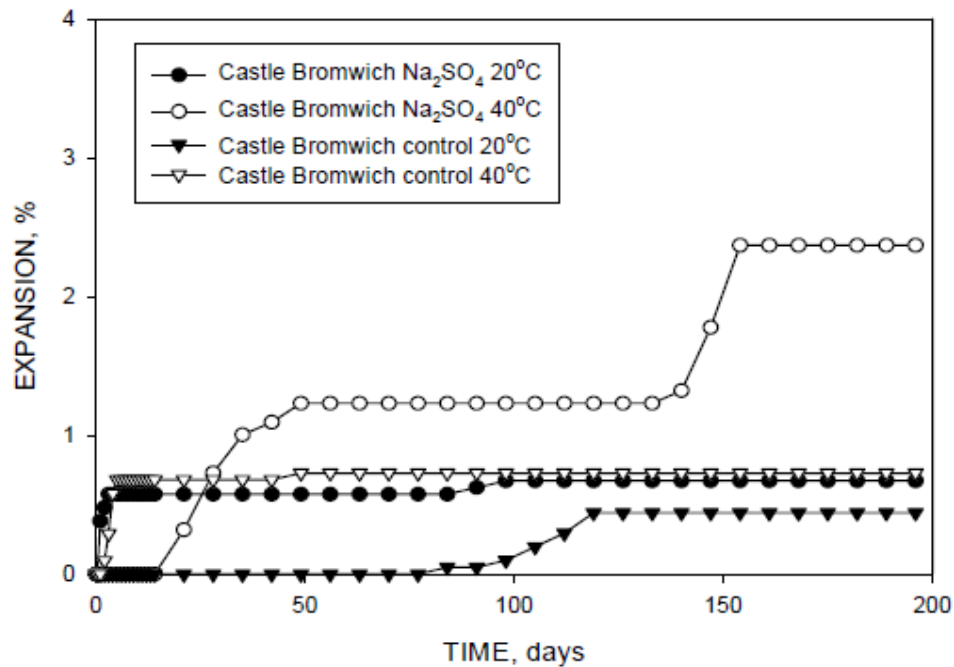


Figure 4-7 Expansion measurements taken from Castle Bromwich IBA specimens containing Na<sub>2</sub>SO<sub>4</sub>

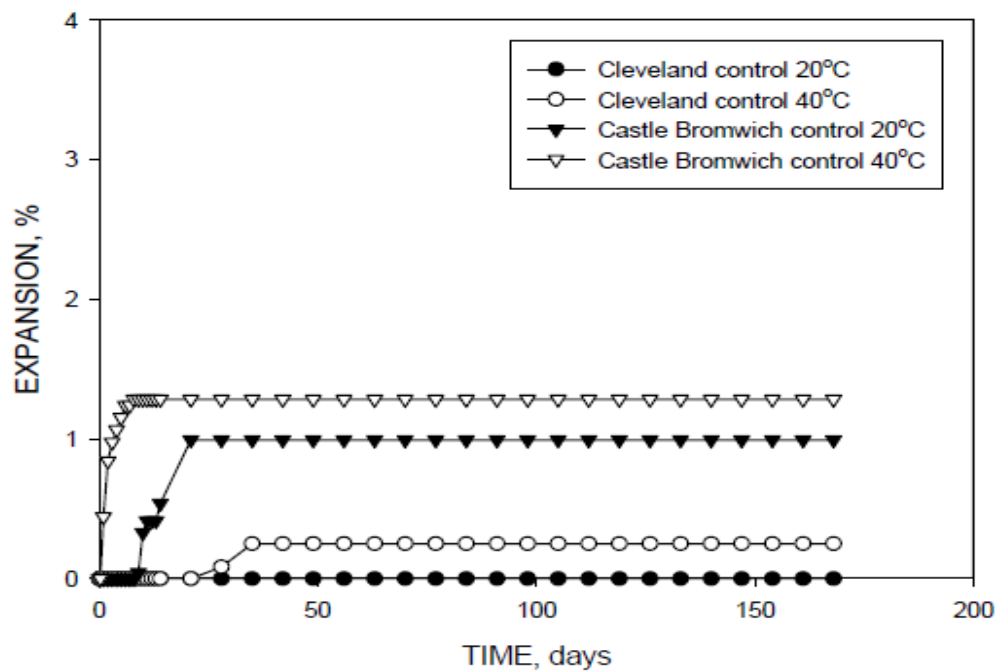


Figure 4-8 Expansion measurements taken from control Castle Bromwich and Cleveland IBA specimens.

## 4.2.2 Specimens Containing NaOH

### 4.2.2.1 Cleveland

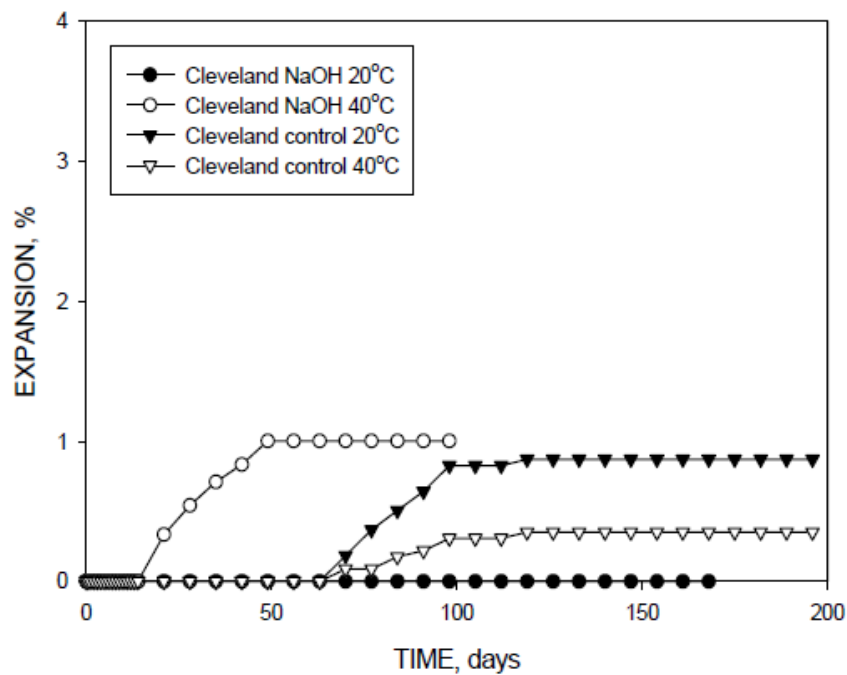


Figure 4-9 Expansion measurements taken from Cleveland IBA specimens containing NaOH

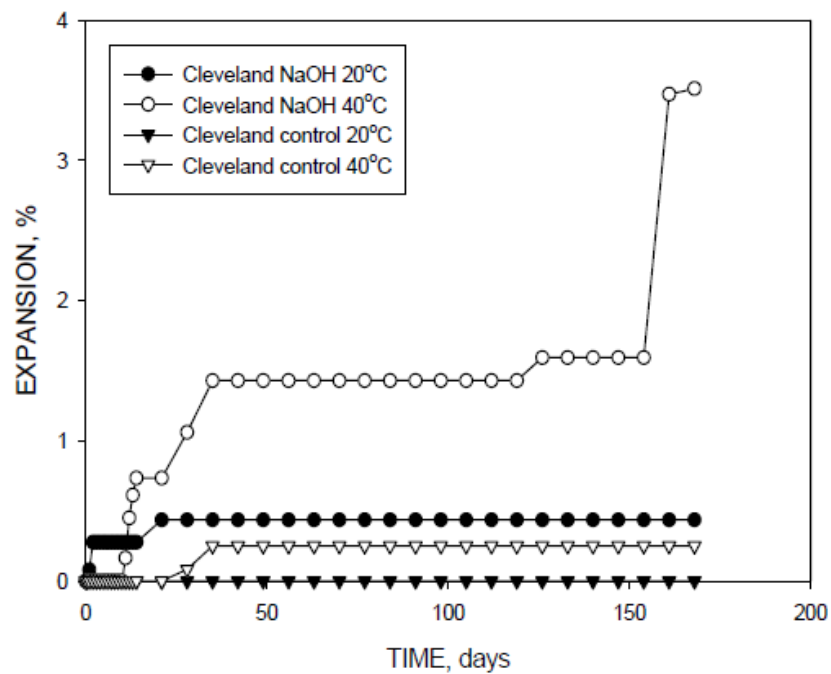


Figure 4-10 Expansion measurements taken from Cleveland IBA specimens containing NaOH with additions of water.

#### 4.2.2.2 *Castle Bromwich*

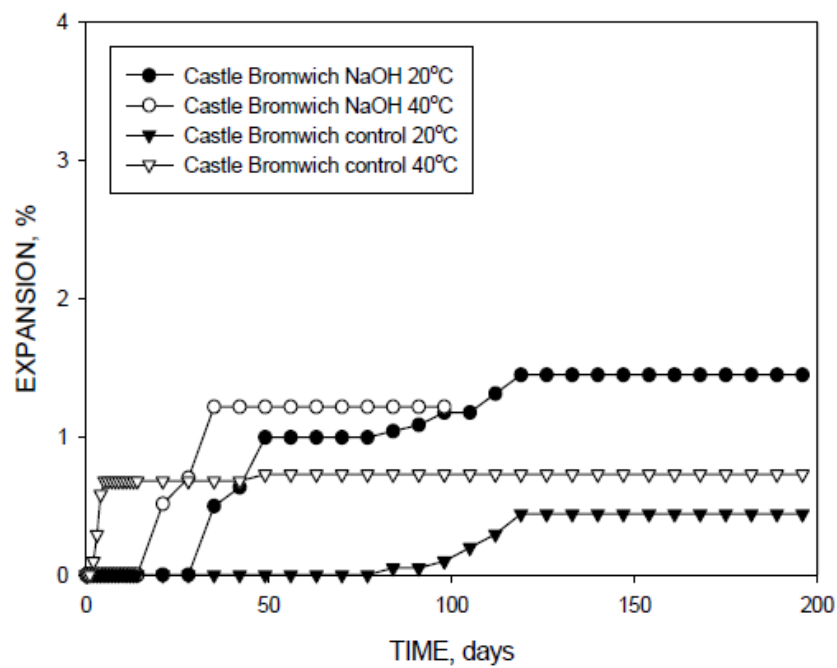


Figure 4-11 Expansion measurements taken from Castle Bromwich IBA specimens containing NaOH

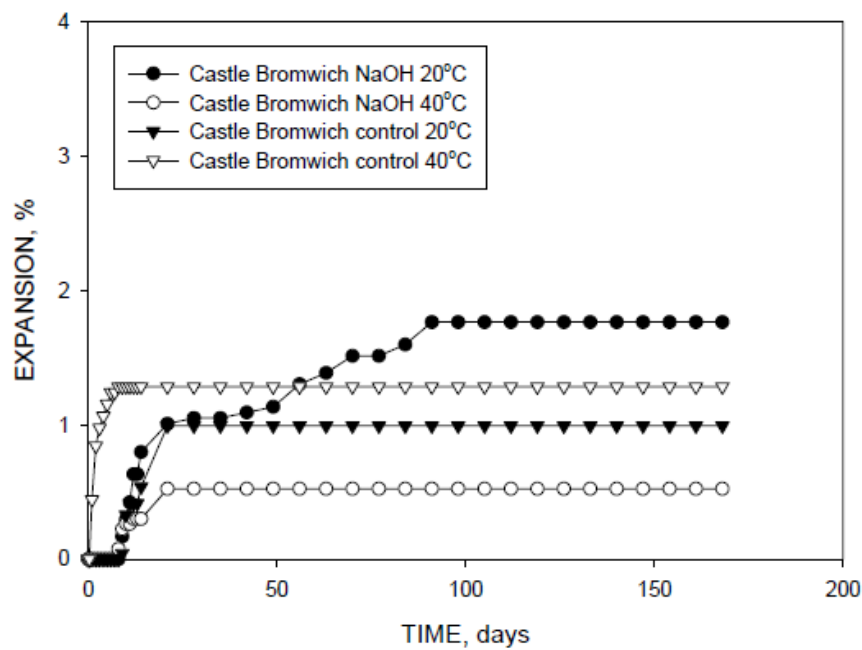


Figure 4-12 Expansion measurements taken from Castle Bromwich IBA specimens containing NaOH with additions of water



### 4.2.3 Specimens Containing $\text{CaCl}_2$

The addition of  $\text{CaCl}_2$  into aggregate was done to establish whether the formation of corrosion products on particles of ferrous metal in the IBA s could be a source of expansion. The mechanism of expansion in specimens containing  $\text{CaCl}_2$  is investigated further during chemical analysis in 4.3.3

#### 4.2.3.1 Cleveland

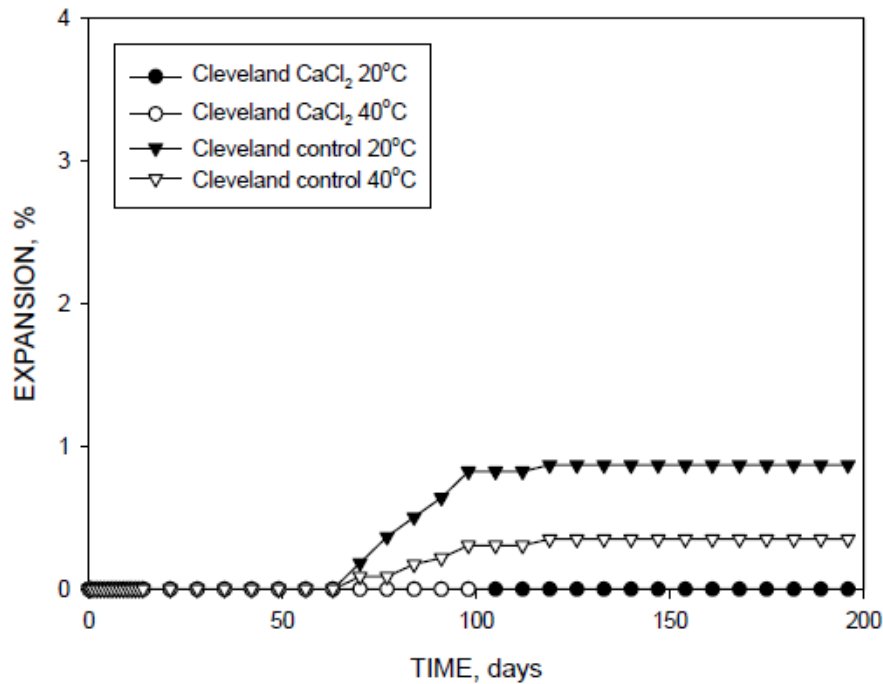


Figure 4-13 Expansion measurements taken from Cleveland IBA specimens containing  $\text{CaCl}_2$

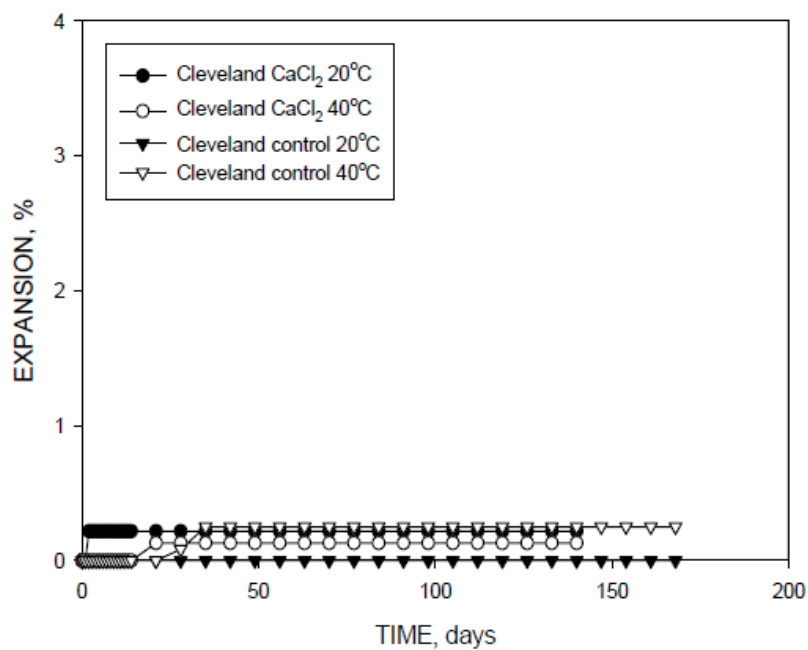


Figure 4-14 Expansion measurements taken from Cleveland IBA specimens containing  $\text{CaCl}_2$  with additions of water

#### 4.2.3.2 *Castle Bromwich*

Figure 4-15 Expansion measurements taken from Castle Bromwich IBA specimens containing  $\text{CaCl}_2$  and Figure 4-16 Expansion measurements taken from Castle Bromwich IBA specimens with added water containing  $\text{CaCl}_2$  show expansion in the Castle Bromwich specimens with the addition of  $\text{CaCl}_2$ .

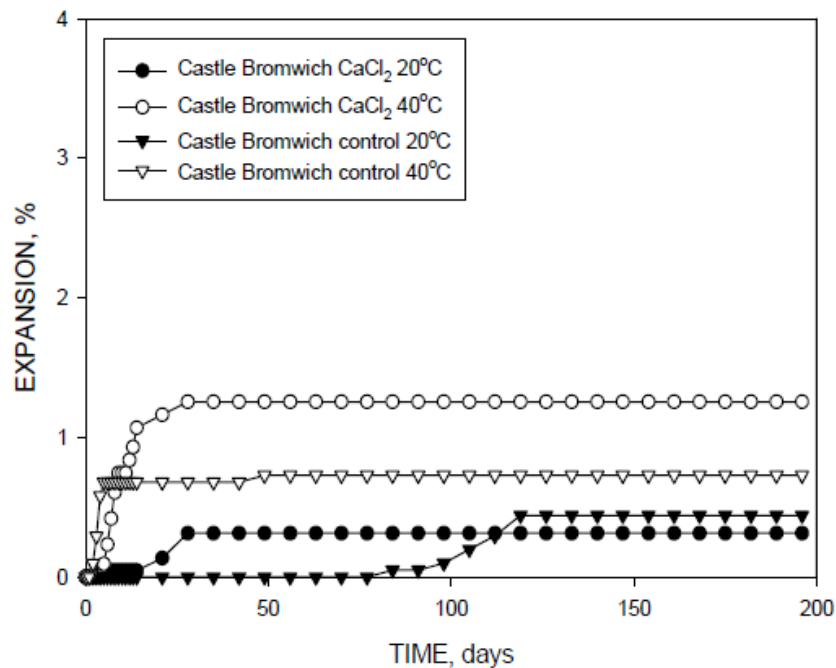


Figure 4-15 Expansion measurements taken from Castle Bromwich IBA specimens containing  $\text{CaCl}_2$

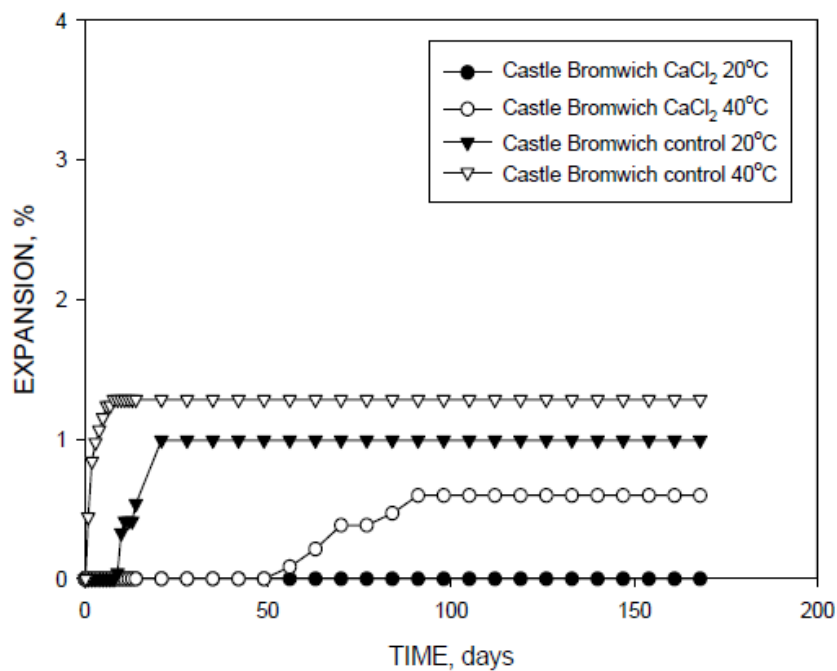


Figure 4-16 Expansion measurements taken from Castle Bromwich IBA specimens with added water containing  $\text{CaCl}_2$

#### 4.2.4 Specimens Containing no Chemical Addition (Control)

Figure 4-17 Expansion measurements taken from control Castle Bromwich and Cleveland IBA specimens and Figure 4-18 Expansion measurements taken from control Castle Bromwich and Cleveland IBA specimens show expansion in the Cleveland specimens with no chemical additions, i.e. the control specimens.

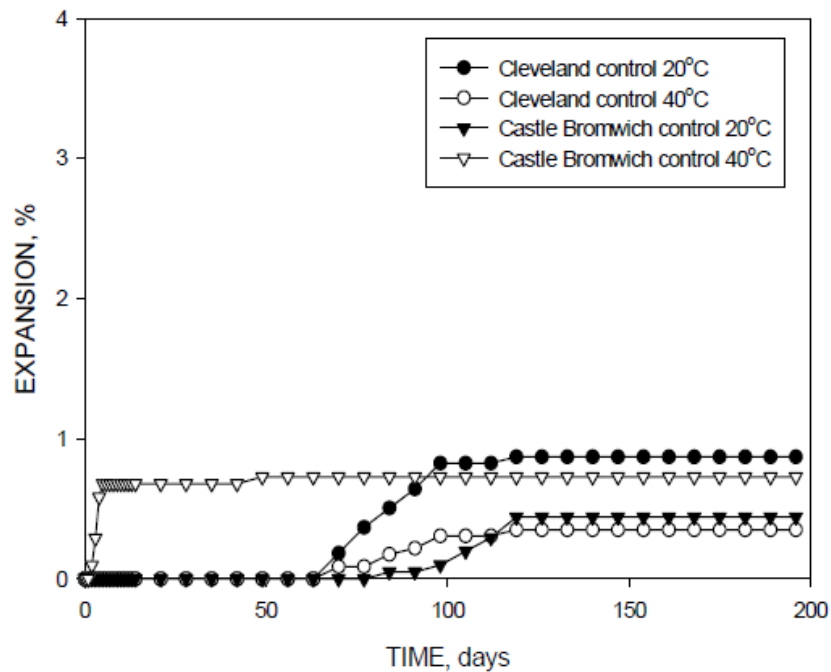


Figure 4-17 Expansion measurements taken from control Castle Bromwich and Cleveland IBA specimens

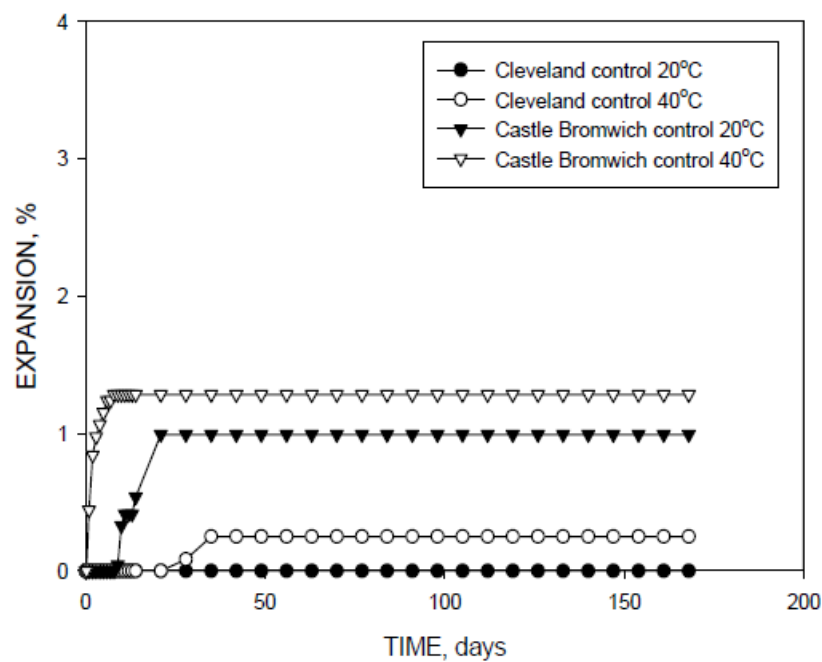


Figure 4-18 Expansion measurements taken from control Castle Bromwich and Cleveland IBA specimens with the additional water.

#### 4.2.5 Discussion of Rapid Evaluation of Expansion Test Results

Before examining the detail of the results obtained, it is worth noting that some variability is evident in the results. Thus, whilst examples of consistent patterns can be identified, there are also instances where uncharacteristic behaviour is observed. Thus, ultimately the overall trends observed are of greater value in interpreting the results. Table 4-3 Summary of Expansion shows the specimens which showed expansive properties; the same labelling applies as stated in Table 3-1 applies.

**Table 4-3 Summary of Expansion**

Chemical Addition	Temperature (°C)	Cleveland	Castle Bromwich
Na <sub>2</sub> SO <sub>4</sub>	20	-----	-----
	40	Expansion	Expansion
	20S	-----	Expansion
	40S	-----	Expansion
NaOH	20	-----	Expansion
	40	Expansion	Expansion
	20S	-----	Expansion
	40S	Expansion	Expansion
CaCl <sub>2</sub>	20	-----	Expansion
	40	-----	-----
	20S	Expansion	Expansion
	40S	Expansion	-----
Control	20	Expansion	Expansion
	40	Expansion	Expansion
	20S	-----	Expansion
	40S	Expansion	Expansion

##### 4.2.5.1 Na<sub>2</sub>SO<sub>4</sub>

For the Cleveland measurements shown in Figure 4-5, expansion is observed in three specimens, CL Na<sub>2</sub>SO<sub>4</sub> 40, CL Control 20 and CL control 40. Both control specimens have expanded as well as CL Na<sub>2</sub>SO<sub>4</sub>. Figure 4-6 shows the effect of water additions on the specimens. Where water is added, and the results are similar, except that CL Na<sub>2</sub>SO<sub>4</sub> 20 S has expanded considerably.

The early reaction of CL Na<sub>2</sub>SO<sub>4</sub> was thought to be related to ettringite formation but after no expansion occurred prior to day 7 it was concluded that the rapid early expansion may have been the result of relaxation of the compacted material – particles near the surface which are under strain from the compaction process are ‘popping’ out. Similar pop outs can also be seen in the early stages of other specimens.

While earlier expansion may be attributed to pop outs, the continuing expansion in the latter stages of testing has indicated that some form of expansion has occurred. The reason for this is unclear, and should be stressed that the results show a lack of consistency which would point to an underlying mechanism. Thus, it suggests that this result of the localised presence of a particularly expansive material which is not present in other specimens.

In the case of the Castle Bromwich specimens (Figure 4-7 and Figure 4-8), significant expansion is mainly observed just for the higher temperature specimen with no added water (CB Na<sub>2</sub>SO<sub>4</sub> 40) and both lower and higher temperature control where water is added (CB Na<sub>2</sub>SO<sub>4</sub> 20 S/40 S). It should also be noted that the lower temperature continued to expand slowly throughout. Compared to control specimens, expansion of the Na<sub>2</sub>SO<sub>4</sub> samples occurs early on in specimens with and without water. The control aggregate begins to expand later on (63 days) for both unsaturated sample and continues steadily, this coincides with the continued expansion of specimens with chemical addition in the unsaturated specimens.

#### 4.2.5.2 **NaOH**

Figure 4-9 and Figure 4-10 show expansion in the Cleveland specimens exposed to NaOH. CL NaOH 20 does not expand whatsoever. However, CL NaOH 40 shows very rapid reactions between day 14 and 49 when expansion ceases completely. The reactive pattern as seen in Figure 4-9 of CL NaOH 40 and CL control specimens is very similar although at a different timescale, this may suggest that NaOH addition has accelerated the expansion of the Cleveland IBA. However, such an effect is absent in the CL NaOH 20 and CL Control 20 samples.

The Cleveland and NaOH specimens exposed to additional water have reacted similarly to the unsaturated specimens, Figure 4-10. CL NaOH 20 S has expanded slightly but again the 40 °C Cleveland specimen, CL NaOH 40 S, shows the highest level of expansion. The initial expansion in this specimen occurs on day 10 and continues gradually until day 35 when expansion was thought to have ceased. However, expansion began to reoccur on 126 days and increased rapidly thereafter. The early expansion strongly suggests that alkali-silica reaction was occurring as the shape of the curves from each 40° CL specimen is highly characteristic of this reaction, which normally goes through a dormant period during which the gel is formed by the reaction expands outwards into the pores of the material. Expansion does not start until the expansive stresses sufficient to disrupt the consolidated material are developed.

Figure 4-11 and Figure 4-12 show expansion in the Castle Bromwich specimens exposed to NaOH. All Castle Bromwich specimens containing NaOH expanded early on in testing. Specimens with no additional water (Figure 4-11) showed early rapid expansion at day 6 for CB NaOH 20 and day 11 for CB NaOH 40. This observation is of interest, because the magnitude of expansion is greater at lower temperatures, which would not be the normal expectation.

A similar pattern can be seen in the specimens with added water - early expansion in both NaOH specimens. However, the specimens with added water display a higher level of expansion with CB NaOH 20 S expanding throughout the first 77 days until expansion ceases. By the end of the testing programme, the specimens with higher water contents had expanded more than the specimens with no added water.

#### 4.2.5.3 ***CaCl<sub>2</sub>***

Figure 4-13 and Figure 4-14 show expansion in the Cleveland specimens exposed to CaCl<sub>2</sub>. For specimens without additional water, expansion did not occur at all.

The specimens with added water only expanded slightly with CL CaCl<sub>2</sub> 20 S expanding on day 1, CL CaCl<sub>2</sub> 40 S expanded on day 14. Expansion then ceased for the remainder of the testing period.

Figure 4-15 and Figure 4-16 show expansion in the Cleveland specimens exposed to CaCl<sub>2</sub>. Expansion is displayed by both CB CaCl<sub>2</sub> 20 and CB CaCl<sub>2</sub> 40 specimens. Limited expansion is seen in the CB NaOH 20 specimen and the final expansion is less than the control specimen. The 40°C specimen with additional water does not expand to the same degree; the specimen containing additional water takes longer to expand than the unsaturated specimen.

#### 4.2.5.4 ***Specimens Containing no Chemical Addition (Control)***

Figure 4-17 shows the expansion of unsaturated control specimens. It can be seen that CB Control 40 expands in the first four days, while Castle Bromwich 20° did not expand until day 77. CL control 20 and CL control 40 did not expand until day 70.

Figure 4-18 shows the Expansion measurements taken from control Castle Bromwich and Cleveland IBA specimens containing additional water. The results of which are the most consistent of all combinations. The Castle Bromwich aggregate CB Control 20 S and CB Control 40 S expand early on, at day 9 and day 1 respectively.

#### 4.2.6 **Summary of Expansion**

It is evident that whilst expansion is observed in many specimens, there is an absence of consistent behaviour with respect to the effect of chemical additions and test temperature. For this reason, it is useful to examine the results in a broader manner. Figure 4-19 plots the full range and average values obtained from the expansion testing for different chemical exposures. Some caution should be used in interpreting this information, since taking an average from the results where other conditions were significantly different will not produce a wholly representative result. However, examining the plot indicates that it would appear that NaOH has the largest impact on expansion, followed by Na<sub>2</sub>SO<sub>4</sub>, with the controls and showing only very small levels of average expansion for CaCl<sub>2</sub> and the controls. It should also be stressed that average levels of expansion are relatively small in all cases.

Figures Figure 4-20 and Figure 4-21 plot average expansion values with respect to temperature and moisture content show very little difference, indicating that these parameters have little influence over expansion.

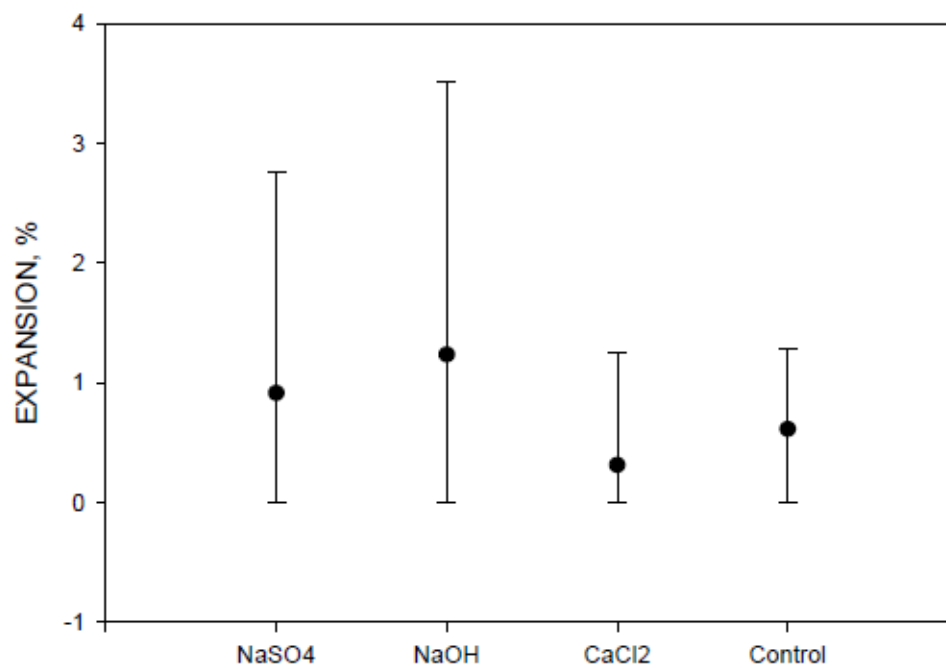


Figure 4-19 Ranges and average expansion values for different types of chemical exposure

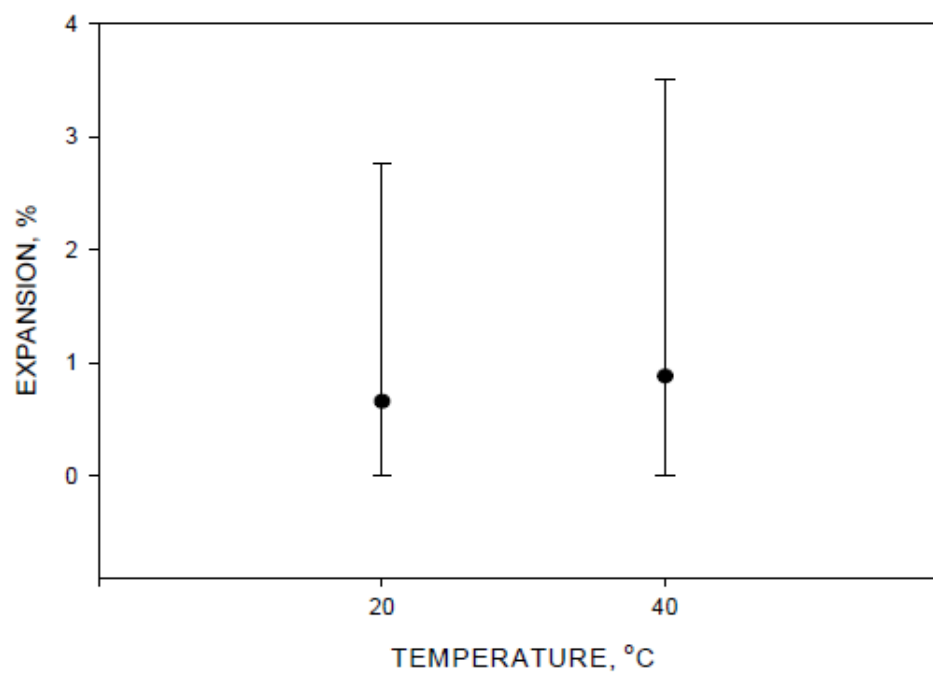


Figure 4-20 Ranges and average expansion values for different test temperatures.

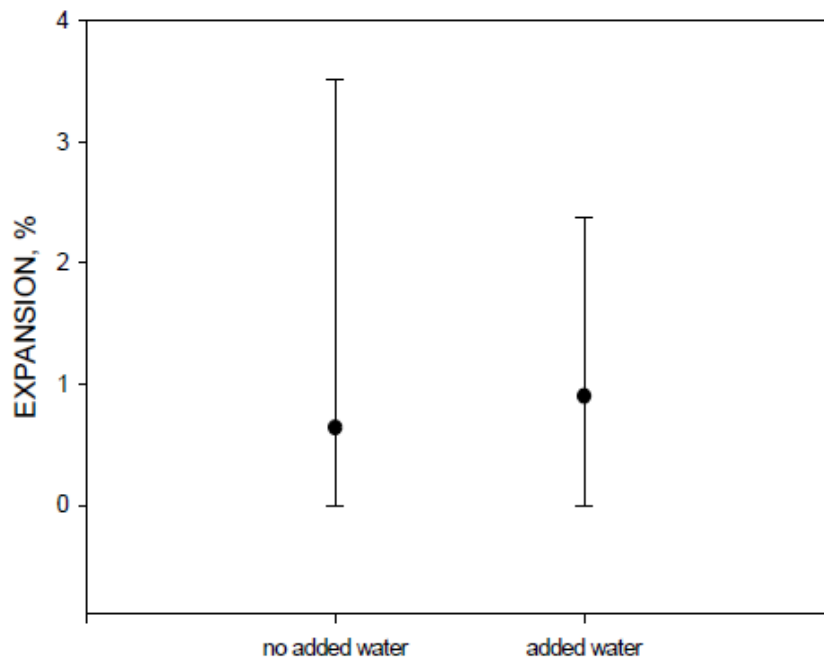


Figure 4-21 Ranges and average expansion values for different moisture conditions.

### 4.3 X-ray Diffraction

X-Ray diffraction analysis was focused on specimens who showed significant expansion. Results of XRD are shown with the reactive specimen shown above the original ash. This is done to highlight the main differences between specimens in a clear manner. A reoccurring trend can be seen in most specimens that were analysed. A broad 'hump' in the background of the traces and a major peak at  $26.7^\circ 2\theta$ . The hump indicates the presence of amorphous phases in the form of glass and possibly amorphous reaction products, such as gels. The peak is quartz.

#### 4.3.1 Specimens Containing $\text{Na}_2\text{SO}_4$

##### 4.3.1.1 *Cleveland*

Figure 4-22 shows CL  $\text{Na}_2\text{SO}_4$  20 S. comparing the original as received ash (CL Original) and ash exposed to  $\text{Na}_2\text{SO}_4$  at  $20^\circ$  with additional water. The main phases highlighted here are calcium oxide and calcite, calcium oxide is usually made by the thermal decomposition of materials such as limestone, which contains calcium carbonate ( $\text{CaCO}_3$ , or calcite). This is accomplished by heating the material to above  $825^\circ\text{C}$ , a process called calcination or lime-burning, to liberate a molecule of carbon dioxide ( $\text{CO}_2$ ). This leaves Calcium dioxide, also known as lime. The lime is not stable and, when cooled, will spontaneously react with  $\text{CO}_2$  from the air until it is completely converted back to calcium carbonate.



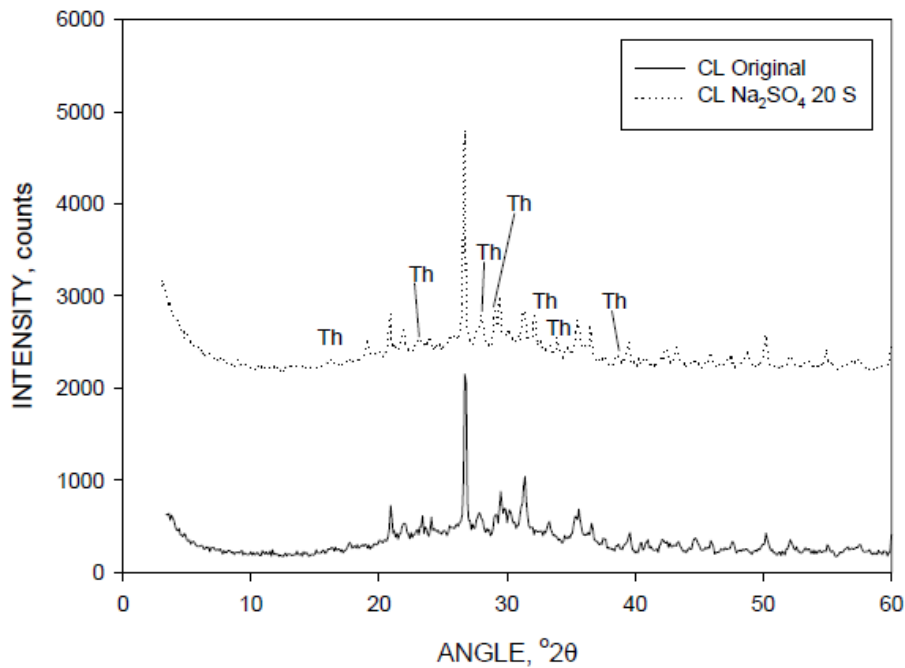


Figure 4-22 X-ray diffraction traces from the Cleveland ash before and after exposure to  $\text{Na}_2\text{SO}_4$  20 with added water. Th = Thernardite ( $\text{Na}_2\text{S}_{04}$ )Castle Bromwich

#### 4.3.1.2 *Castle Bromwich*

The Castle Bromwich specimen which expanded significantly is CB  $\text{Na}_2\text{SO}_4$  40 (Figure 4-23). In this case the  $\text{Na}_2\text{SO}_4$  has clearly reacted in some manner, since there is no evidence of this compound. However, there is little evidence of any crystalline hydration products. There is, however, evidence of the dissolution of some of the original constituents, namely the feldspar compounds and possibly some calcite. As for the accelerated chemical reaction study, the amorphous 'bump' is more pronounced in the reacted specimen relative to the original. This is discussed in further detail at the end of this section.

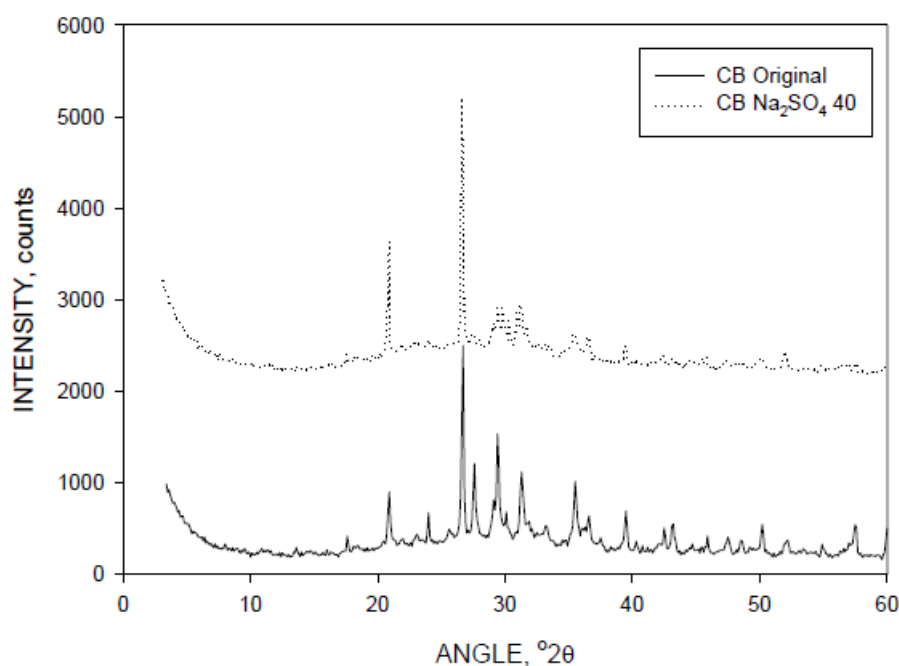


Figure 4-23 X-ray diffraction traces from the Castle Bromwich ash before and after exposure to  $\text{Na}_2\text{SO}_4$  40°C

#### 4.3.2 Specimens Containing NaOH

##### 4.3.2.1 *Cleveland*

The main component of CL NaOH 40 ash is the presence of aluminium hydroxide ( $\text{Al}(\text{OH})_3$ ), mainly in the form of bayerite (Figure 4-24). The formation of bayerite is likely to originate from the reaction of aluminium metal. Initially aluminium hydroxide gel will be formed which will ultimately convert to crystalline forms of aluminium hydroxide. This mirrors the observations made during the accelerated chemical reactions study previously discussed in Section 4.2

The XRD analysis also indicates the presence of small quantities of a hydrated aluminosilicate phase cancrinite ( $\text{Na}_6\text{Ca}_2((\text{CO}_3)_2\text{Al}_6\text{Si}_6\text{O}_{24}) \cdot 2\text{H}_2\text{O}$ ). This indicates some form of interaction between the products of the reaction of aluminium and silicates, probably deriving from the reaction of glass and similar substances in the alkaline conditions.

Figure 4-25 shows the XRD trace from CL NaOH 40 S. Cancrinite is again present. Additionally, small quantities of calcium aluminates are present, which reflects the results of the accelerated chemical reactions study.

Figure 4-26 shows the XRD trace for CB NaOH 20. Ettringite ( $\text{Ca}_6\text{Al}_2(\text{SO}_4)_3(\text{OH})_{12} \cdot 26\text{H}_2\text{O}$ ) has been formed as a result of the reactions of aluminium, soluble forms of calcium in the ash and hydroxide ions. This result also mimics the findings of the accelerated chemical reactions study. In this case, the reaction has not progressed as far as the accelerated reactions, since only the presence of ettringite is clearly evident, and this compound will always appear before other calcium aluminate hydrates, due to its greater stability. The presence of bayerite provides further evidence of the reaction of aluminium.

Figure 4-27 shows the XRD trace from CB NaOH 40. Again, aluminium hydroxide is present, but in this instance the range of phases is more diverse – bayerite is detected along with gibbsite. There is possibly also a small quantity of nordstrandite.

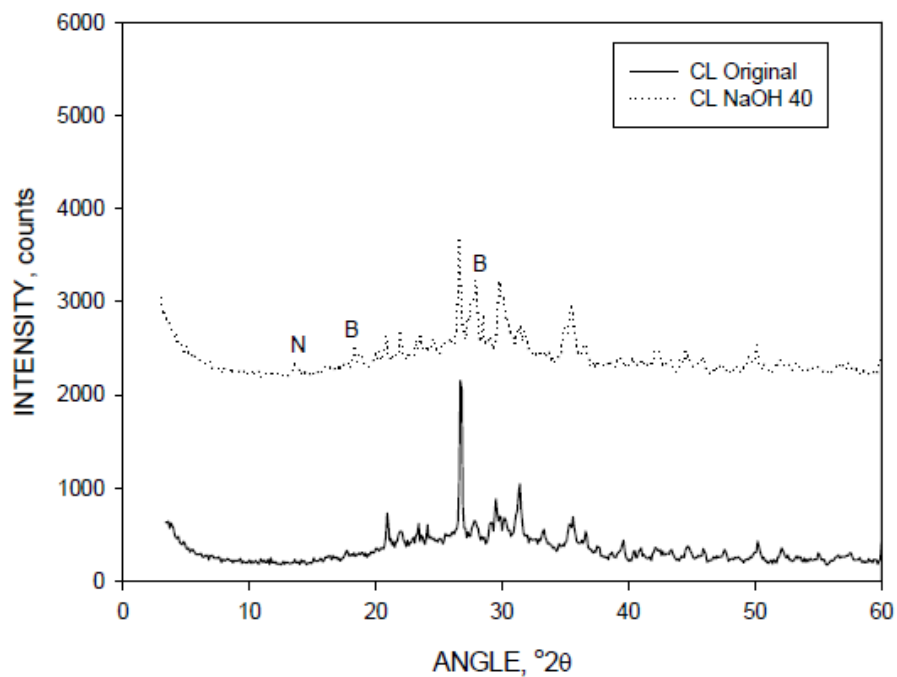


Figure 4-24 X-ray diffraction traces from the Cleveland ash before and after exposure to NaOH at 40°C. N = cancrinite; B = bayerite.

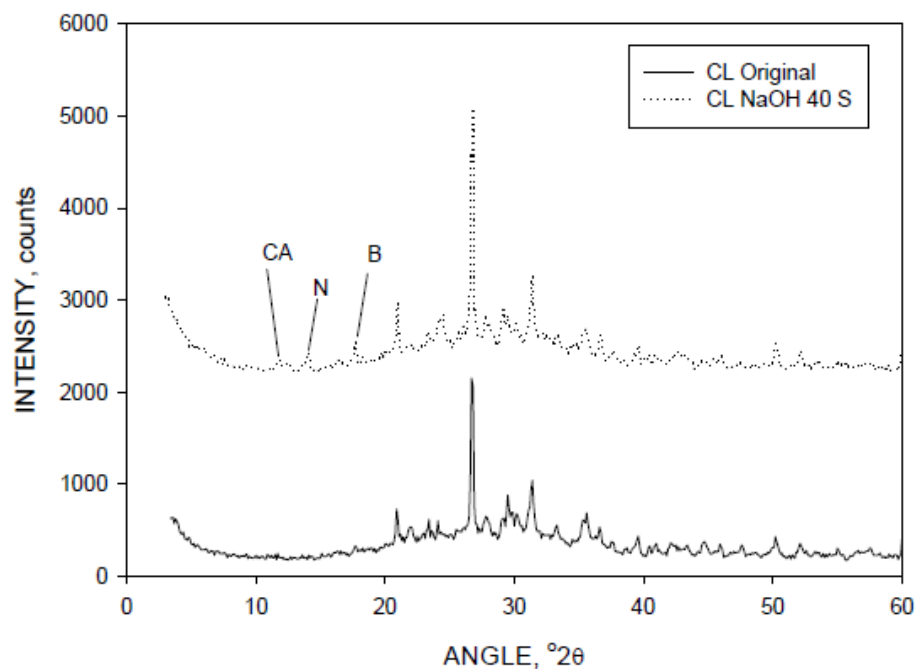


Figure 4-25 X-ray diffraction traces from the Cleveland ash before and after exposure to NaOH with added water. N = cancrinite; B = bayerite; CA = calcium aluminates

The trace in this case looks significantly different from the 'original' trace. This is not entirely the result of the presence of reaction products – some of the compounds present must have been present prior to testing and highlight the potential for specimen variability. These compounds are mullite and tridymite (high temperature polymorphs of quartz) and indicate the presence of fired clay ceramic- type materials in the specimen.

The XRD trace from CB NaOH 20 S (Figure 4-28) shows similar crystalline reaction products to previous Castle Bromwich specimens exposed to NaOH – gibbsite, cancrinite and calcium aluminates

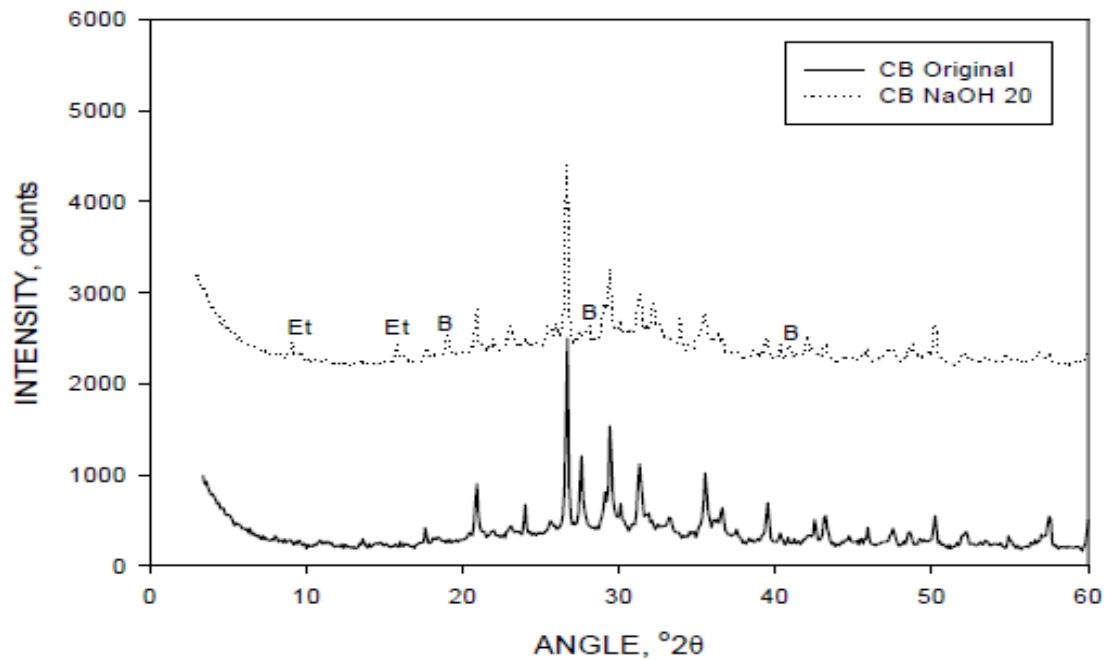


Figure 4-26 X-ray diffraction traces from the Castle Bromwich ash before and after exposure to NaOH at 20°C. Et = ettringite; B = bayerite.

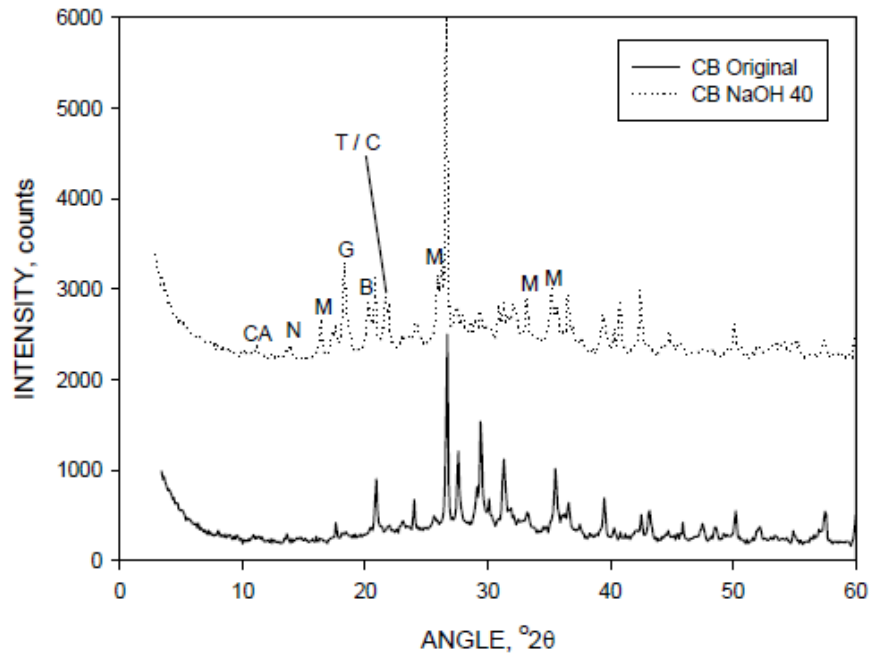


Figure 4-27 X-ray diffraction traces from the Castle Bromwich ash before and after exposure to NaOH at 40°C. CA = calcium aluminate; N = cancrinite; M = mullite; G = gibbsite; B = bayerite; T = tridymite; C = cristobalite.

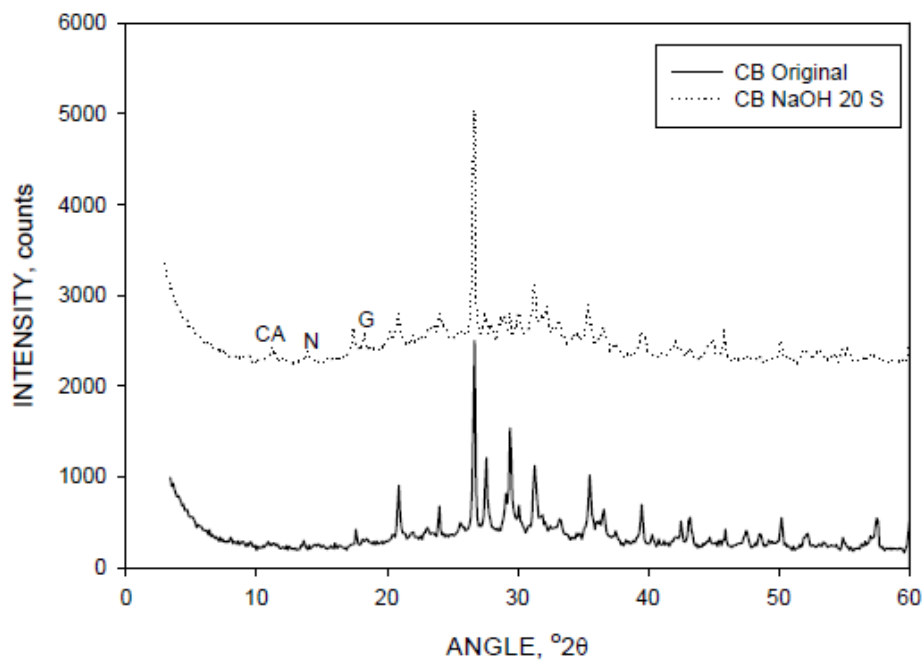


Figure 4-28 X-ray diffraction traces from the Castle Bromwich ash before and after exposure to NaOH at 20°C with added water. Ca = calcium aluminates; N = cancrinite; G = gibbsite

### 4.3.3 Specimens Containing $\text{CaCl}_2$

#### 4.3.3.1 *Castle Bromwich*

The XRD trace from CB  $\text{CaCl}_2$  40 (Figure 4-29) also indicates the formation of a calcium aluminate hydrate phase. Whilst this compound was not observed in any great quantities in the accelerated

chemical reaction study for the Castle Bromwich IBA, it was seen in the Cleveland specimen. Again, its formation can be attributed to reactions of aluminium metal.

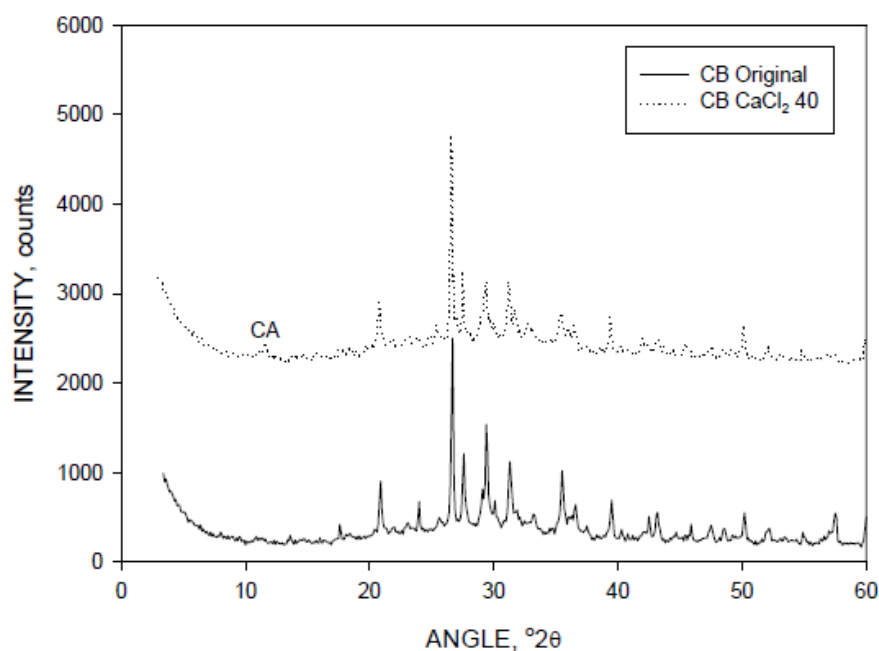


Figure 4-29 X-ray diffraction traces from the Castle Bromwich ash before and after exposure to  $\text{CaCl}_2$  at  $40^\circ\text{C}$

#### 4.3.4 Specimens Containing No Chemical Addition (Controls)

Bayerite was the only crystalline reaction product present in the Cleveland control after storage at  $20^\circ\text{C}$  (Figure 4-30)

The XRD trace from CB control 20 S (Figure 4-31) shows small quantities of calcium aluminate hydrates and possibly an even smaller quantity of bayerite. The trace from CB Control 40 S shows no new crystalline reaction products.

As previously touched upon, crystalline products of reaction do not provide a full picture of what is potentially being formed during exposure. X-ray diffraction is not able to identify any hydration products which do not have a well-defined crystal structure. Such substances can include glasses, gels and substances present as very fine particles. However, the amorphous material does show up as a broad 'bump' that covers a wide angular range on the XRD trace. Figures Figure 4-32 and Figure 4-33 show the backgrounds of traces obtained from the Cleveland and Castle Bromwich IBAs respectively. It is clear that, in both cases, the amorphous bump is larger in both cases after exposure – an event which was only observed for the Castle Bromwich IBA in the accelerated chemical reactions study. The initial bump is likely to be largely the result of the presence of glass in the ash. After exposure, the additional amorphous material present is most likely the result of the formation of gels. It should be stressed that this development of reaction gels is observed in all of the specimens, and that simply measuring the area under this curve does not give a quantitative measure of how much gel has been formed. This is because glass and gels are indistinguishable.

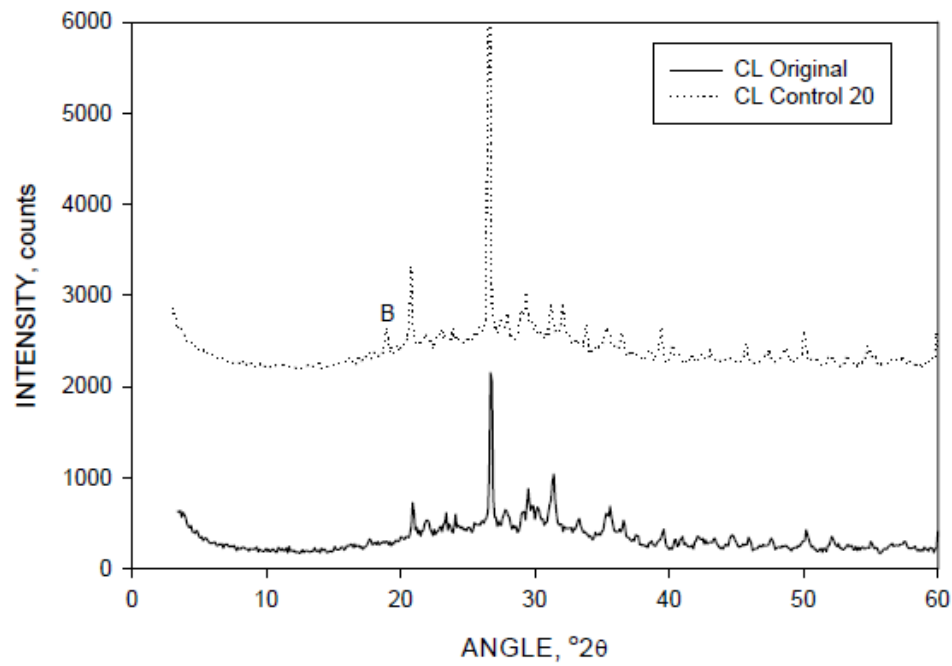


Figure 4-30 X-ray diffraction traces from the Cleveland ash with no chemical addition before and after storage at 20°C. B = bayerite

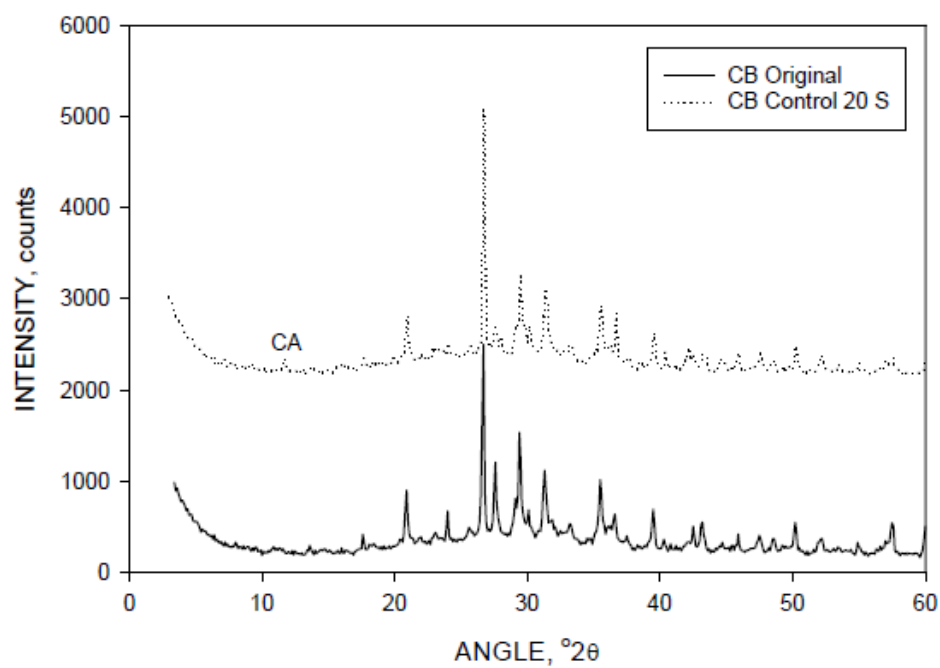


Figure 4-31 X-ray diffraction traces from the Castle Bromwich ash with no chemical addition before and after storage at 20°C with additional water. CA = calcium aluminate

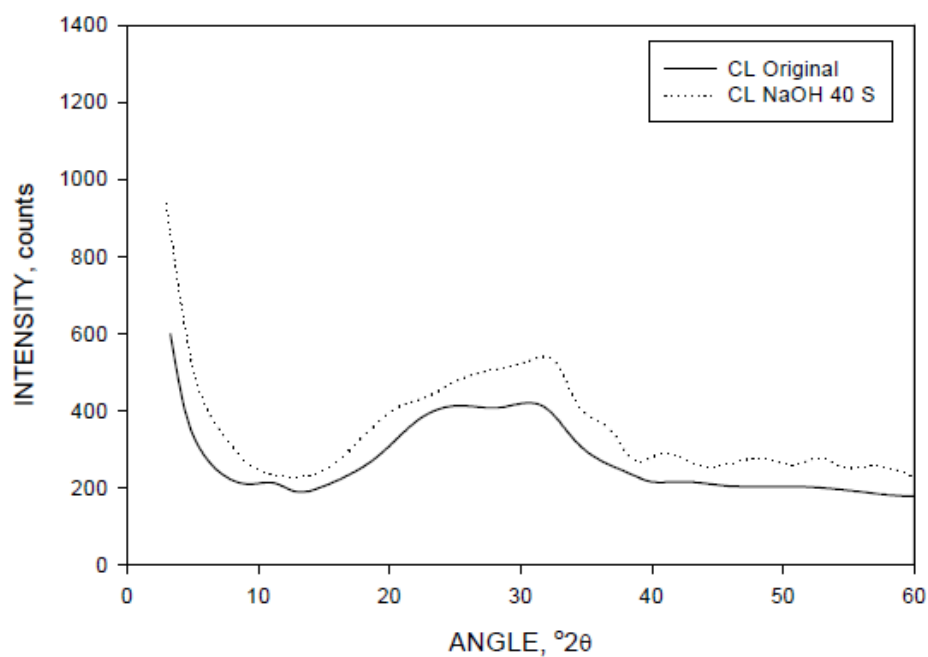


Figure 4-32 Background of the Cleveland IBA XRD trace and the background of the same material after exposure to NaOH at 40°C with additional water

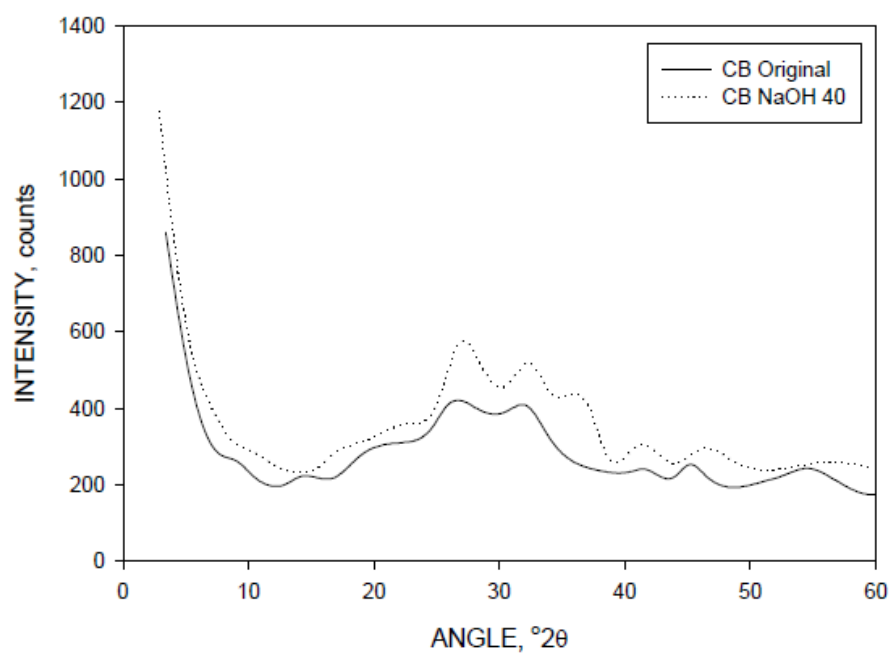


Figure 4-33 Background of the Castle Bromwich IBA XRD trace and the background of the same material after exposure to NaOH at 40°C



#### 4.3.5 Summary of X-Ray Diffraction

X-ray diffraction found evidence of only small quantities of crystalline reaction products in the materials which had undergone expansion testing. Specimens containing  $\text{Na}_2\text{SO}_4$  highlights calcium oxide and calcite. Specimens containing  $\text{NaOH}$  displayed reaction products, mainly the formation of aluminium hydroxide ( $\text{Al}(\text{OH})_3$ ) in the form of Bayerite and some ettringite. The specimens containing  $\text{CaCl}_2$  indicate the formation of calcium aluminate hydrate phase as well as gibbsite, cancrinite and calcium aluminates. Samples with no chemical addition showed small quantities of calcium aluminate hydrates and possibly even smaller quantities of bayerite.

#### 4.4 pH Testing

The results of pH measurements from the expansion specimens where liquid was found remaining in the cylinders are shown in Table 4-3. Testing was done using a calibrated HANNA Pocket pHep5 pH tester. The specimens containing added  $\text{NaOH}$  display high pHs, as would be expected. In the case of the specimens containing  $\text{Na}_2\text{SO}_4$ , and the Castle Bromwich control, the pH is largely unaltered. However, in the case of the specimen exposed to  $\text{CaCl}_2$ , there has been a drop in pH. The most likely explanation for this decline in pH is that the likely accelerated corrosion of ferrous metal induced by the presence of the chloride salt is acting as a sink for hydroxide ions and thus reducing the pH.

Table 4-4 pH values obtained from IBA specimens with excess liquid.

Aggregate	pH level
CL $\text{NaOH}$ 20 S	13.5
CB $\text{NaOH}$ 20 S	13.4
CB $\text{NaOH}$ 20 S	13.4
CB $\text{Na}_2\text{SO}_4$ 20 S	9.7
CB $\text{Na}_2\text{SO}_4$ 40 S	9.8
CB 20	8.9
CL $\text{CaCl}_2$ 20	6.6

#### 4.5 Microscopic Analysis

Microscopic analysis was carried out using a geological microscope manufactured by Leica. The results of which are shown below. The microscopic analysis highlights the surface of a cross section of the specimens broken early on in the testing process. The high metallic content of the aggregate is highlighted in the figures (present as very bright region) as well as some possible formation of gel like materials. Gel like materials are likely to develop on the interface of aggregate particles.

However, after initial testing of four samples testing of this fashion proved to give an interesting view of the makeup of the aggregate, but no conclusive evidence was found. The analysed specimens are shown below.

#### 4.5.1 Specimens Containing $\text{Na}_2\text{SO}_4$

##### 4.5.1.1 *Cleveland*

Figure 4-34 shows the interface of a particle of metal and other materials. The metal is clearly visible and the interface between the materials clearly defined. A similar feature is shown in Figure 4-35. An image from CL  $\text{Na}_2\text{SO}_4$  40 S is shown in Figure 4-37, and a line of reaction products appears to be forming. This observation cannot be conclusively confirmed as the evolution of the gel has not been chronologically photographed.

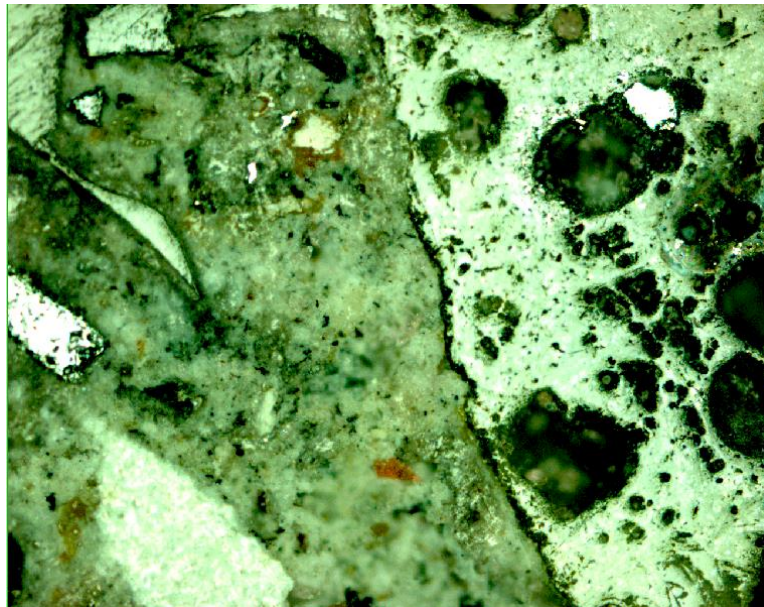


Figure 4-34 Microscopic image from a particle taken from CL  $\text{Na}_2\text{SO}_4$  40 specimen

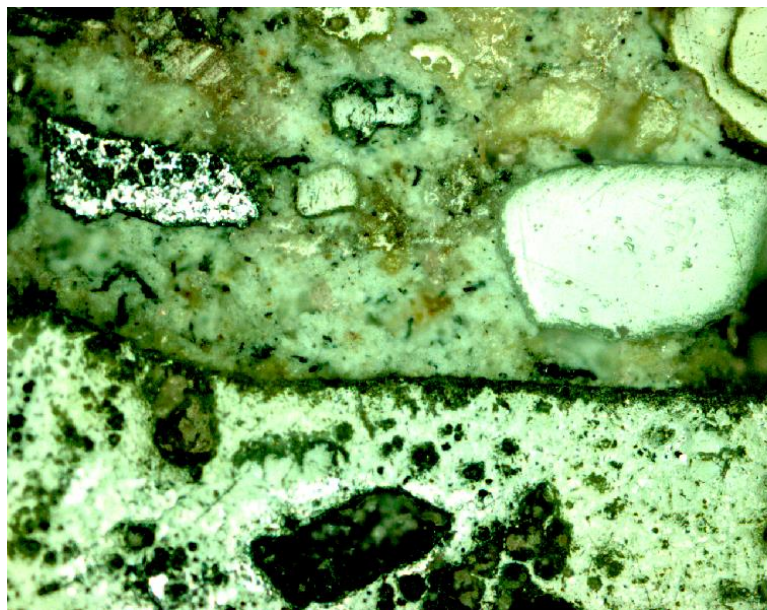


Figure 4-35 CL Microscopic image from a particle taken from  $\text{Na}_2\text{SO}_4$  40 specimen



#### 4.5.1.2 *Castle Bromwich*

The Castle Bromwich specimen (Figure 4-36 and Figure 4-37) shows more metallic particles showing up. The surface here appears to consist of two separate types of metal.

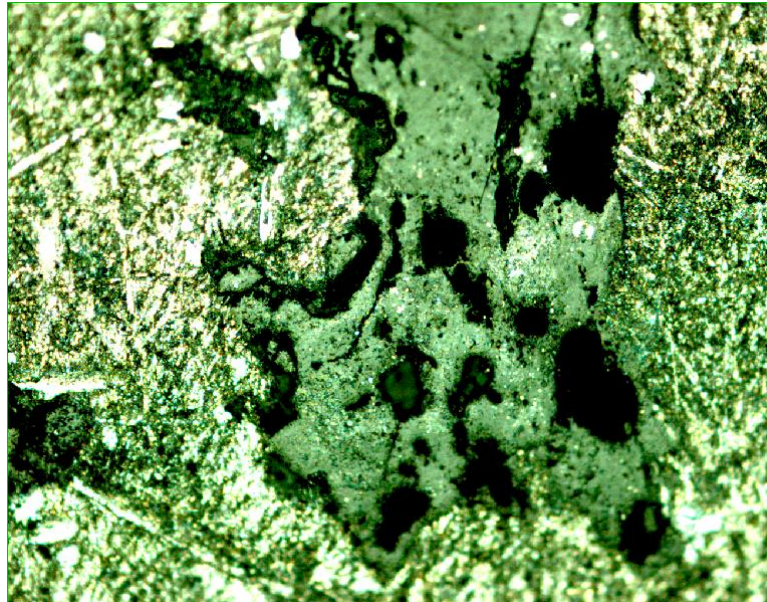


Figure 4-36 Microscopic image from a particle taken from CB Na<sub>2</sub>SO<sub>4</sub> 40 specimen

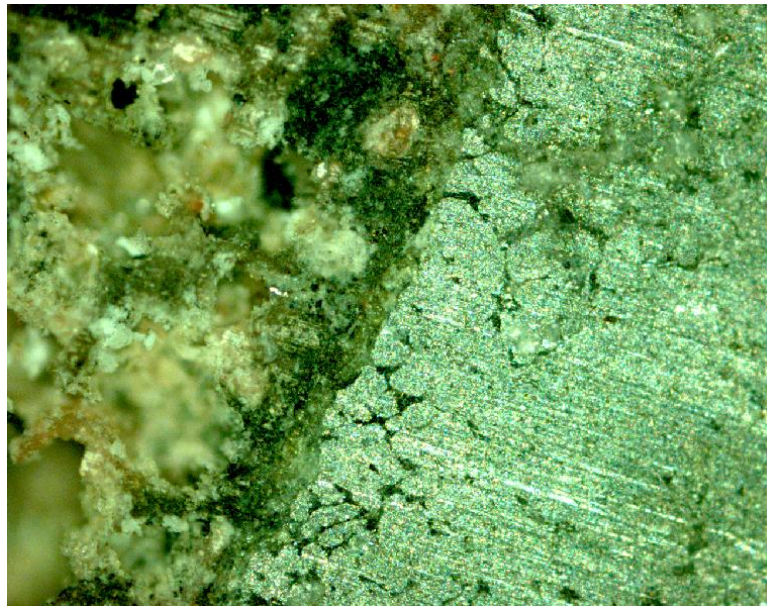


Figure 4-37 Microscopic image from a particle taken from CB Na<sub>2</sub>SO<sub>4</sub> 40 S specimen

## 4.5.2 Specimens Containing NaOH

### 4.5.2.1 *Cleveland*

Figure 4-38 is a cross section of Cleveland aggregate containing NaOH. The image shows the interface between a particle of glass and other material. Under such conditions it might be expected that ASR would occur, leading to the formation of gel. However there does not appear to be gel present in the image.

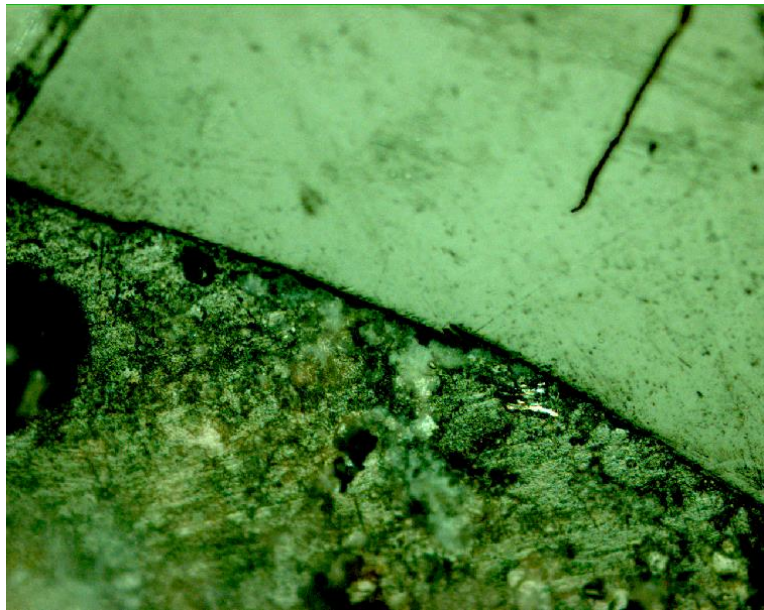


Figure 4-38 Microscopic image from a particle taken from CL NaOH 40 specimen

## 4.6 Scanning Electron Microscope and EDAX analysis

Specimens were chosen for Scanning Microscope (SEM) examination by visual inspection. A sample was chosen from each of the swelling test specimens displaying expansion to investigate whether expansive products. EDAX analysis was carried out during SEM examination; EDAX analysis focuses on the point of magnification to establish the chemical composition of several specimens. It is important to note that the EDAX analysis always finds very high levels of gold (Au) and palladium (Pd) in the analysis. This is because, for the specimens were plasma coated with a thin Au-Pd coating to allow them to conduct electricity.

### 4.6.1 Specimens Containing $\text{Na}_2\text{SO}_4$

Figure 4-39 is a SEM image of the surface of a particle from the CL  $\text{Na}_2\text{SO}_4$  40 specimen. Long narrow crystals are evident. Such crystals may be ettringite, which is associated with sulfate expansion. However, the absence of ettringite on the X-ray diffraction traces suggests that these may in fact be  $\text{Na}_2\text{SO}_4$  crystals. EDAX analysis was to be carried out on these specimens to confirm what these crystals are.

#### 4.6.1.1 *Cleveland Samples*

The following specimens have been taken from CL  $\text{Na}_2\text{SO}_4$  40 specimen who was broken at 91 days, both of the SEM images (Figure 4-39Figure 4-40) shows similar columnar crystalline formation. The EDAX analysis retrieved from the SEM analysis shows high levels of Calcium, sodium, aluminium, chlorine and carbon (Figure 4-41). This is most possibly the mineral cancrinite. There is no evidence in the literature of cancrinite being expansive, and little to suggest an expansive effect in these images.



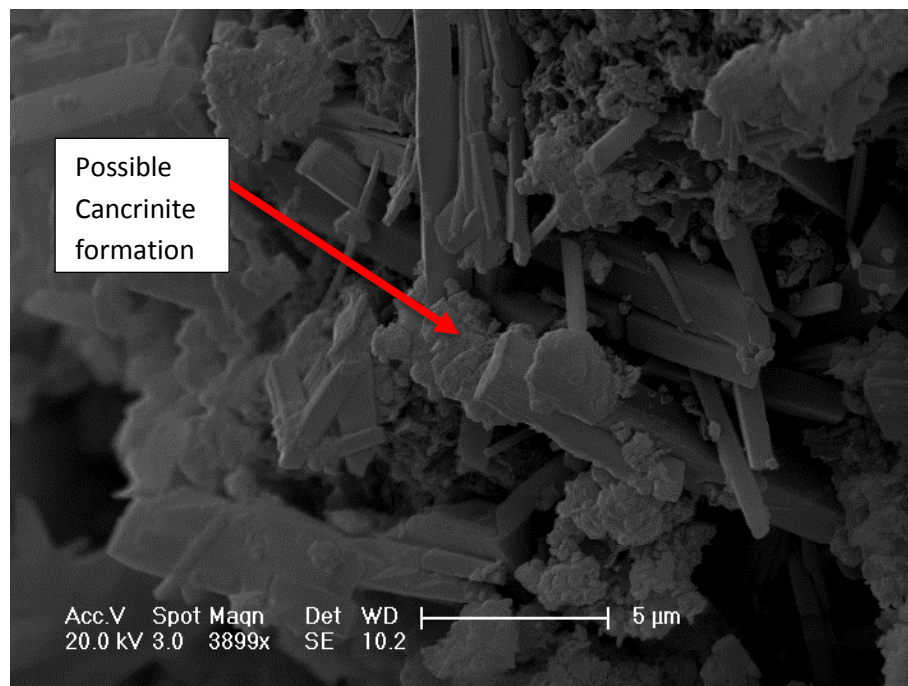


Figure 4-39 SEM image from a particle taken from the CL Na<sub>2</sub>SO<sub>4</sub> 40 Specimen

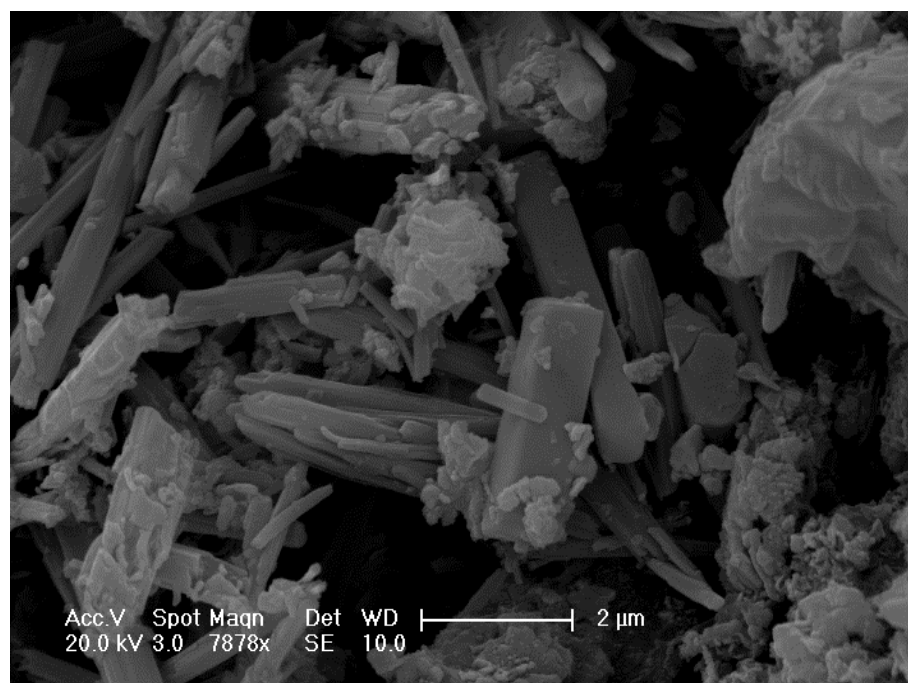


Figure 4-40 SEM image from a particle taken from the CL Na<sub>2</sub>SO<sub>4</sub> 40 specimen

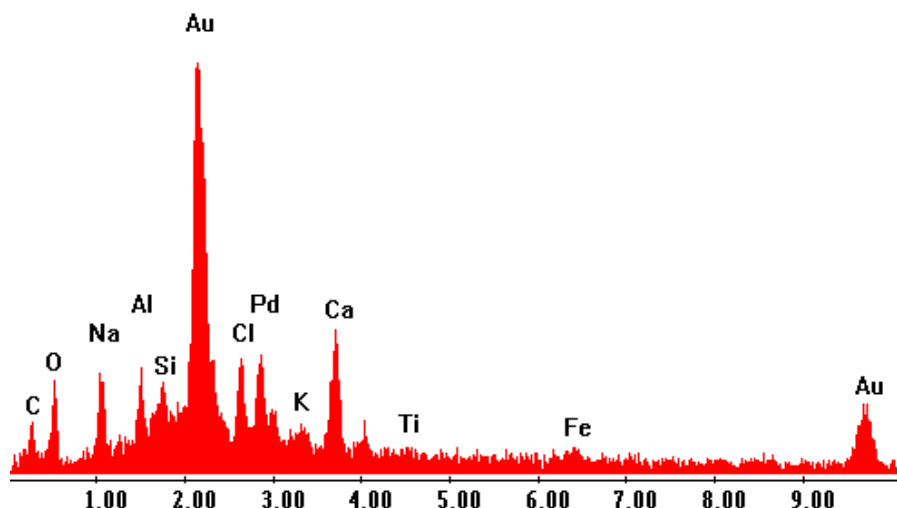


Figure 4-41 EDAX spectrum from the crystals present on the CL Na<sub>2</sub>SO<sub>4</sub> 40 specimen

An SEM image from a particle taken from CL Na<sub>2</sub>SO<sub>4</sub> 40 S can be seen in Figure 4-42 SEM image from a particle taken from the CL Na<sub>2</sub>SO<sub>4</sub> 40 S. There is another columnar crystal of what is possibly cancrinite. The many clusters of very small crystals were found by EDAX to consist of Na<sub>2</sub>SO<sub>4</sub>, which was found to persist in this specimen using X-ray diffraction. Thermal analysis identified significant quantities of what was most probably aluminium hydroxide gel. This was not evident on the surface of this particle.

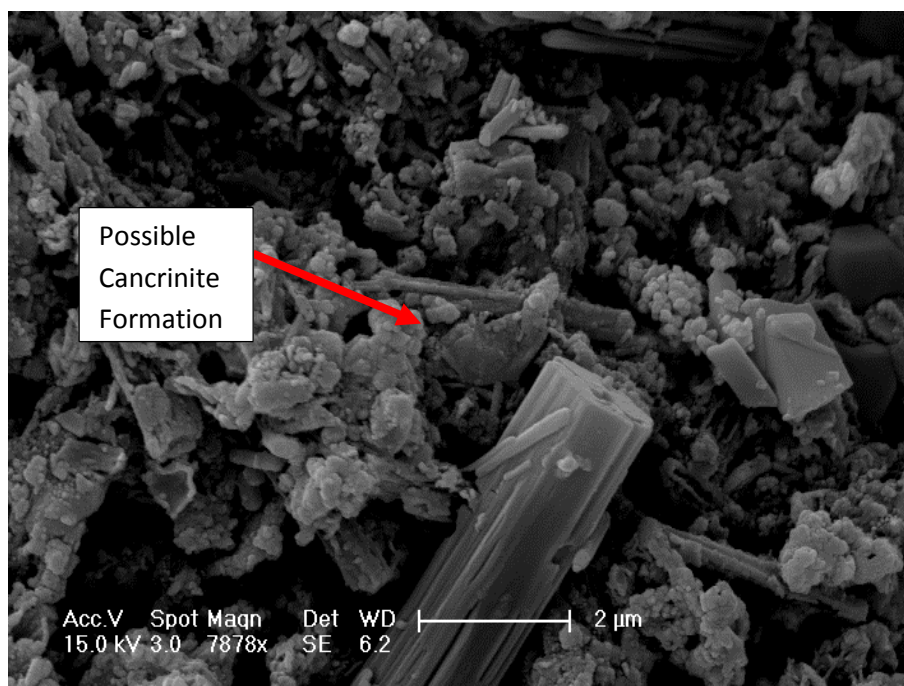


Figure 4-42 SEM image from a particle taken from the CL Na<sub>2</sub>SO<sub>4</sub> 40 S specimen

#### 4.6.1.2 *Castle Bromwich*

Figure 4-43 shows the presence of gel on the surface of a particle taken from specimen CB  $\text{Na}_2\text{SO}_4$  40, this specimen was broken on day 196 which gave the gel adequate time to form. Figure 4-44 shows aluminium hydroxide gel forming in glass.

Figure 4-44 shows a similar formation of gel on the same particle. The results of EDAX analysis can be seen in Figure 4-45, which confirm it as being most probably aluminium hydroxide gel. The morphology of the gel is significant – during specimen preparation the gel has undergone shrinkage and cracking. This is a significant observation since it indicates that this gel swells when it imbibes water (and thus contracts on drying). This is a strong indication that the gel is expansive in nature.

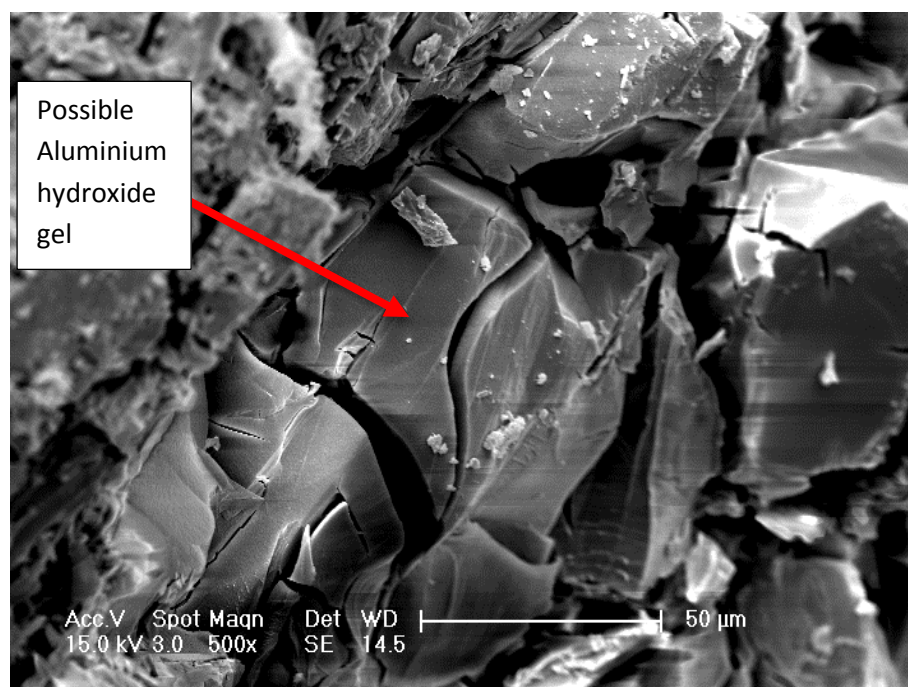


Figure 4-43 SEM image from a particle taken from the CB  $\text{Na}_2\text{SO}_4$  40 specimen



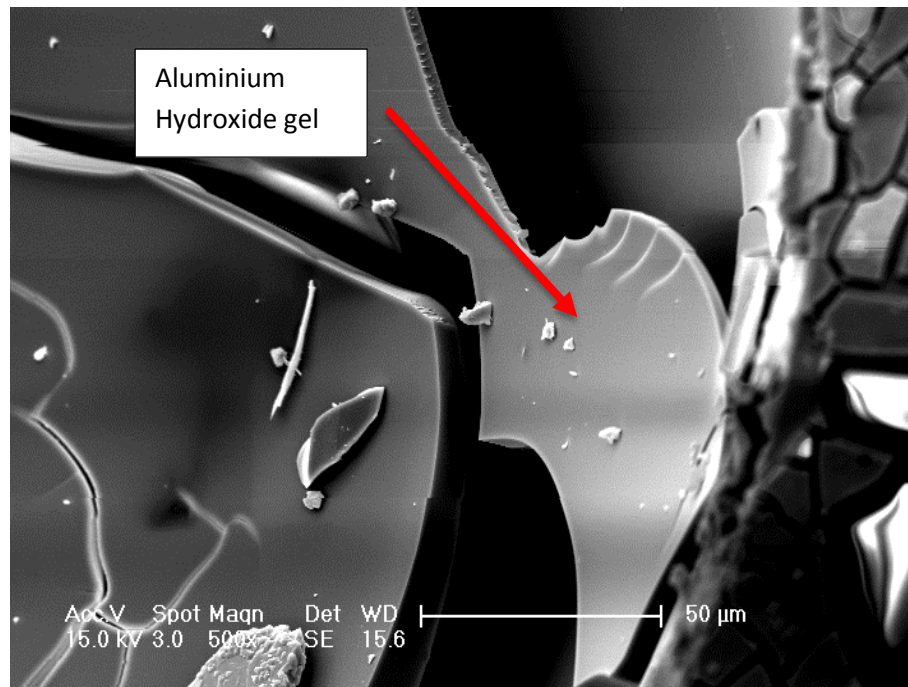


Figure 4-44 SEM image from a particle taken from the CB Na<sub>2</sub>SO<sub>4</sub> 40 specimen

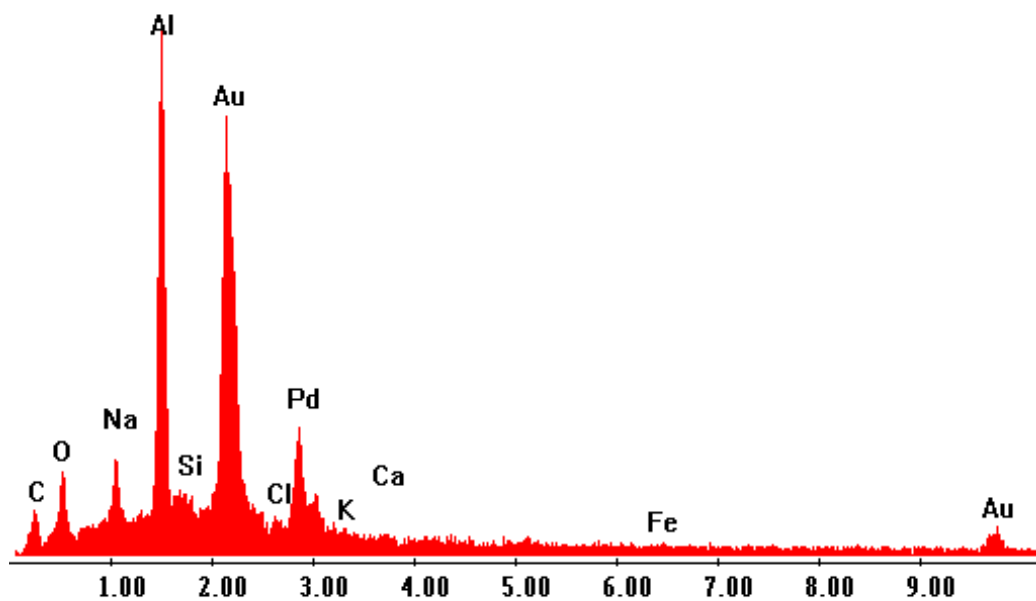


Figure 4-45 EDAX spectrum of particle taken from the CB Na<sub>2</sub>SO<sub>4</sub> 40 specimen

#### 4.6.2 Specimens Containing NaOH

##### 4.6.2.1 *Cleveland*

Figure 4-46 shows the surface of a particle taken from the CL NaOH 40 specimen. A layer of material is present on the surface of the particle resembling a porous framework. The images are taken from CL NaOH 40 specimen broken at 98 days after initial expansion had ceased. EDAX analysis (Figure

4-47) shows high levels of sodium, aluminium, silicon, chlorine and calcium, and is thus most likely to be cancrinite, albeit with a very different morphology than that seen in previous images. It is likely that these crystals are much less mature than those seen before.

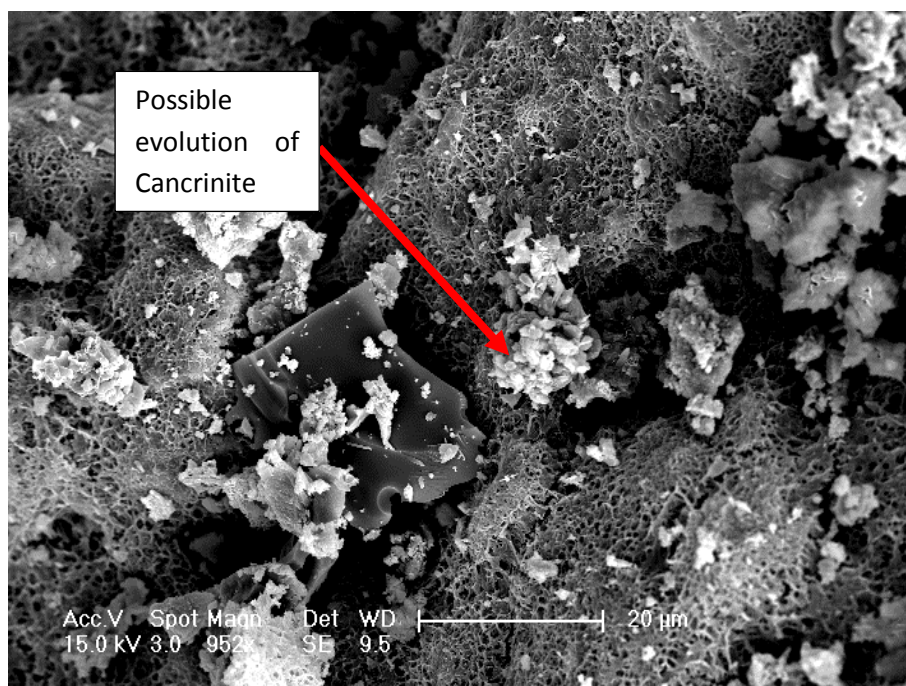


Figure 4-46 SEM image from a particle taken from CL NaOH 40

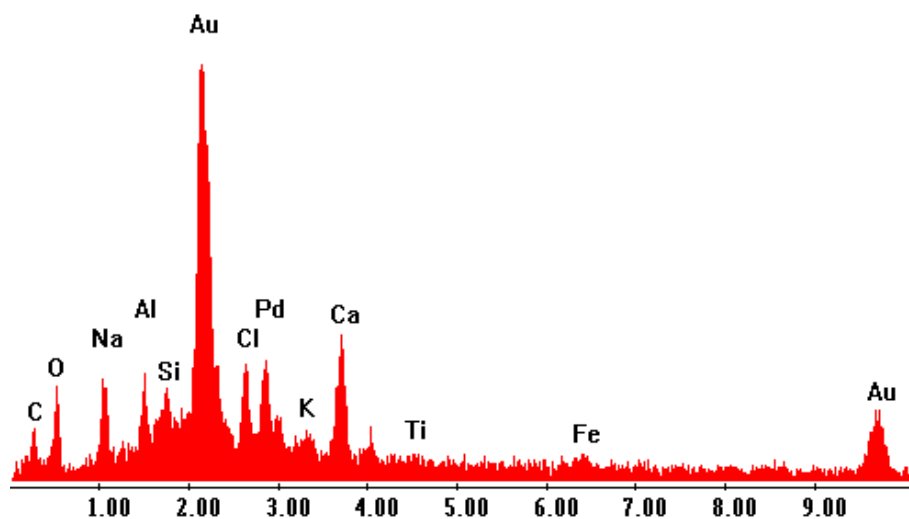


Figure 4-47 EDAX spectrum of particle taken from the CL Na<sub>2</sub>SO<sub>4</sub> 40 specimen

Figure 4-48 shows a layer of material growing on a surface of a glass particle taken from specimen CL NaOH 40 S. The material is most probably a gel and has undergone cracking which, as discussed previously, is characteristic of a desiccated expansive gel. The EDAX spectrum in Figure 4-49 shows that the main constituents here are silica, sodium, oxygen and calcium. This strongly suggests that this is gel resulting from alkali-silica reaction (ASR). Figure 4-50 shows a similar reaction product, albeit much less well developed.

The suspected presence of ASR gel fits well with the findings of thermal analysis, from which similar conclusions were drawn, and with the expansion results, where significant expansion was observed.

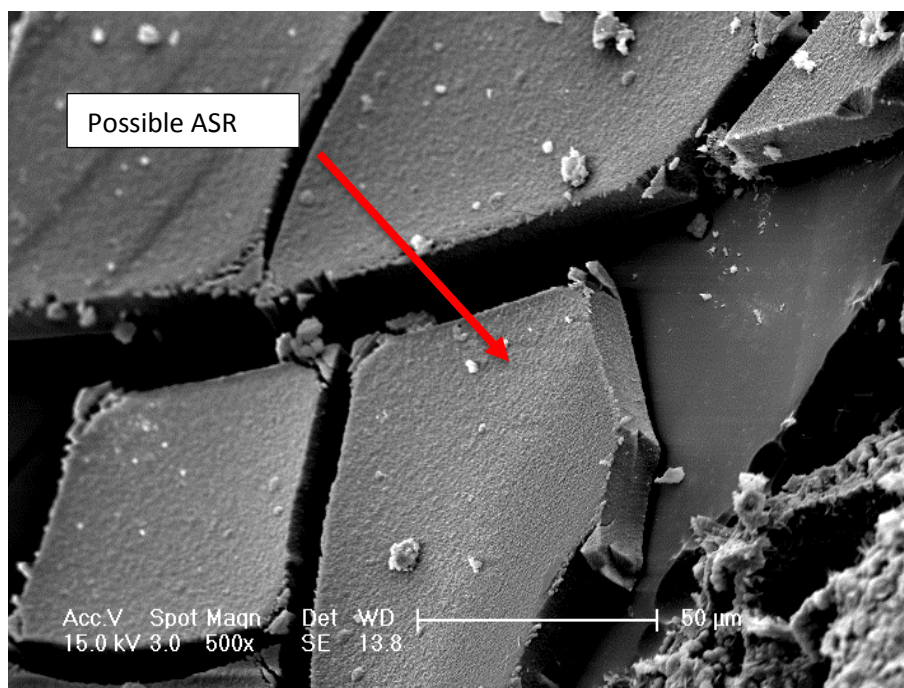


Figure 4-48 SEM image from a particle taken from the CL NaOH 40 S specimen

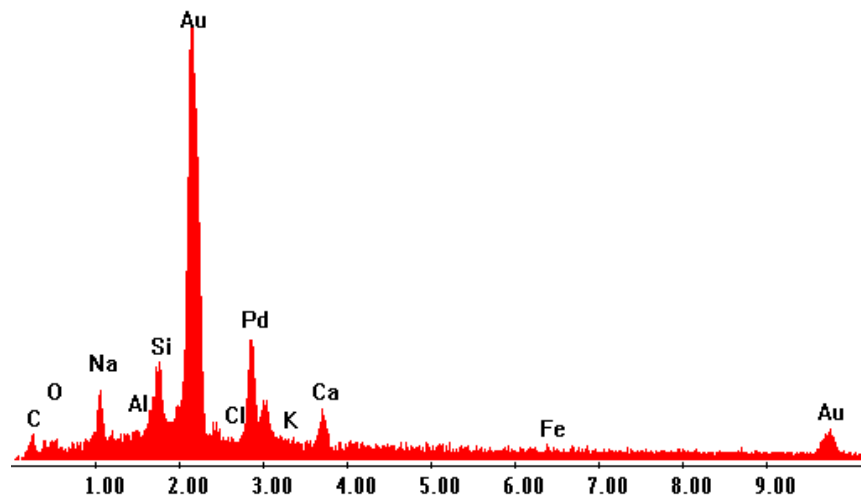


Figure 4-49 EDAX spectrum from the reaction product present on the particle taken from the  
CL NaOH 40 S specimen

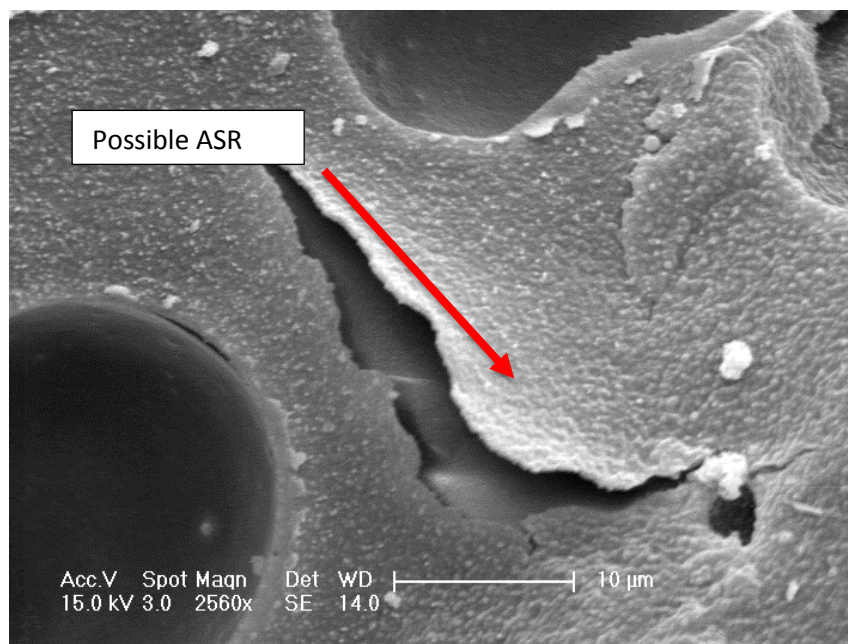


Figure 4-50 SEM image of a thin layer of material developing on a glass particle taken from the CL NaOH 40 S specimen.

Figure 4-51 is an SEM image from the same particle taken from specimen CL NaOH 40 S. It shows another reaction product significantly different from the previous products seen on this particle. EDAX analysis (Figure 4-52) indicates that this is most probably calcium silicate hydrate (CSH) gel. CSH gel is also formed by pozzolanic materials and Portland cement and is non-expansive. CSH gel is also a by-product of ASR, since some of the gel formed by ASR gradually dissolves and reacts with calcium. Thus, this image provides evidence of pozzolanic reactions occurring in the specimen. Such reactions should be viewed as being beneficial, since they will contribute towards the strength of compacted IBA

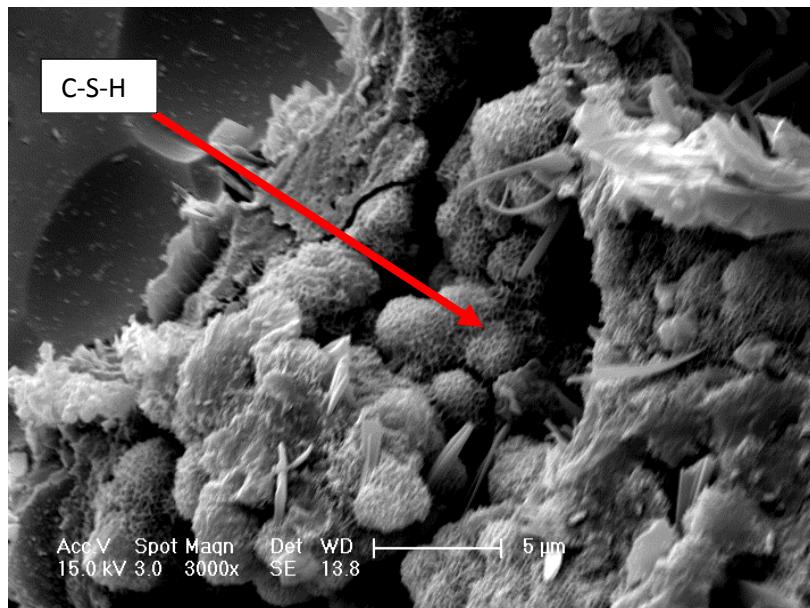


Figure 4-51 SEM image of reaction products on the surface of a glass particle taken from the CL NaOH 40 S

Specimen

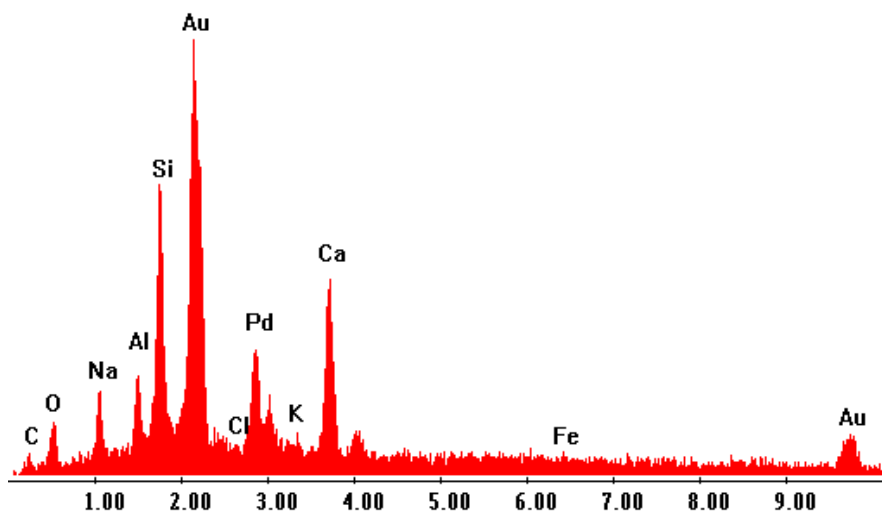


Figure 4-52 EDAX spectrum of suspected CSH gel on the CL NaOH 40 S specimen.

#### 4.6.2.2 *Castle Bromwich*

Figure 4-53 is an SEM image of the surface of a particle taken from CB NaOH 20. Whilst the crystals in this image were initially thought to be reaction products, EDAX analysis (Figure 4-82) shows that they are in fact particles of unreacted NaOH



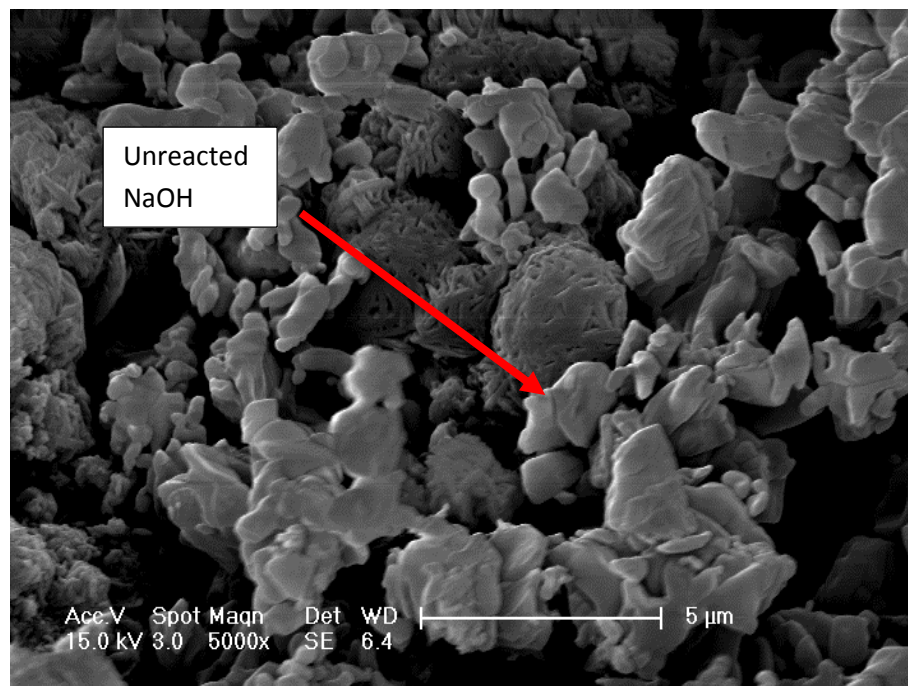


Figure 4-53 SEM image from the surface of a particle taken from the CB NaOH 20 specimen

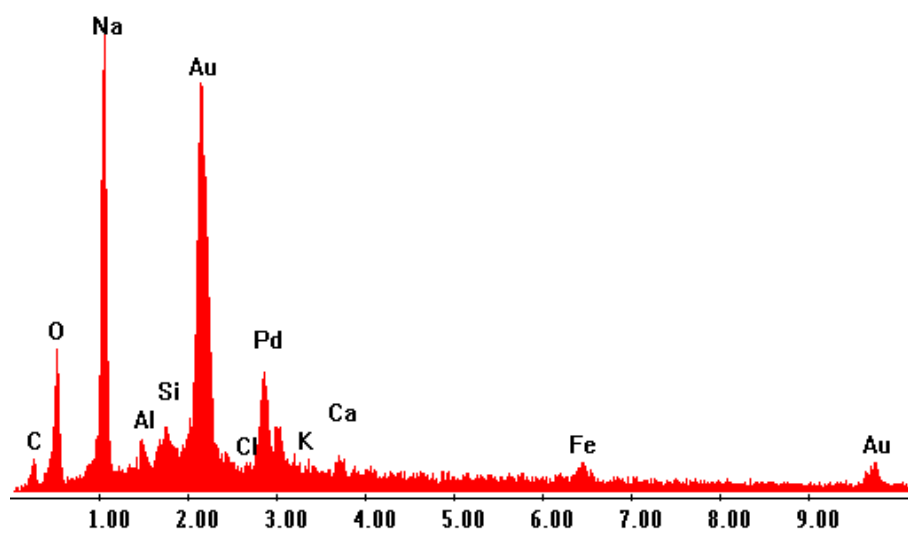


Figure 4-54 EDAX spectrum of particle taken from the CB NaOH 20 specimen

An image from CB NaOH 40 (Figure 4-55) again shows a cracked gel-like product at the surface of a particle. The gel is almost certainly aluminium hydroxide gel. Also identified on the surface of particles coming from this specimen were groups of needle-like crystals and hexagonal plate-shaped crystals (Figure 4-56 and Figure 4-57). Figure 4-57 is a magnified image of Figure 4-56 which gives a clearer image of the particles. Gibbsite and bayerite were found by X-ray diffraction to be present in this specimen, and it is likely that the needles are gibbsite and the hexagonal plates are bayerite.

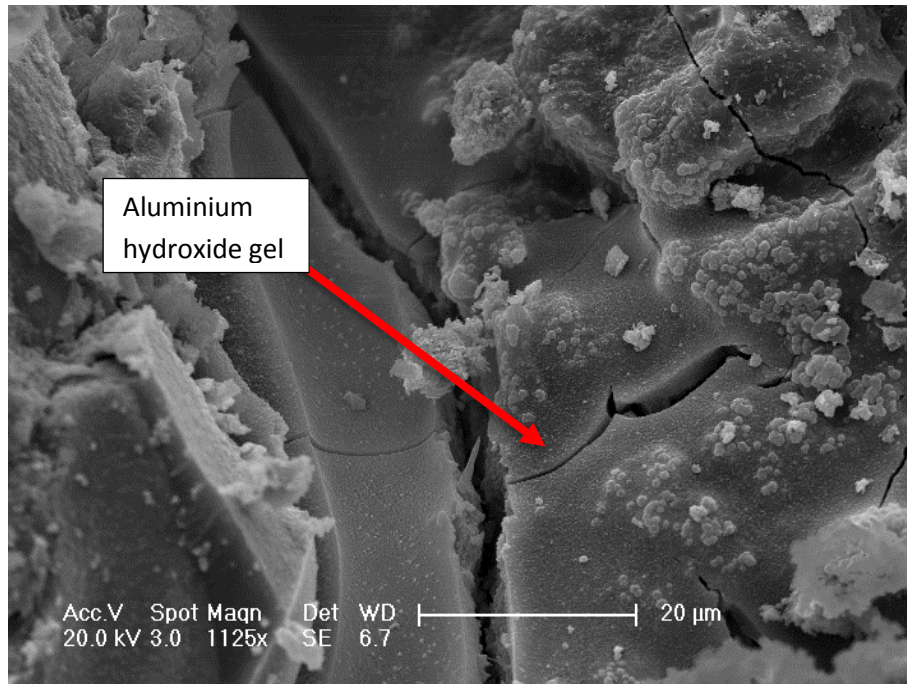


Figure 4-55 SEM image from a particle taken from the CB NaOH 40 specimen

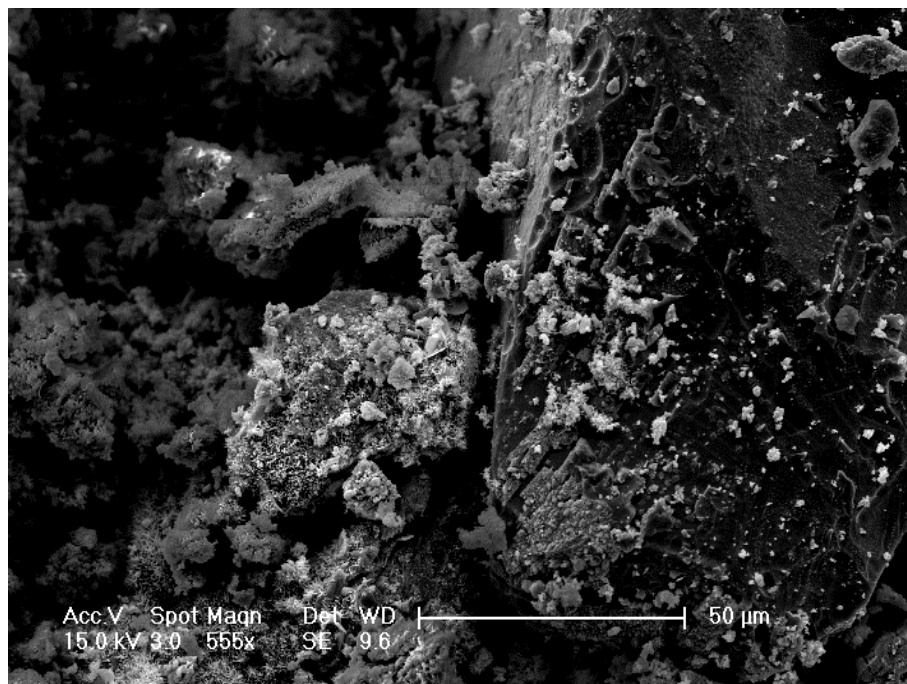


Figure 4-56 SEM image of Clusters of needle like crystals in the CB NaOH 40 specimen (1 of 2)

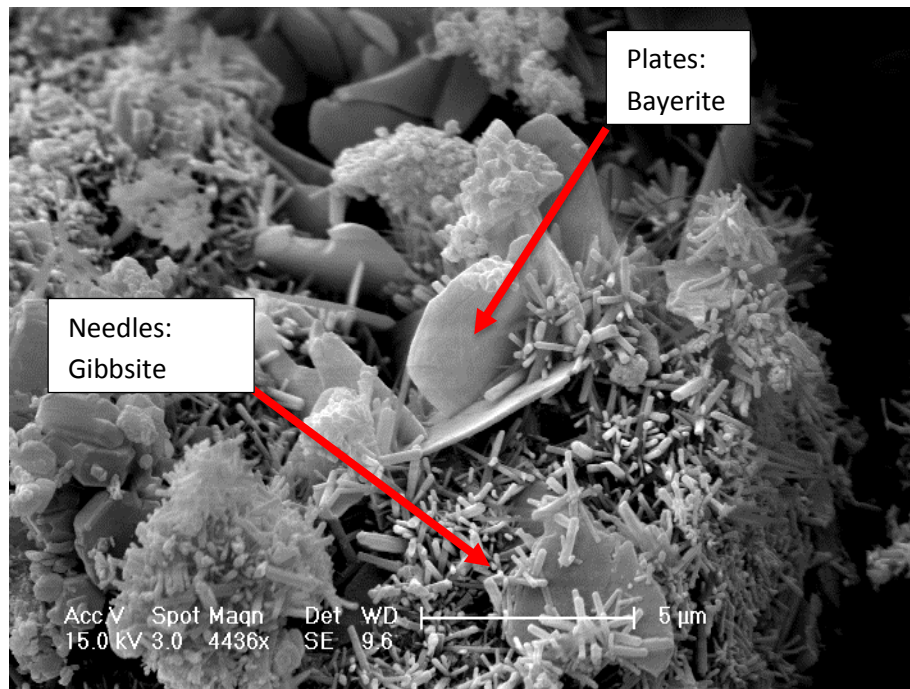


Figure 4-57 SEM image of Needle shaped and hexagonal crystals in the CB NaOH 40 specimen. (2 of 2 @ 10x magnification)

Figure 4-58 and Figure 4-59 show the SEM image and EDAX spectrum taken from the surface of CB NaOH 20 S respectively. The EDAX confirms the presence of calcium, silicon, aluminium, sodium, carbon and oxygen, which is most probably cancrinite. The morphology of the reaction products is unusual – the products take the form of spheres composed of smaller crystals. This morphology is very commonly encountered during cancrinite formation. A very interesting image from the same specimen is shown in Figure 4-60. The same spheres of cancrinite are visible here, but within the spheres is a less well defined material. What is being seen here is possibly the transformation of amorphous gel (possibly aluminium hydroxide) into cancrinite.



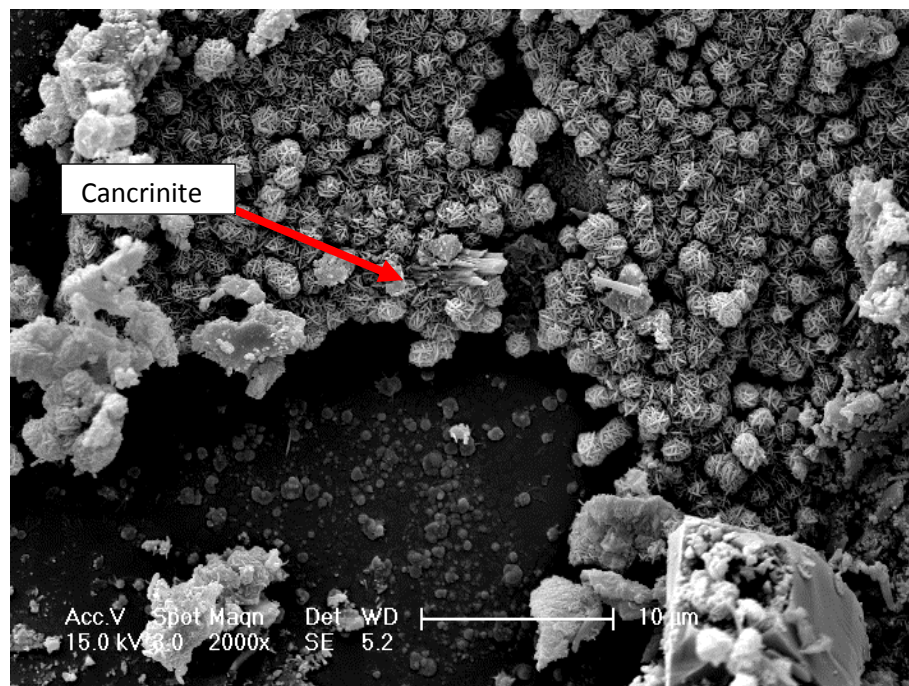


Figure 4-58 SEM image from a particle taken from the CB NaOH 20 S specimen

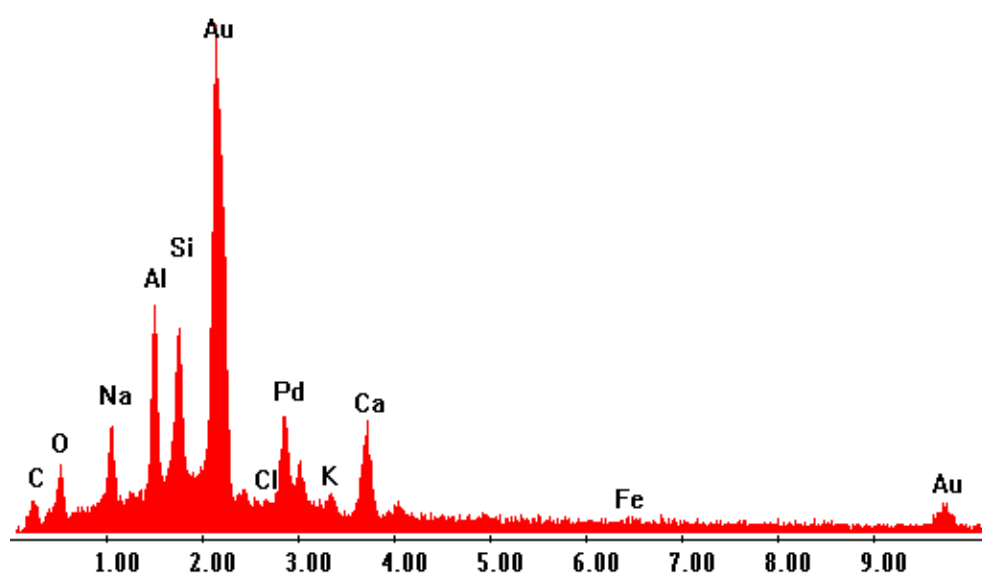


Figure 4-59 EDAX spectrum of particle taken from the CB NaOH 20 S specimen

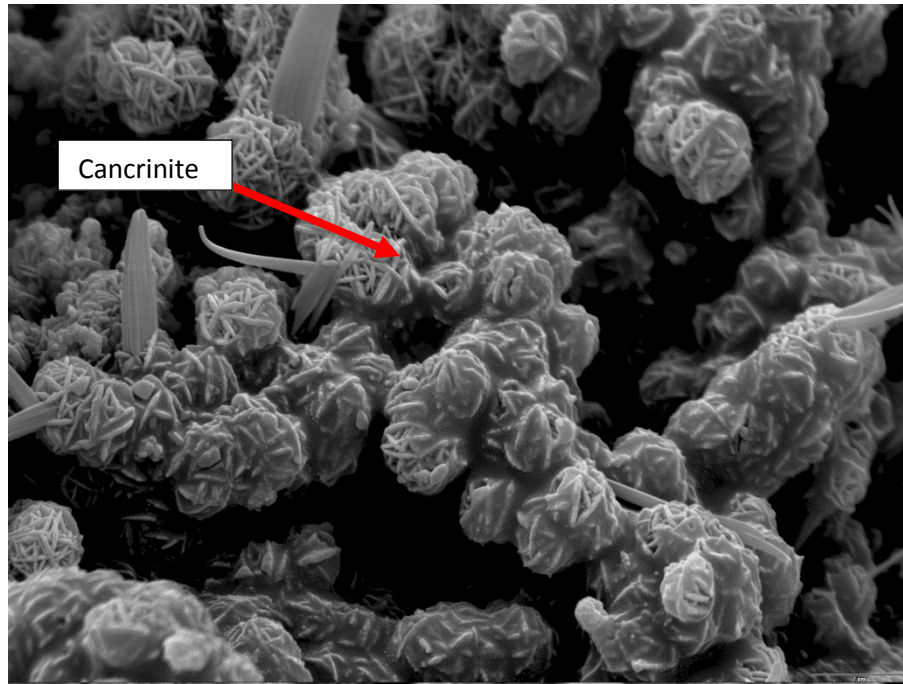


Figure 4-60 SEM image of reaction products from a particle taken from the CB NaOH 20 S specimen

#### 4.6.3 Specimens Containing $\text{CaCl}_2$

##### 4.6.3.1 *Cleveland*

Figure 4-61 shows material growing on the surface of a particle of glass from the CL  $\text{CaCl}_2$ 40 specimen. Two features are evident in this image. Firstly, there is a smooth nodule of material attached to the surface which EDAX confirms as  $\text{CaCl}_2$ . Secondly, there is a rough layer of material attached to the surface of the glass particle which would otherwise appear smooth. This rough layer is possibly ASR gel in a very early condition – it resembles the thin layer seen previously and would appear have only developed to a very limited depth.

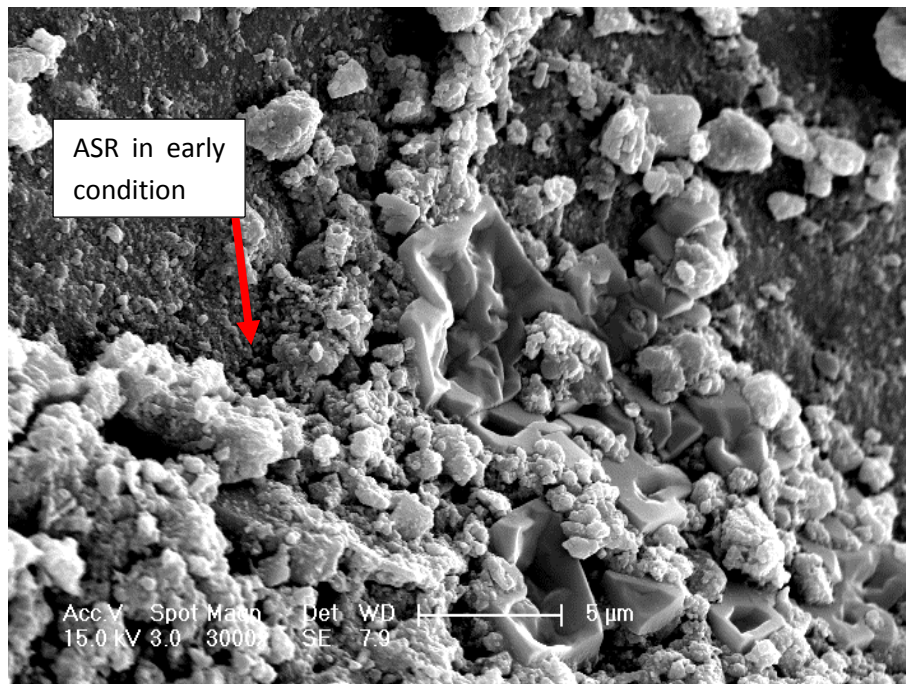


Figure 4-61 SEM images of the surface of a particle from the CL CaCl<sub>2</sub> 40 specimen

#### 4.6.3.2 *Castle Bromwich*

Figure 4-62– from the surface of a particle from CB CaCl<sub>2</sub> 40 S – also shows unreacted CaCl<sub>2</sub>. In other areas of the particle surface gel-like products are forming. Figure 4-63 shows a layer of aluminium hydroxide gel forming on an area of the IBA particle. Figure 4-64 shows a close up of the previous image. The gel has a cracked and wrinkled texture after drying which is indicative of an expansive gel. However, it is worth noting that expansion in this specimen was not significant.

Figure 4-65 shows a layer of material on the surface of the same aggregate particle. This was first thought to be the formation of rust due to the presence of CaCl<sub>2</sub> in the specimen. However, EDAX analysis (Figure 4-66) shows silicon, aluminium and calcium as the most prominent elements, suggesting it is a calcium aluminate gel. There is little sign of cracking or other features which would indicate an expansive gel.



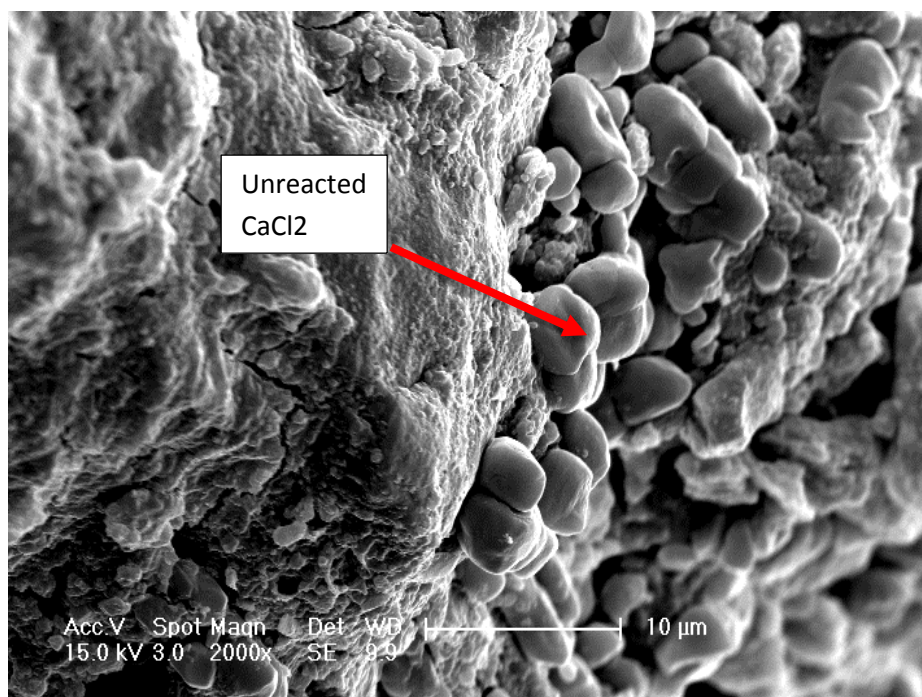


Figure 4-62 SEM image of Crystals of  $\text{CaCl}_2$  powder on surface of a particle taken from CB  $\text{CaCl}_2$  40 S,

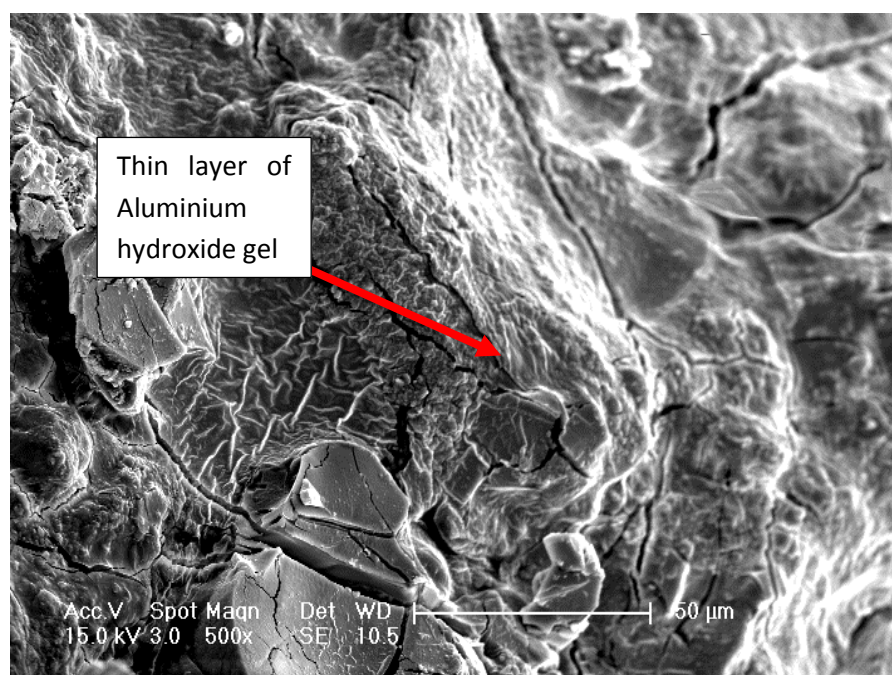


Figure 4-63 SEM images of a Gel layer on the surface of a particle taken from CB  $\text{CaCl}_2$  40 S

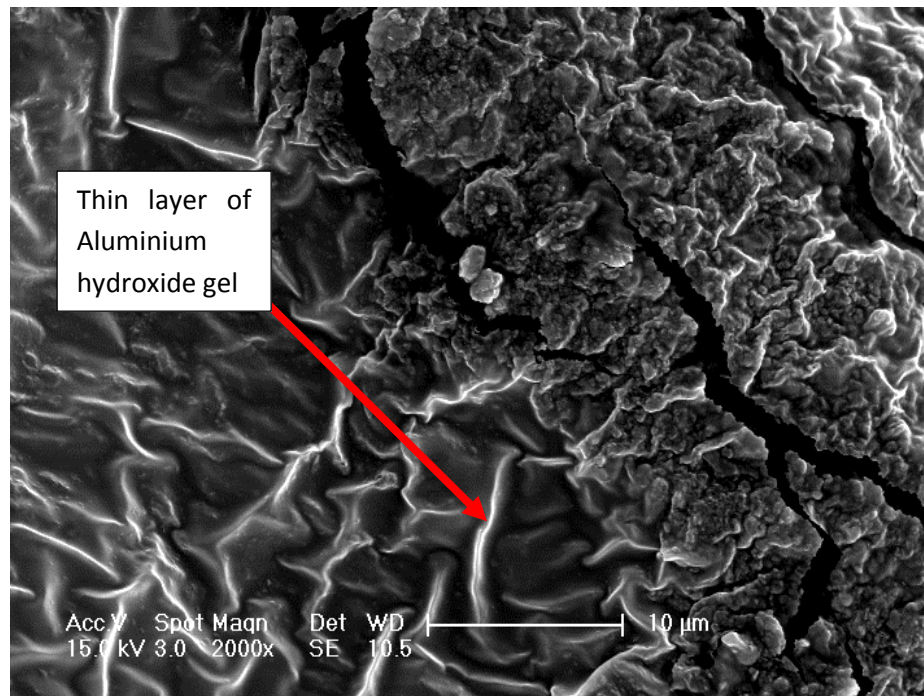


Figure 4-64 SEM images of a particle taken from CB  $\text{CaCl}_2$  40 S specimen. (2) @ 5x magnification, gel like surface leading to aggregate not yet reacted

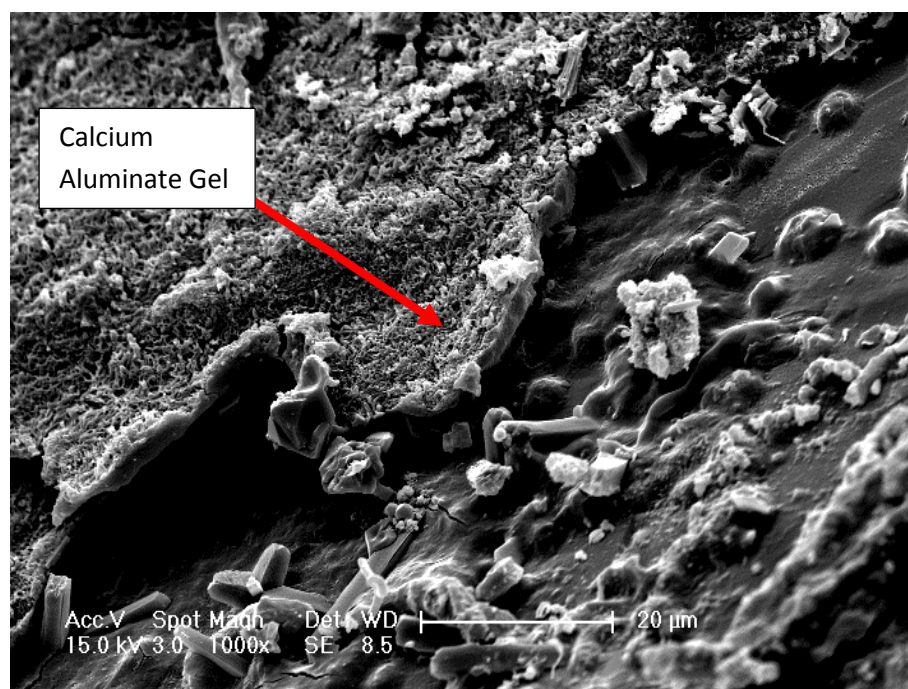


Figure 4-65 SEM images of a particle taken from CB  $\text{CaCl}_2$  40 S specimen

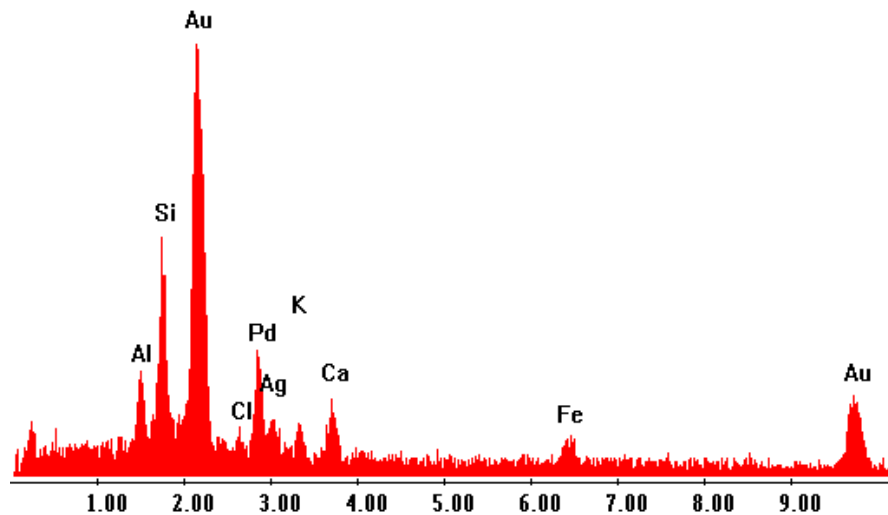


Figure 4-66 EDAX spectrum of particle taken from the CB  $\text{CaCl}_2$  40 specimen

#### 4.6.4 Specimens without chemical addition

##### 4.6.4.1 *Cleveland*

Figure 4-67 shows the surface of a particle taken from specimen CL control 20. The image, when considered alongside the EDAX spectrum from the material (Figure 4-68) clearly shows the occurrence of rust. There was little evidence of significant quantities of iron oxides and hydroxides in this specimen, and so the image should not be viewed as being characteristic of the material as a whole. However, it does at least provide an understanding of what sort of morphologies these products adopt.

Figure 4-69 is another image from the same sample, showing larger crystals of iron corrosion products (confirmed by the EDAX spectrum in Figure 4-70).



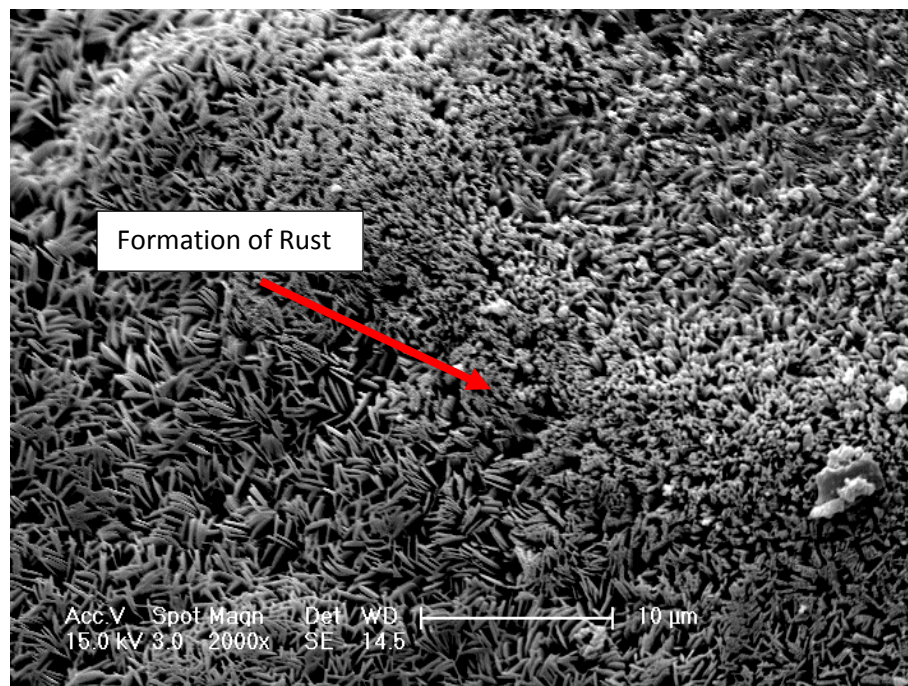


Figure 4-67 SEM images of Corrosion products on the surface of a particle taken from CL control 20 specimen

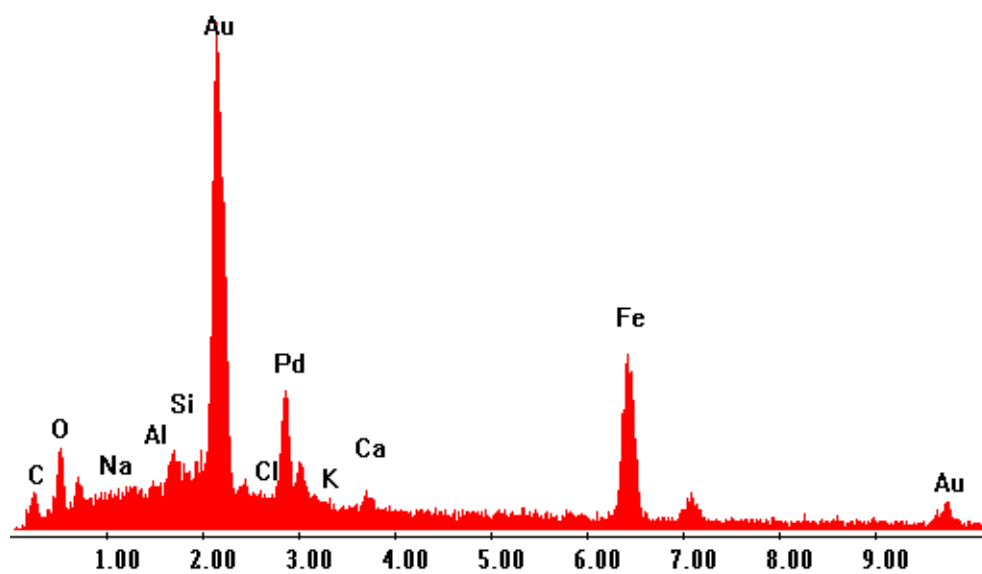


Figure 4-68 EDAX spectrum from the CL control 20 specimen

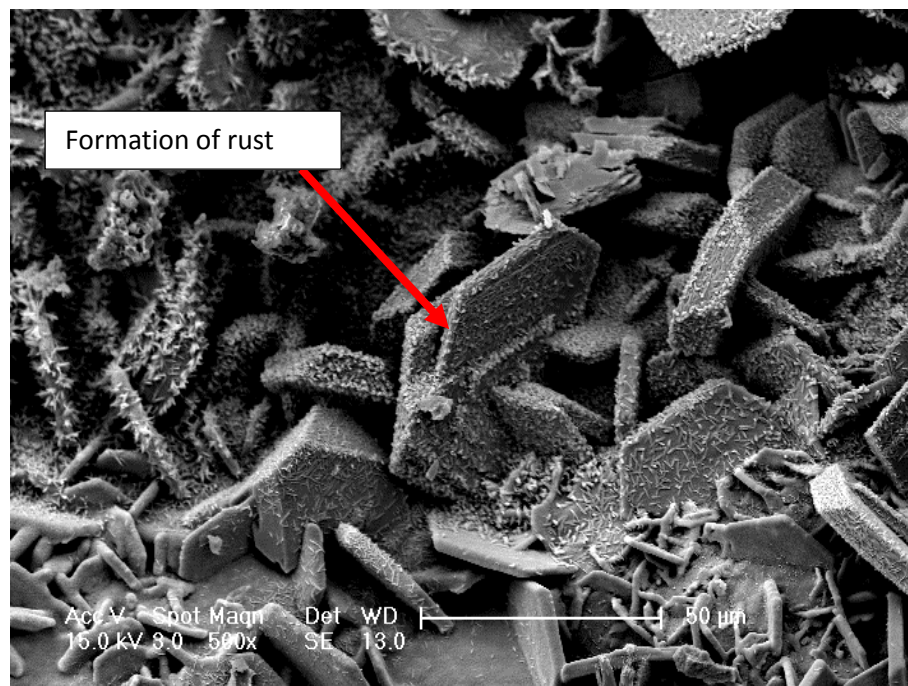


Figure 4-69 SEM images of Corrosion products on the surface of a particle taken from the CL Control 20 specimen

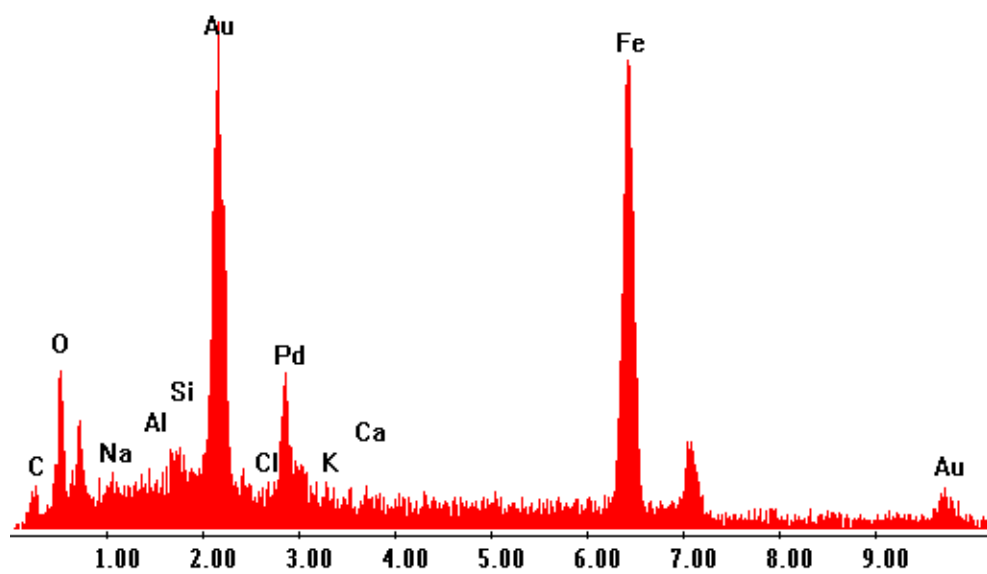


Figure 4-70 EDAX Spectrum from CL control 20 specimen



#### 4.6.4.2 *Castle Bromwich*

The image from a glass particle from CB Control 20S (Figure 4-71) shows a thin layer of material growing on its surface. This layer resembles similar features seen in previous images. However, EDAX (Figure 4-72) indicates that it is an aluminosilicate gel, which has previously not been encountered. The CB Control 20 S specimen also contained some partially combusted organic material (probably timber) (Figure 4-73). The EDAX analysis in Figure 4-74 shows high levels of carbon.

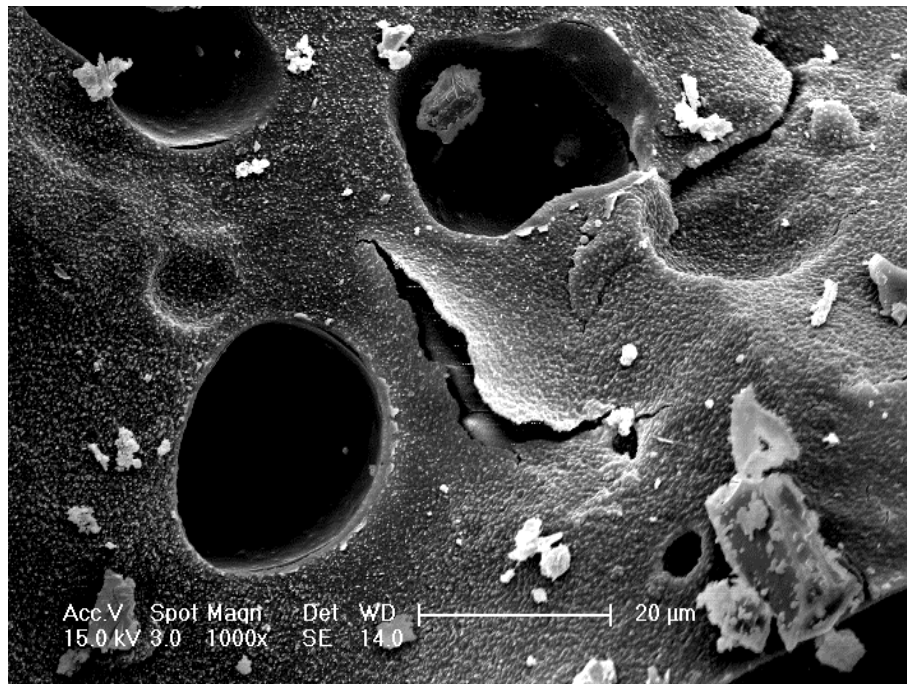


Figure 4-71 SEM images of a layer of reaction product on the surface of a particle from CB Control 20 S

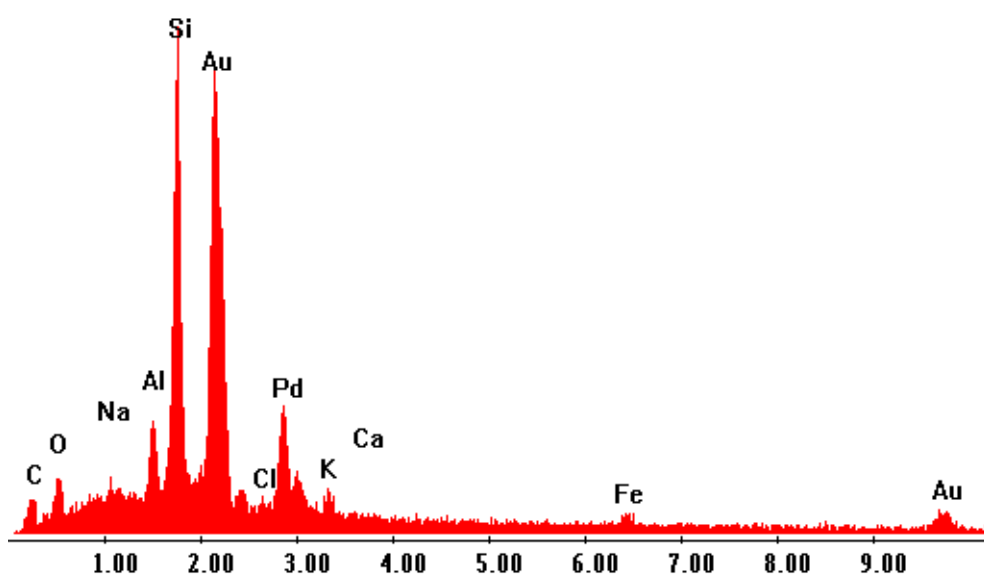


Figure 4-72 EDAX spectrum from CB Control 20 S

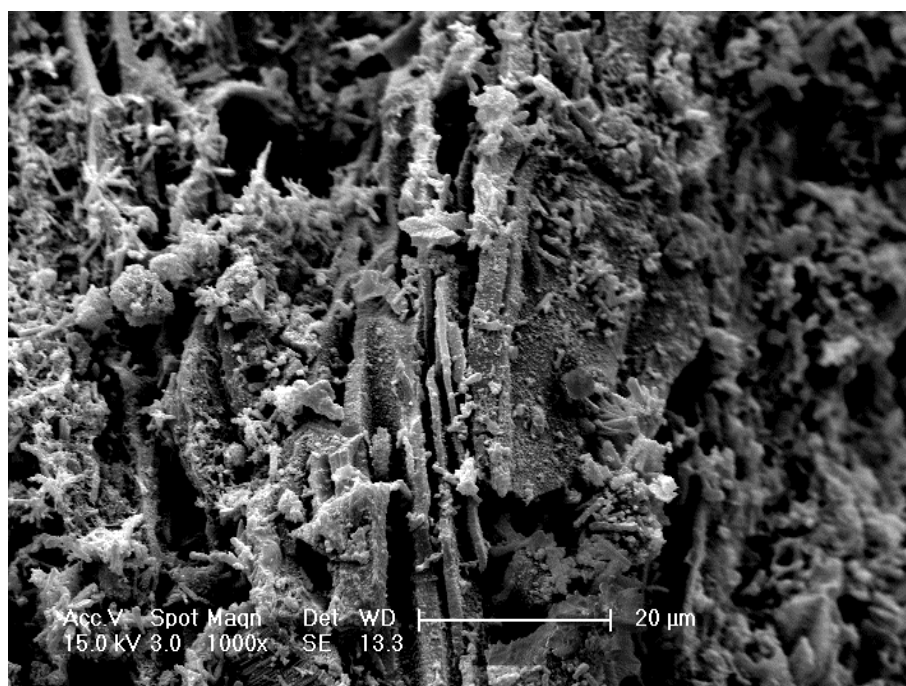


Figure 4-73 SEM image of Unburnt organic material on a particle taken from CB Control 20 S specimen

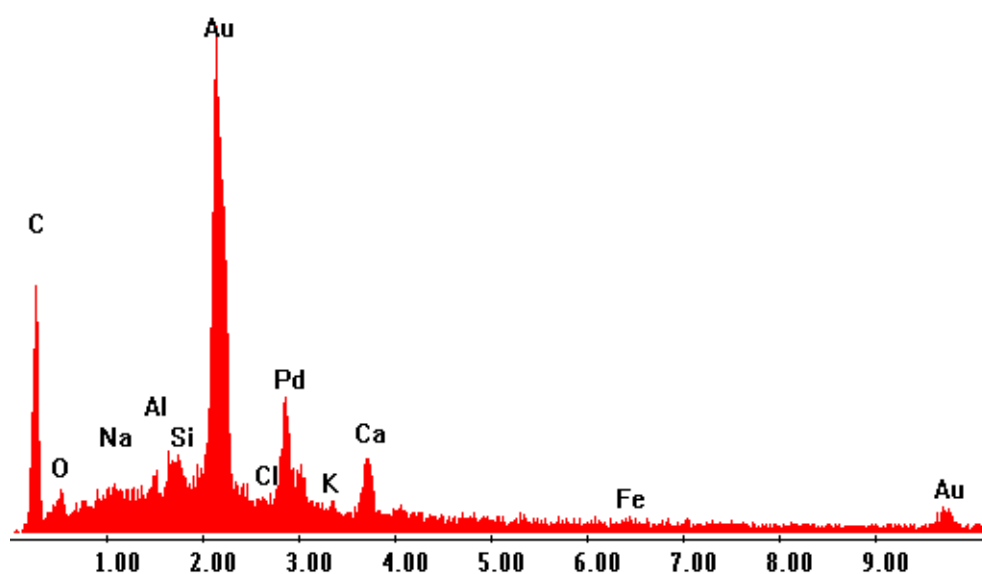


Figure 4-74. EDAX spectrum of unburnt organic material in CB Control 20 S

Figure 4-75 shows an image from the surface of a particle taken from the CB control 40 S specimen. In general the material showed similar features to the CB Control 20 specimen. The image shows corrosion products from ferrous metal confirmed by EDAX in Figure 4-76

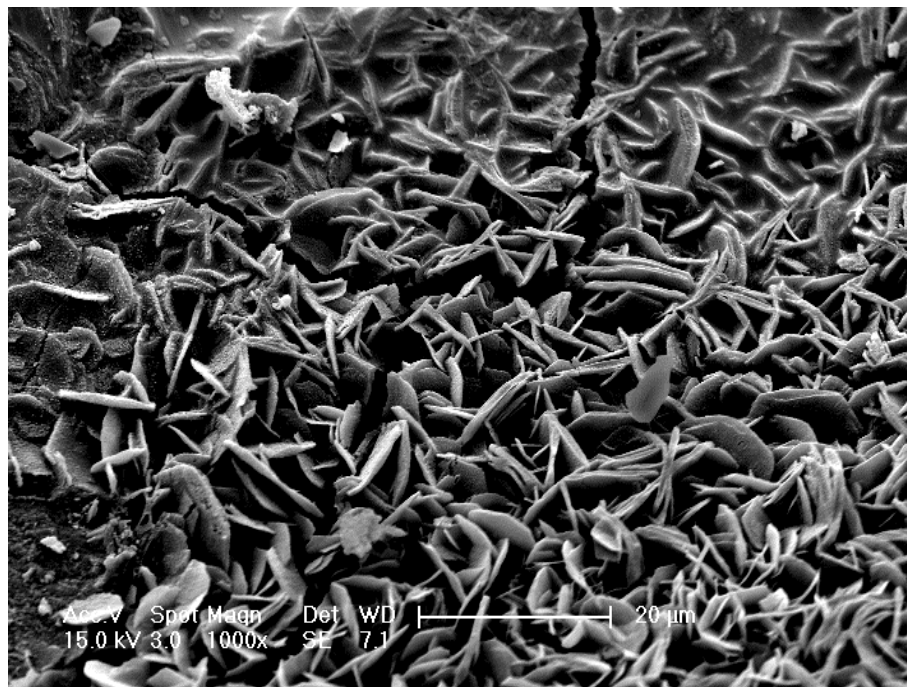


Figure 4-75 SEM images of a particle taken from CB Control 40 S specimen

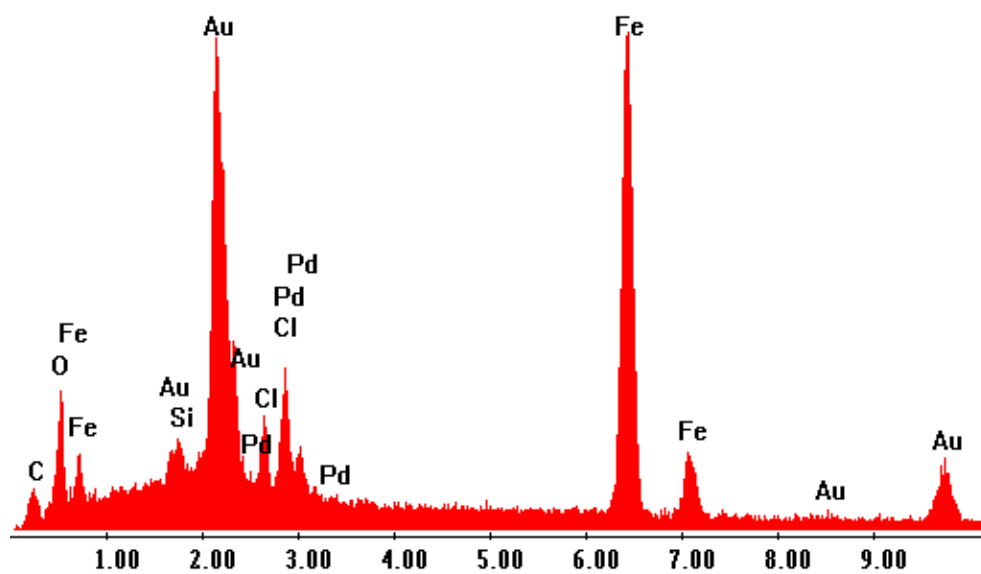


Figure 4-76 EDAX spectrum of particle taken from the CB Control 40 S specimen

Table 4-5 Summary of reaction products found in EDAX and Thermal analysis

Chemical Addition	Cleveland	Castle Bromwich
<b>Na<sub>2</sub>SO<sub>4</sub></b>	Ettringite Cancrinite Aluminium Hydroxide gel	Aluminium Hydroxide Gel
<b>NaOH</b>	Cancrinite Alkali Silica Gel Calcium Silicate Hydrate (CSH)	Aluminium hydroxide gel Gibbsite Bayerite
<b>CaCl<sub>2</sub></b>	Alkali Silica Gel	Calcium Aluminate gel
<b>.3</b>	Forms of Ferrous Metals	Forms of Ferrous Metals

Table 4-5 shows a summation of the reaction products found in EDAX and Thermal analysis which were discussed in this section. Sodium Sulfate and sodium hydroxide show the most reactive products with Calcium chloride and control specimens also containing reactive products.

## 4.7 Thermal Analysis

The results of thermal analysis are shown below, it should be noted that the horizontal portion, or plateau that indicates constant sample weight and the curved portion; the steepness of the curve indicates the rate of mass loss. Thermal analysis in Figure 4-77. Figure 4-77 shows very little mass loss as the result of heating the specimen to 100°C. Exposure to water (Figure 4-78) has the effect of increasing the proportions of some of the troughs visible in the original material. In particular, the trough at 87°C is present as a much larger feature in Figure 4-78 (reaching a minimum at 78°C). This feature is most likely the dehydration of aluminium hydroxide ( $\text{Al}(\text{OH})_3$ ) gel, which has presumably formed as a result of the solution in the reaction vessel (rendered alkaline by contact with the ash) reacting with aluminium metal in the ash. However, it should be stressed that a number of other gel-like materials, including calcium silicate hydrates, calcium aluminate hydrates and aluminosilicate hydrates may also contribute to this feature on the thermal analysis trace.

Also of note is the increase in magnitude of the loss of mass at around 250°C. This is most probably the dehydration of iron hydroxyl-oxide  $\text{FeO}(\text{OH})$ . This therefore represents the formation of rust in the ash in moist conditions.

When the material is brought into contact with a solution of sodium hydroxide (Figure 4-79), it is clear that the feature attributed to aluminium hydroxide is much pronounced, which is to be expected, since alkaline conditions will promote the conversion of aluminium to aluminium hydroxide. Calcium chloride also promotes the reaction of aluminium metal to form its hydroxide gel (Figure 4-80). There also appear to be higher quantities of rust relative to the unreacted specimen. This is to be expected since chlorides promote the corrosion of iron and steel.

Figure 4-81 show the thermal analysis results for the Castle Bromwich specimen exposed to sodium sulphate ( $\text{Na}_2\text{SO}_4$ ). There is little evidence of much further reaction relative to the unreacted specimen.

Figure 4-82 presents a series of X-ray diffraction traces of the full range of Castle Bromwich powdered specimens. It is evident that, overall, the traces all resemble each other, indicating that the magnitude of reactions occurring is relatively minor. In the case of exposure to water only and calcium chloride, there is very little difference between the original and reacted material.

Where exposure to sodium hydroxide has occurred, the main difference between the original and reacted specimens is the presence of a series of peaks at lower angles. The two peaks around 9 and 10 °2θ can be attributed to the formation of ettringite and monocarbonate, which are both calcium aluminate hydrates, presumably formed as the result of the reaction of aluminium metal in the presence of calcium. Ettringite has in some cases been associated with expansion of concrete. However, the quantities here are very small and unlikely to present a problem. There is a new peak at around 13 °2θ, which is probably the aluminosilicate hydrate nacrite. There is also some evidence of the formation of small quantities of bayerite, a crystalline form of aluminium hydroxide, which has a peak at around 18 °2θ.

There are a number of additional peaks on the trace obtained from the specimen exposed to sodium sulphate. However, these result from the presence of sodium sulphate itself, indicating that this compound has not been involved in reactions to any great extent.

Whilst X-ray diffraction is an extremely powerful technique, it is not able to provide detailed characterisation of any amorphous materials, which show up as broad 'humps' on the traces. However, it is worth examining the nature of these features, since they provide some further insight into the reactions occurring. Figure 4-83 shows the original trace obtained for the Castle Bromwich ash with the trace obtained from the same material after exposure to sodium hydroxide superimposed. The larger magnitude of the amorphous hump is very much evident. The most probable explanation of this is that reactions which have occurred have produced relatively significant quantities of amorphous reaction products. This observation is true of all of the Castle Bromwich specimens.

The results obtained from the Cleveland IBA (Figure 4-84 -Figure 4-87) are broadly similar, and so it is more meaningful to highlight any differences observed. The thermogravimetry traces are largely the same as those observed for Castle Bromwich. However, in the case of the X-ray diffraction traces, a number of differences can be identified. Firstly, in the case of the material exposed to sodium hydroxide, the quantity of calcium aluminates formed is clearly much higher. Secondly, where exposure has been to water only, gypsum is present, which may reflect the higher levels of sulphate in the Cleveland IBA. Thirdly, exposure to calcium chloride has led to the formation of Friedel's salt, which is a calcium aluminate formed in the presence of chlorides.

Figure 4-90 shows the original material's trace with the trace obtained after exposure to sodium hydroxide. There is very little evidence of the formation of amorphous reaction products, and possibly a decline in the amount of amorphous material present. Again, this is true of all the specimens.

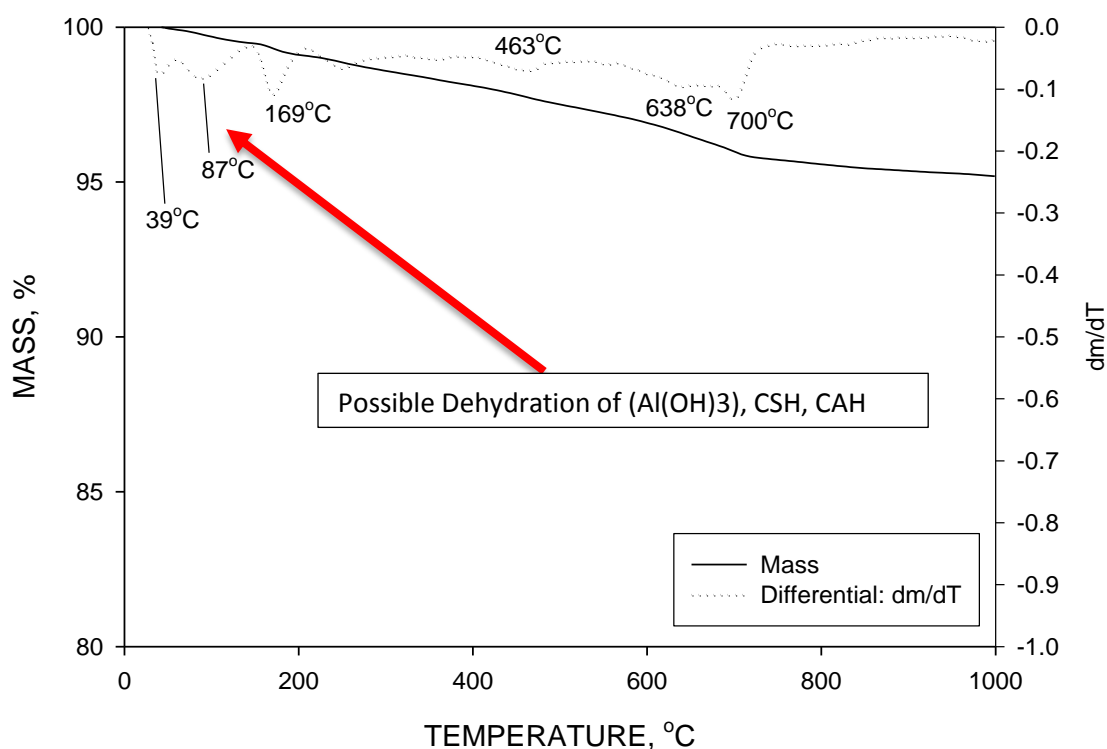


Figure 4-77 Thermal analysis results from the unreacted Castle Bromwich IBA

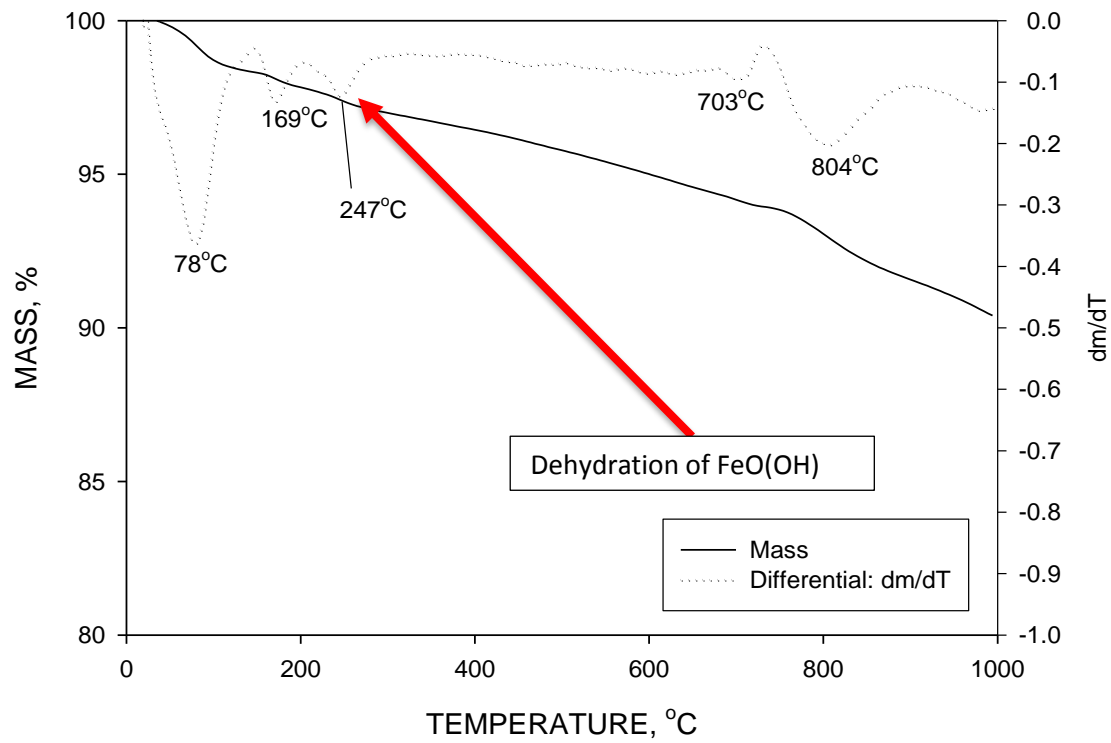


Figure 4-78 Thermal analysis results from the powdered Castle Bromwich IBA after storage in the presence of water at 40°C for 6 weeks.

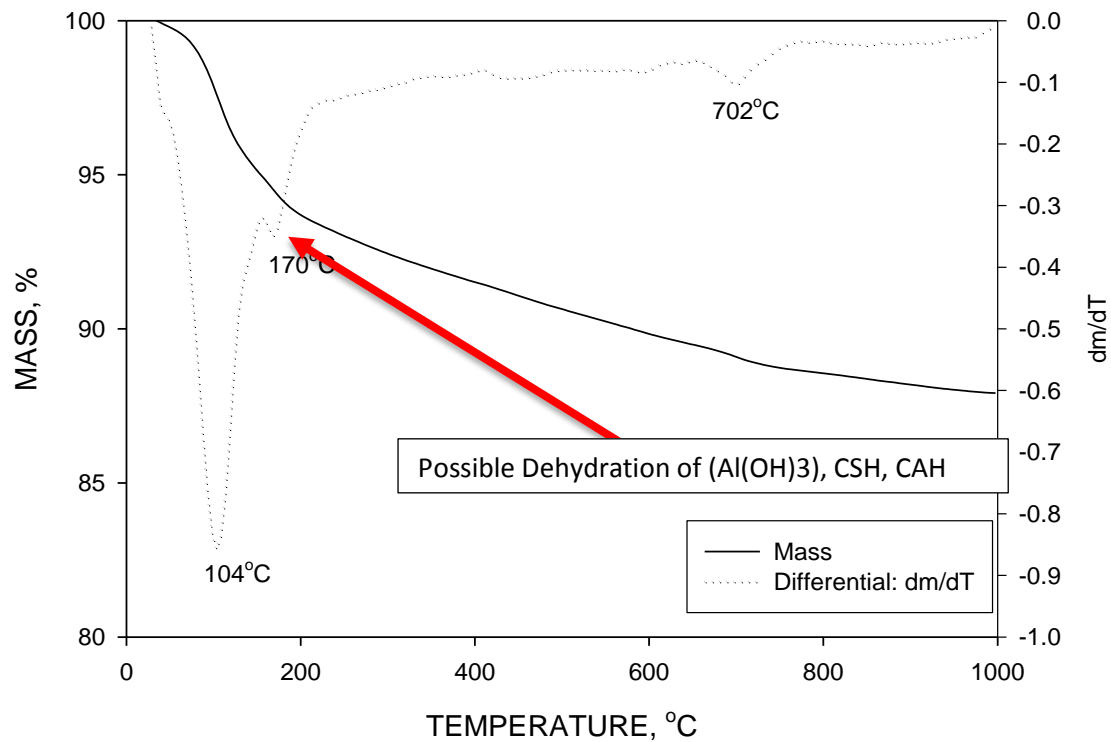


Figure 4-79 Thermal analysis results from the powdered Castle Bromwich IBA after storage in the presence of a solution of NaOH at 40°C for 4 weeks



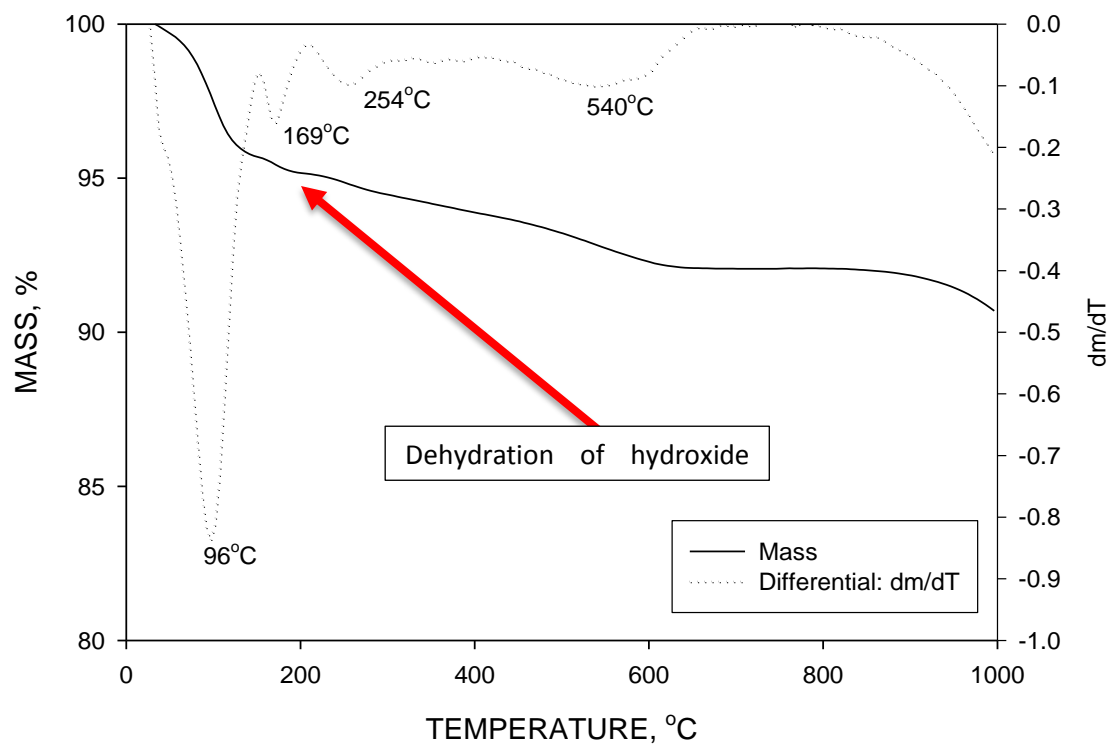


Figure 4-80 Thermal analysis results from the powdered Castle Bromwich IBA after storage in the presence of a solution of  $\text{CaCl}_2$  at  $40^\circ\text{C}$  for 4 weeks

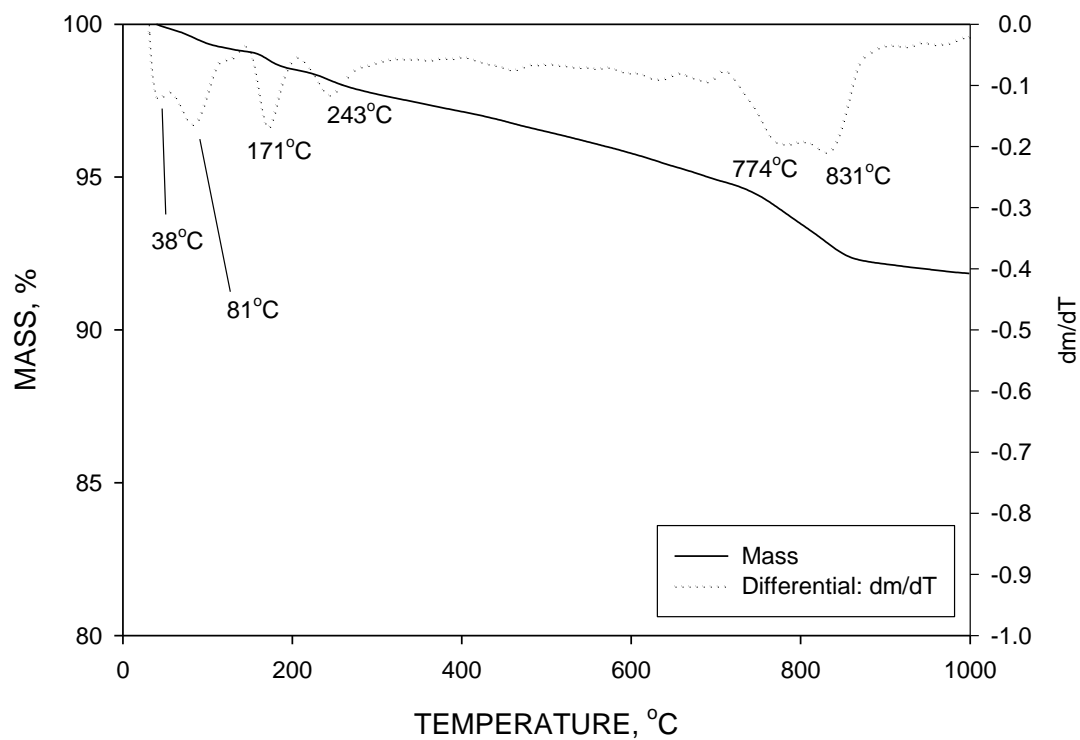


Figure 4-81 Thermal analysis results from the powdered Castle Bromwich IBA after storage in the presence of a solution of  $\text{Na}_2\text{SO}_4$  at  $40^\circ\text{C}$  for 4 weeks



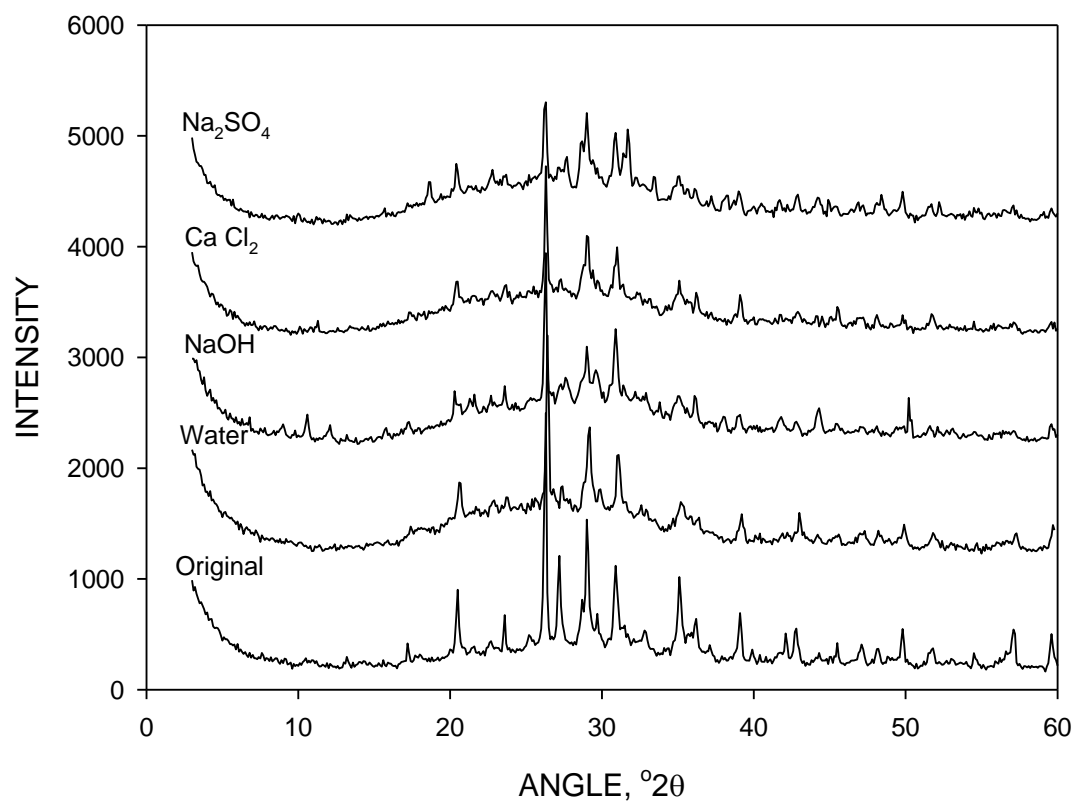


Figure 4-82 X-ray diffraction traces from the powdered Castle Bromwich specimens exposed to different chemical environments.

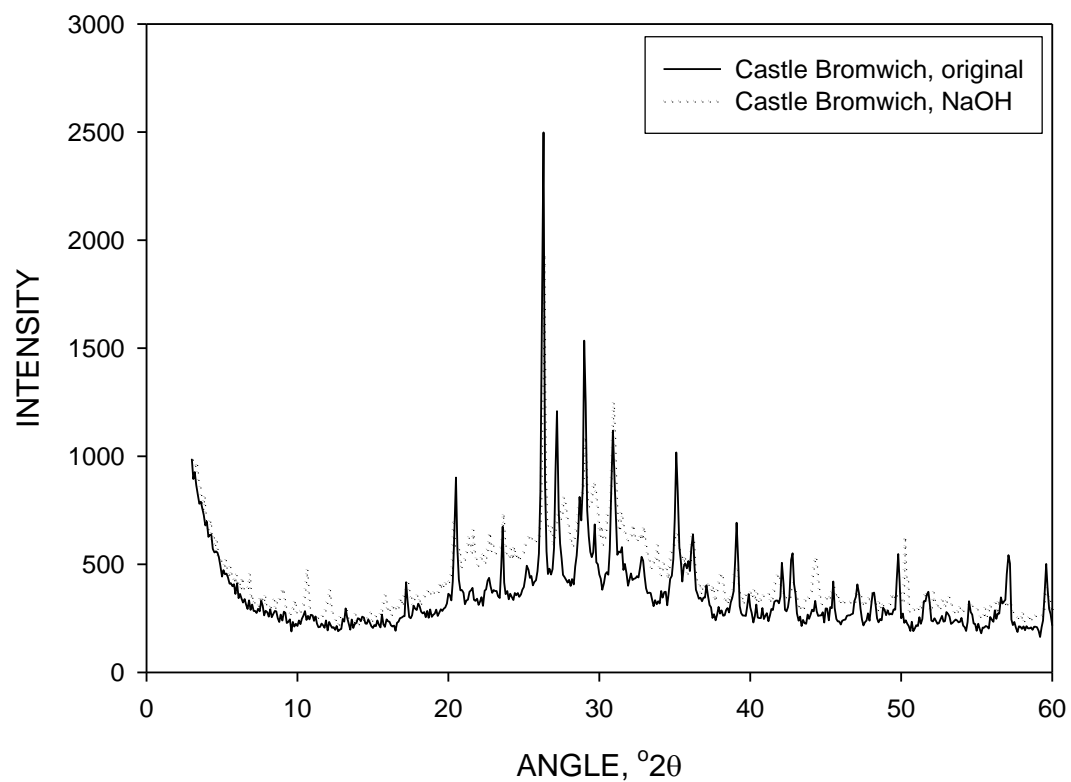


Figure 4-83 X-ray diffraction traces from the original powdered Castle Bromwich specimen, plus the material after exposure to NaOH.

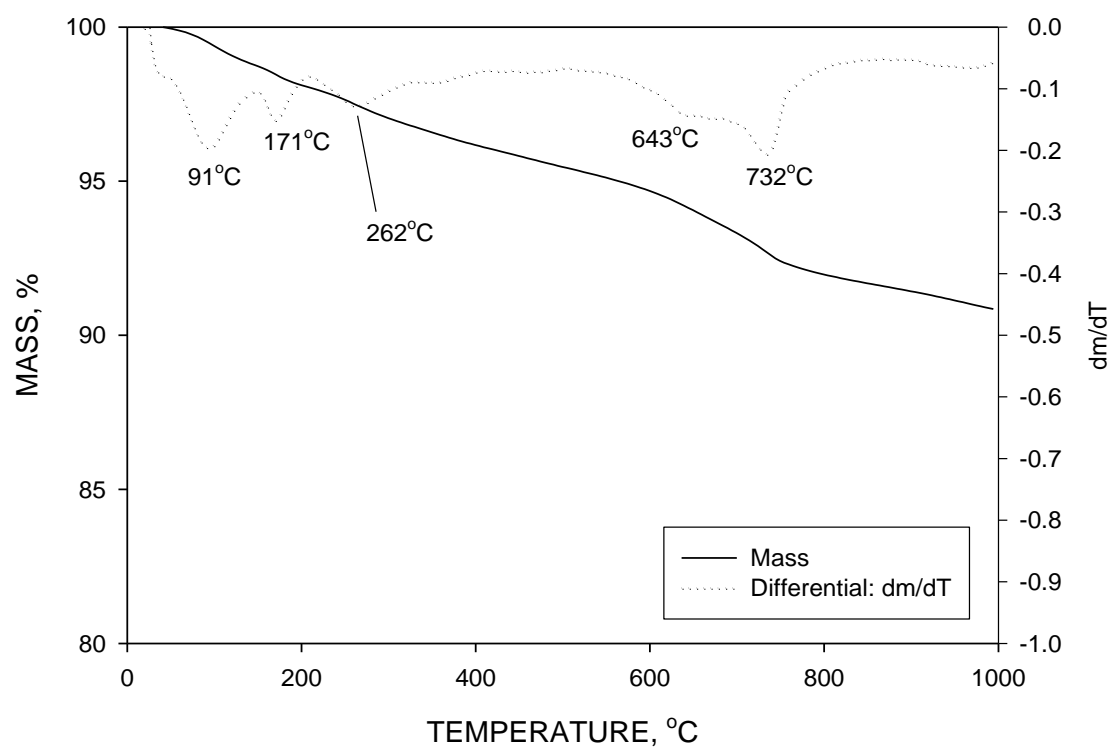


Figure 4-84 Thermal analysis results from the unreacted Cleveland IBA

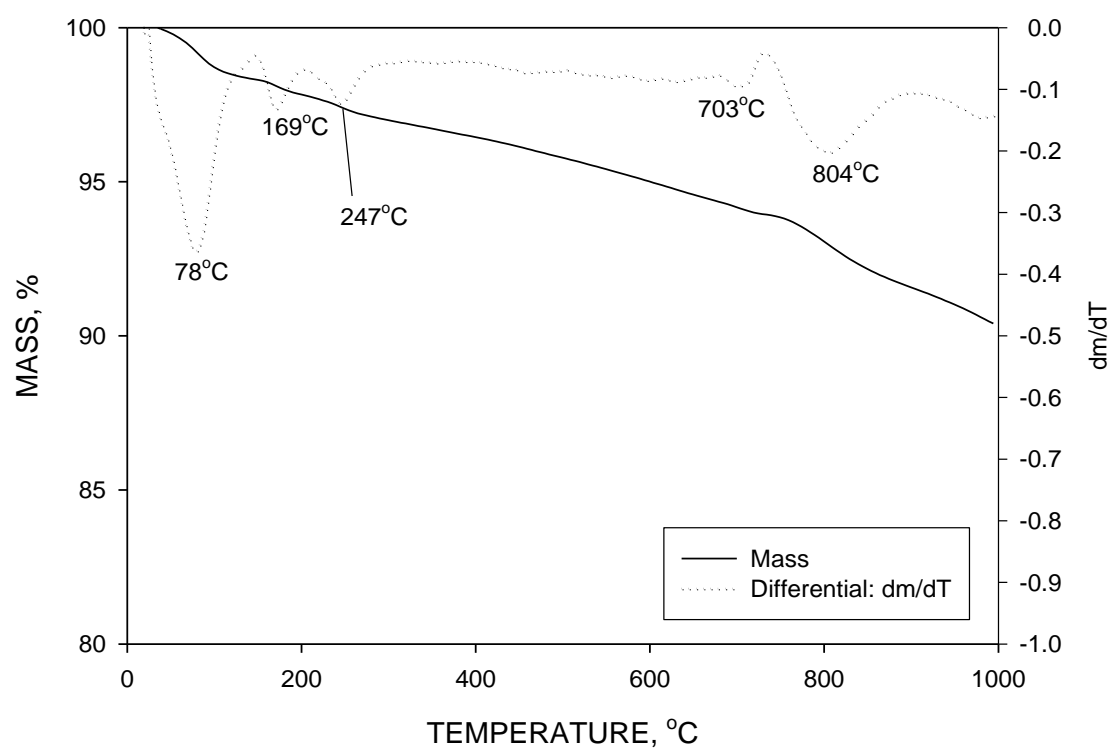


Figure 4-85 Thermal analysis results from the powdered Cleveland IBA after storage in the presence of water at 40 $^{\circ}C$  for 6 weeks.

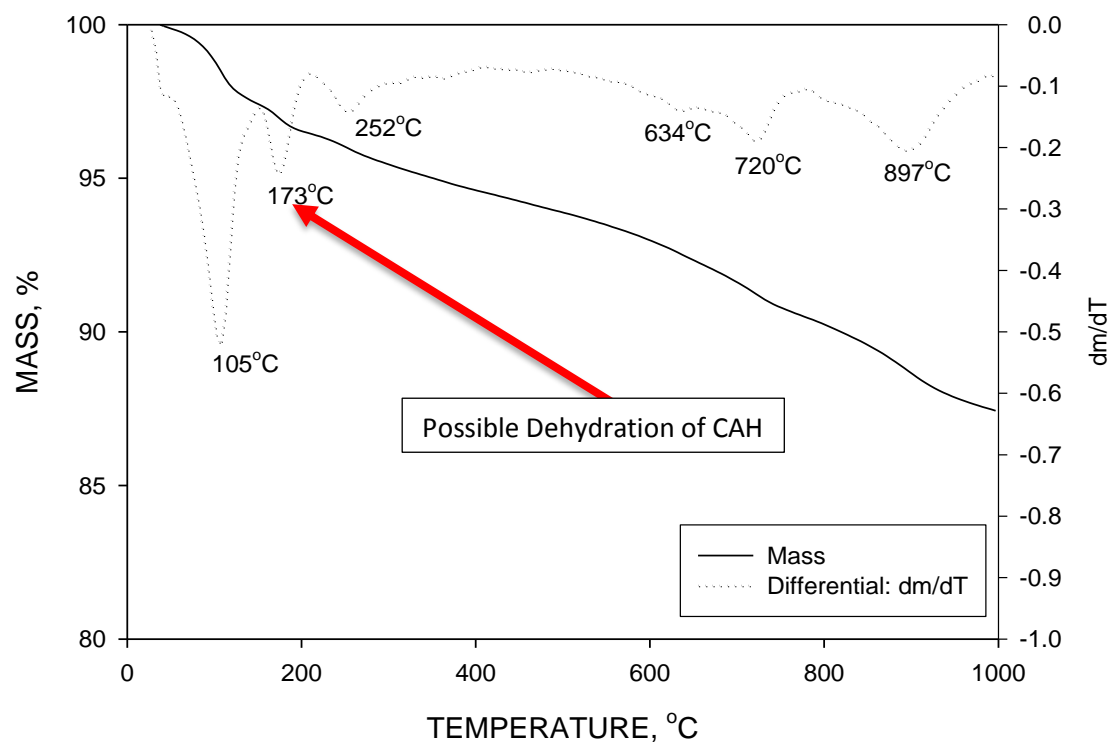


Figure 4-86 Thermal analysis results from the powdered Cleveland IBA after storage in the presence of a solution of NaOH at 40°C for 4 weeks

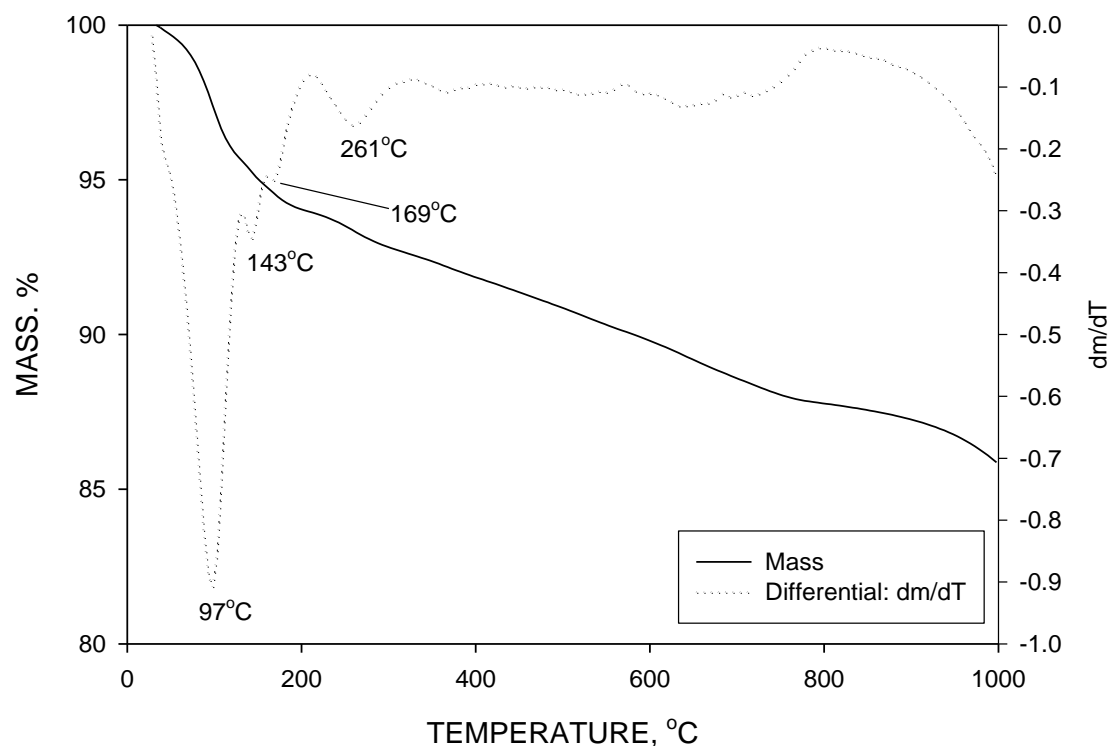


Figure 4-87 Thermal analysis results from the powdered Cleveland IBA after storage in the presence of a solution of CaCl<sub>2</sub> at 40°C for 4 weeks.

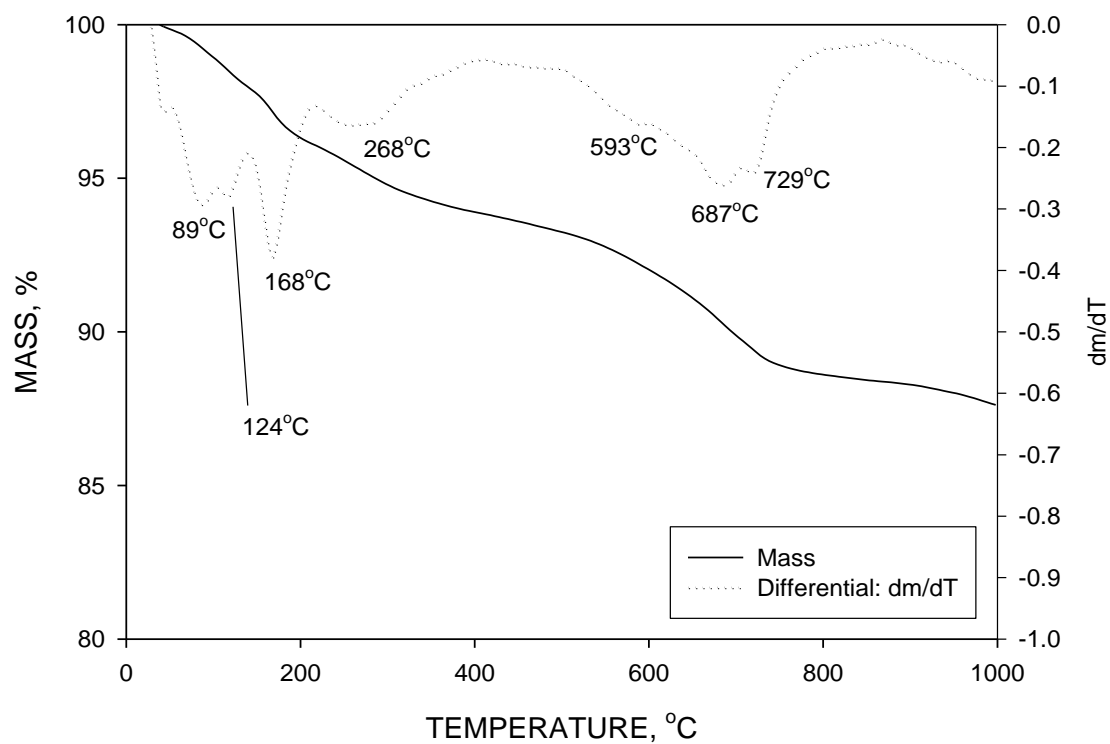


Figure 4-88 Thermal analysis results from the powdered Castle Bromwich IBA after storage in the presence of a solution of  $\text{Na}_2\text{SO}_4$  at 40°C for 4 weeks

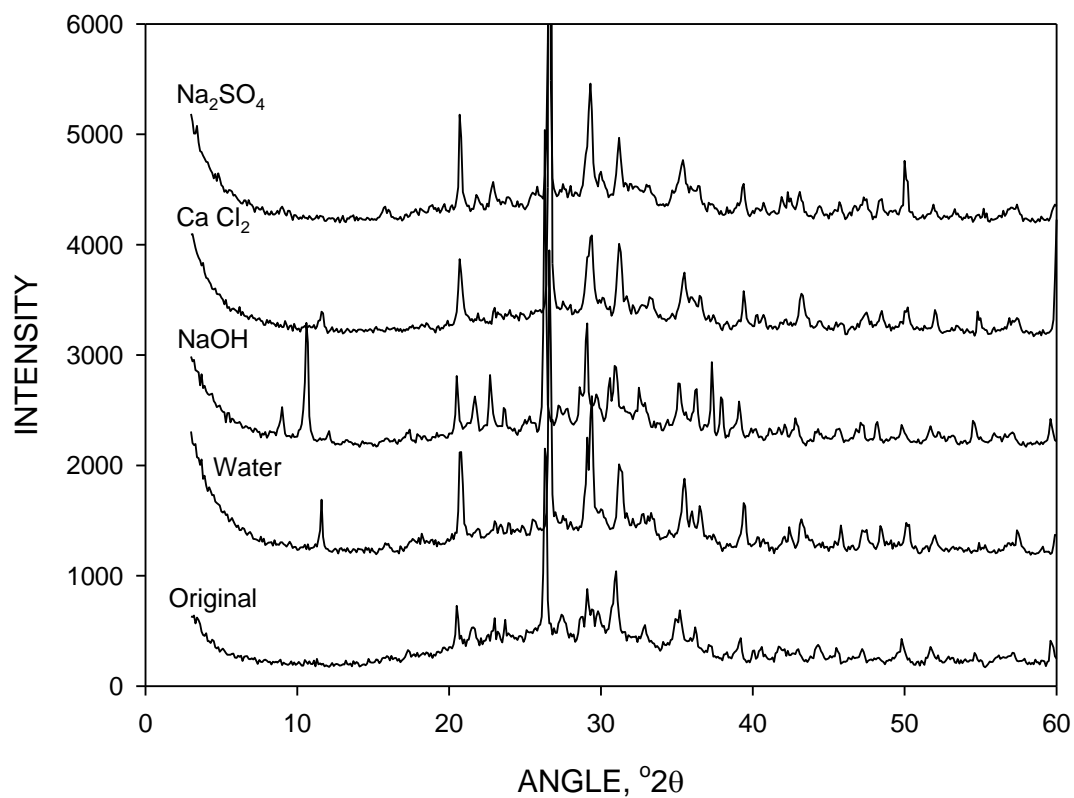


Figure 4-89 X-ray diffraction traces from the powdered Cleveland specimens exposed to different chemical environments

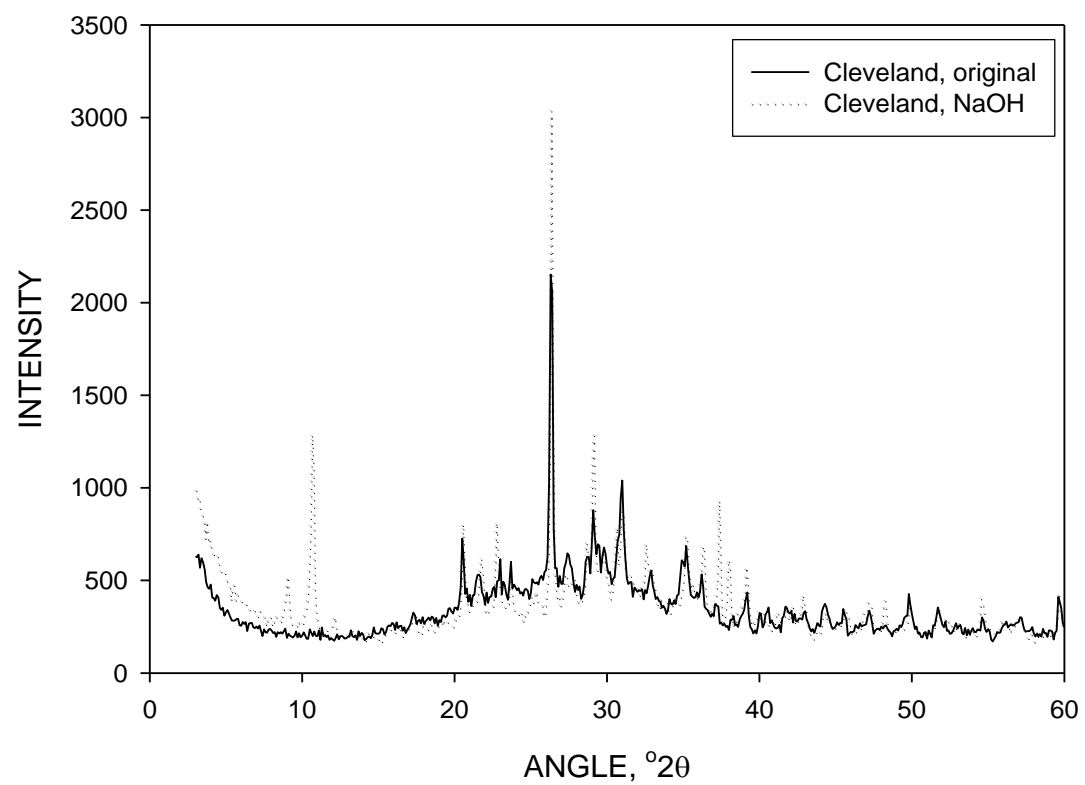


Figure 4-90 X-ray diffraction traces from the original powdered Cleveland specimen, plus the material after exposure to NaOH

## 5 Discussion of Results

The results of the testing programme are best interpreted by considering the different studies in parallel. Initially it is beneficial to summarise the key findings of the different investigations which made up the entire study:

- The expansion study identified little correlation between the conditions that the IBA was exposed to and the magnitude and nature of expansion. Most specimens underwent a small quantity of expansion. Generally most specimens did not expand, but a small number did.
- X-ray diffraction found evidence of only small quantities of crystalline reaction products in the materials which had undergone expansion testing. However, thermal analysis measured quantities of chemically-bound water in some materials which must have been present in the form of amorphous gels. Generally, high levels of bound water (and hence gels) were found in specimens which had undergone significant expansion. The gel most often present is probably aluminium hydroxide gel. Many of the crystalline materials found in the tested IBAs appear to be the result of further reaction of the amorphous gels.
- Microscope examination of the ashes has identified a number of gels in the tested IBAs. The most common of these is an aluminium hydroxide whose morphology implies an expansive nature. Alkali-silica reaction gel has also been identified in some cases, but it appears to be largely present in small volumes and unlikely to be responsible for expansion.

Whilst expansion results were, in places, inconsistent and seemingly sensitive to specimen variability, the overall conclusion that can be drawn from the results is expansion during the testing programme appeared to occur through at least two mechanisms. The first of these appears to be a relaxation of the compacted mass of IBA, which occurs unpredictably producing relatively small levels of expansion. In a wholly confined environment, such expansion would not be observed. On a typical construction site, where loads of aggregate for use as fill or pavement layers are generally spread and compacted as and when they arrive, any relaxation is most likely to occur relatively rapidly and before any superceding or superimposed activity takes place. The risk of 'relaxation' of compacted IBA causing damage expressed as expansion is negligible.

There would appear to be a second expansion process which is, at least in part, promoted by alkaline conditions. This process involves a reaction of constituents in the ash to form amorphous gels, some of which are expansive. The precise nature of these gels has proven difficult to identify through conventional chemical analysis techniques (XRD, thermogravimetry) since they are non-crystalline and share common characteristics. However, expansive gels of aluminium hydroxide are likely to be the main contributor here.

Aluminium hydroxide gels are formed as a result of a reaction between aluminium metal and alkaline solutions. Associated with this would be the release of hydrogen gas. However, this mechanism seems less likely as expansion resulting from this process would be expected early in the expansion test, whereas expansion is observed over a broad time range.

When considering this phenomenon in real construction scenarios, most applications where IBAA is used, it would not be exposed to conditions of high pH. Therefore, it is most unlikely, except where IBAA is used in poured concrete mixes, to have the amounts of alkaline, wet conditions that would promote the creation of such gels. General fill and pavement foundation layers are laid in 'dry' conditions and surface water, which may permeate through the IBAA is typically of neutral pH. It is reasonable therefore to consider the risk of any expansion to be low and, even if it were to occur, it is most likely to be less than 1% in typical circumstances.

Because of the mixtures of different gels formed and the chemical similarities between the gels, relating the quantity of gel formed to the magnitude of expansion has not been possible. Moreover, it may well be the case that there is very little correlation between the two. However, given the absence of any other reaction products which could be responsible for expansion, it is concluded that the gel-formation mechanism is a highly probable explanation. It should be stressed that the IBA used in the experiments reported in this document were fresh from production. In reality, IBAA is typically aged for at least three weeks prior to use. During this period it is likely that most of the gel forming reactions would have taken place, thus considerably reducing the risk of damage from expansion when the IBAA is used.

Interpreting the expansion results in terms of their implications from an engineering perspective is complicated by the variable nature of these results. Considering the magnitudes of expansion of the full population of IBA specimens, expansion over 2% was rare, and most magnitudes of expansion were less than 1%. It should also be noted that the few samples which did show expansion in excess of 1%, had been subjected to abnormal conditions, deliberately intended to promote a reaction.

Therefore, the observation of more significant expansion in a handful of specimens needs to be taken in context. These results indicate that within a large volume of IBA, there is potential for small pockets of larger expansion under chemically aggressive conditions. Based on the above analysis, these pockets are most likely to correspond to the presence of occasional large particles of glass or aluminium metal, though IBAA has been through a process to take out metal particles and processor information suggests a residual metal content of less than 0.05% by mass. In very large volumes of ash, the overall expansion observed is likely to be very low, since larger expansion in localised parts of the volume will be dissipated throughout the rest of the volume.

Thus, in most instances, the risk of expansion of IBAA is remote. However, means of mitigating the risk of expansion have been devised for applications. These are:

- ***Weathering periods:*** as discussed above, periods of weathering will to reduce the pH of the IBAA and also weather particles of glass and aluminium to such an extent that potential reactivity would be very limited.
- ***Removal of aluminium metal:*** removal of aluminium metal through the use of eddy current apparatus is considered best practice and is a routine part of IBA processing, where high percentages of recovery are achievable.

The applications for IBAA are generally above water table in pH conditions near neutral where it is a valuable alternative aggregate. Whilst it may have a remote potential for expansion if used in wet, very alkaline conditions, the benefits of relatively low bulk density, self-setting and sustainability should encourage potential users to keep it as a feasible option.



## 6 Conclusions

This document reports on an experimental programme in which incinerator bottom ash (IBA) was characterised and tested to evaluate its propensity to expand when compacted into a confined space under different chemical and environmental conditions.

As set out in the aims and objectives, the literature review outlined the origin and background of IBA, the formation, chemical and physical composition of IBA, the application of the material and possible mechanisms of expansion to establish experimental procedures which could be undertaken in the study. This was done through researching past studies on IBA which classify the typical characteristics of the material. The literature review also outlined the methods of classification which were then used in the experimental programme.

Through the findings of the Literature review a laboratory based experimental programme was conducted which examined the physical and chemical characteristics of IBA. An experimental programme was laid out to classify the tendency for compacted IBAA to undergo expansion under a range of different conditions. These conditions were elevated temperatures, increased moisture contents and the addition of high concentrations of chemical substances which had the potential to cause reactions which lead to expansion. Once expansion had ceased, further analysis of the expansive material was carried out.

The experimental programme results, obtained through laboratory testing were then presented and discussed in detail, beginning with the expansion of the specimens. The influence of the ambient conditions in which the specimens were stored were shown to have an effect on the overall expansion. The results of the expansion led to additional testing as stated in the aims and objectives. Further testing of the IBA included X-ray Diffraction, X-ray fluorescence, magnetic separation analysis, thermogravimetry, Scanning electron microscopy and accelerated chemical reactions. These test methods were all undertaken to highlight the reactions occurring in the ash when rapid evaluation of expansion had ceased.

The practical outcomes, found through the research and experimental programme of the programme were as follows:

The results of the expansion testing programme were evidently very sensitive to specimen variability, despite relatively large sample sizes. The specimen variability was due to the use of three

chemical solutions,  $\text{Na}_2\text{SO}_4$ ,  $\text{NaOH}$  and  $\text{CaCl}_2$ . The specimen variability led to different expansion mechanisms through the use of the additional chemical solutions.

Expansion appears to be through two mechanisms: Relaxation of the compacted mass of IBA produced small levels of expansion, which occurred unpredictably. Each sample was prepared in the same manner; however, varying particles in the IBAA such as organic materials, ceramics and/or metals may have affected the compaction of the material. This can be seen in the early rapid expansion of several specimens in particular the specimens containing no chemical addition. The early expansion is most likely attributed to the settling of materials. The formation of expansive gels promoted by alkaline conditions; this was seen on several occasions. For instance, aluminium hydroxide gels whose morphology implies an expansive nature. Alkali-silica reaction gel has also been identified in some cases, but it appears to be largely present in small volumes and unlikely to be responsible for expansion.

In a wholly confined environment, as would be the case in a real civil engineering application, expansion as a result of relaxation would not be observed, since the material would be wholly confined. On site, material is compacted in several layers at an optimum moisture content. Additionally, relaxation would most likely occur on site relatively rapidly and before any subsequent construction activity takes place. Samples which did show expansion in excess of 1% linear strain through gel formation had been subjected to high pH conditions intended to promote a reaction. Most IBAA applications would not expose IBAA to the high pH conditions necessary for this reaction.

If expansion of this type were to occur, expansion would be relatively small – in the study expansion >2% linear strain was rare, and most magnitudes of expansion were <1%.

IBA used in the study was fresh from production, no storage or aging or processing had taken place. In reality, IBA is typically aged for at least three weeks. During this period, much of the gel forming reactions that could cause potential swelling would have taken place.

Based on the highly variable nature of the ash performance, the expansive potential of IBAA is based around small pockets of occasional reactive particles present within a larger volume of unreactive material; E.g., some local expansions are caused by metallic aluminium and therefore the number and size of the particles of aluminium metals in the IBA which can come into contact with alkaline solutions will have a large effect on the possibility of expansion in the base course through the formation of aluminium hydroxide gels

As a result of this, in very large volumes of ash, overall expansion is likely to be very low, since localised expansion will be dissipated throughout the rest of the volume. Thus, in most instances, it is likely that the risk of expansion of IBAA is remote.

The conclusions from this dissertation lead to the following recommendations for further studies.

## **6.1 Proposed further study**

The research undertaken for this dissertation has highlighted a number of topics in which further research would be beneficial. The literature review highlighted areas where information was lacking, in particular the expansive properties of IBAA. Whilst some of these were addressed by the research in this dissertation, others remain. There are a number of additional areas of study which would further benefit the understanding of IBA. The ash used in this study was fresh ash, no aging or additional processing had occurred. In further studies it may be beneficial to process the ash as it would be if used in industry to give an “as used” representation of the material. Furthermore a wider range of IBA could be included in the study, many MSW plants on the continent produce IBA, these materials could further expand the scope.

Tests were carried out in this study to establish the base composition of IBA, the as received moisture content of bottom ash in the two plants vary from 6% - 13% by mass. The moisture contents may have been affected significantly by the weather conditions and the water quenching methods used in the plants. The effect of weathering and water quenching on the IBA may be studied further. This would aid in finding the optimum condition of the IBA when leaving the plant leading to a more consistent material.

In this study, IBA was tested under normal and elevated temperature conditions. The varying weather in the UK, from very hot summers to bitterly cold winters, particularly in recent years may have an effect on IBA performance as a sub-base material. Testing under varying colder conditions using tests for freeze-thaw and frost heave will give an indication of IBA’s vulnerability to the each phenomenon.

## 7 Bibliography

### Journals and Books

Al-Dulaijan, S.U. (2007) "Sulfate resistance of plain and blended cements exposed to magnesium sulfate solutions" Construction and Building Materials **21**(8):1792-1802

Al-Rawas, A. A., A. Wahid Hago, et al. (2005). "Use of incinerator ash as a replacement for cement and sand in cement mortars." Building and Environment **40**(9): 1261-1266.

Alkemade, M. M. C., M. M. T. Eymael, et al. (1994). "How to Prevent Expansion of MSWI Bottom Ash in Road Constructions?" Studies in Environmental Science. H. A. v. d. S. J.J.J.M. Goumans and G. A. Th, Elsevier. **Volume 60**: 863-876.

Arm, M. (2003). "MECHANICAL PROPERTIES OF RESIDUES AS UNBOUND ROAD MATERIALS – experimental tests on MSWI bottom ash, crushed concrete and blast furnace slag." PhD.

Bayuseno, A. P. and W. W. Schmahl (2010). "Understanding the chemical and mineralogical properties of the inorganic portion of MSWI bottom ash." Waste Management **30**(8–9): 1509-1520.

Casanova, I. Agulló, L. Aguado, A. (1996), "Aggregate expansivity due to sulfide oxidation — I. Reaction system and rate model", Cement and Concrete Research, **26** ( 7): 993-998

Casanova, I. Agulló, L. Aguado, A. (1997), "Aggregate expansivity due to sulfide oxidation — II. Physico-chemical modeling of sulfate attack", Cement and Concrete Research, **27** (11): 1627-1632

Chimenos, J. M., M. Segarra, et al. (1999). "Characterization of the bottom ash in municipal solid waste incinerator." Journal of Hazardous Materials **64**(3): 211-222.

European Environment Agency (2013). Municipal Waste Management in the United Kingdom, Copenhagen Resource Institute, Copenhagen.

Dyer, T. (2014) Concrete Durability, Ebook, CRC Press,

McDonagh, S. (2001) Why are we Deaf to the Cry of the Earth? Dublin: Veritas.

: Author/Editor Last name, Initials. (Year) Title. Edition. Place of publication: Publisher

Farny, S., Koshimatka (1997). "Diagnosis and control of Alkali-Aggregate Reactions in concrete."

Federico, L. M. and S. E. Chidiac (2009). "Waste glass as a supplementary cementitious material in concrete – Critical review of treatment methods." Cement and Concrete Composites **31**(8): 606-610.

Forteza, R., M. Far, et al. (2004). "Characterization of bottom ash in municipal solid waste incinerators for its use in road base." Waste Management **24**(9): 899-909.

D. François , A. Jullien (2009) "A framework of analysis for field experiments with alternative materials in road construction" Waste Management **29**: 374–382

Ginés, O., J. M. Chimenos, et al. (2009). "Combined use of MSWI bottom ash and fly ash as aggregate in concrete formulation: Environmental and mechanical considerations." Journal of Hazardous Materials **169**(1-3): 643-650.

Hobbs, D. W. (1988). Alkali-silica reaction in concrete. London, Thomas Telford.

Ichikawa, T. and M. Miura (2007). "Modified model of alkali-silica reaction." Cement and Concrete Research **37**(9): 1291-1297.

Izquierdo, M., X. Querol, et al. (2011). "Procedural uncertainties of Proctor compaction tests applied on MSWI bottom ash." Journal of Hazardous Materials **186**(2-3): 1639-1644.

Juric, B., L. Hanzic, et al. (2006). "Utilization of municipal solid waste bottom ash and recycled aggregate in concrete." Waste Management **26**(12): 1436-1442.

Klein, R., T. Baumann, et al. (2001). "Temperature development in a modern municipal solid waste incineration (MSWI) bottom ash landfill with regard to sustainable waste management." Journal of Hazardous Materials **83**(3): 265-280.

Müller, U. and K. Rübner (2006). "The microstructure of concrete made with municipal waste incinerator bottom ash as an aggregate component." Cement and Concrete Research **36**(8): 1434-1443.

Musson, S.E. Xu, Q. Townsend, T.G. (2008) "Measuring the gypsum content of C & D debris fines", Waste Management, **28** (11): 2091-2096

Pera, J., L. Coutaz, et al. (1997). "Use of incinerator bottom ash in concrete." Cement and Concrete Research **27**(1): 1-5.

Ping, X, Beaudoin JJ, (1992) "Effects of transition zone microstructure on bond strength of aggregate-portland cement paste interfaces", Cement and Concrete Research, **22**(1)

Qiao, X. C., M. Tyrer, et al. (2008). "Novel cementitious materials produced from incinerator bottom ash." Resources, Conservation and Recycling **52**(3): 496-510.

Siddique, R. (2008). "Waste Materials and By-Products in Concrete." 265-300.

Scherer G.W, (2004) "Stress from crystallization of salt, Cement and Concrete Research", **34** (9): 1613-1624

Tam, V. W. Y., X. F. Gao, et al. (2008). "New approach in measuring water absorption of recycled aggregates." Construction and Building Materials **22**(3): 364-369.

George Wang, Yuhong Wang, Zhili Gao (2010) "Use of steel slag as a granular material: Volume expansion prediction and usability criteria" Journal of Hazardous Materials **184** 555–560

## Standards

Building Research Establishment (2004.). "'Alkali-Silica reaction in concrete.'" Digest 330 part 1, BRE, Watford

Building Research Establishment (2004). "Alkali-silica reaction in concrete." BRE digest 330 part 2, BRE, Watford

Building Research Establishment (2001). "Concrete in Aggressive Ground." BRE digest 363 part 1, BRE, Watford

The Highways Agency (2004), Design manual for Roads and Bridges, Volume 7, section 1, part 2 HD 35/04, Conservation and the use of Secondary Recycled Materials, The Stationary Office, Norwich

British Standards Institution (1995). BS 812-2: 1995 testing aggregates. Methods for determination of density. British Standards Institution. London.

British Standards Institution (1990). BS 812-109: 1990. Testing Aggregates - part 109: methods for determination of moisture content, British Standards Institution. London

British Standards Institution (1990) BS 1377-4: 1990. Soils for civil engineering purposes: part 4 compaction related tests, British Standards Institution. London

British Standards Institution (2005). BS EN 196-2:2005. Methods of testing cement. Part 2: Chemical analysis of cement, British Standards Institution. London

British Standards Institution (2012). BS EN 933-1:2012. Tests for geometrical properties of aggregates Part 1: Determination of particle size distribution - Sieving method, British Standards Institution, London

Concrete.Society (1999). "Alkali-silica reaction: minimising the risk of damage to concrete." Technical report No. 30.

CEN (Comité Européen de Normalisation), 2005a. EN 13286-2 standard, Unbound and hydraulically bound mixtures. Part 2: Test methods for laboratory reference density and moisture content. Proctor compaction

## Websites

Health and Safety Executive (2010) Foamed concrete explosion - HSE investigation update, Available at: <http://www.hse.gov.uk/construction/liveissues/foamedconcrete.htm> [Accessed 21/09/2015]

Virtual Soil lab modules (2012) Soil Bulk Density, available at: <http://soilweb.landfood.ubc.ca/labmodules/compaction/soil-bulk-density> [Accessed 05/04/2012]